

# **Promoted Cobalt Based Catalyst for Fischer Tropsch Synthesis Application**



**By**

**Muhammad Arslan**

**Reg. No. NUST201463504MCES64114F**

**Session 2014-16**

**Supervised by**

**Prof. Dr. Naseem Iqbal**

**US Pakistan Center for Advance Studies in Energy**

**National University of Sciences and Technology**

**H-12, Islamabad 44000, Pakistan**

**November, 2016**

# **Promoted Cobalt Based Catalyst for Fischer Tropsch Synthesis Application**



**By**

**Muhammad Arslan**

**Reg. No. NUST201463504MCES64114F**

**Session 2014-16**

**Supervised by**

**Prof. Dr. Naseem Iqbal**

**A Thesis Submitted to the Centre for Energy Systems in partial  
fulfillment of the requirements for the degree of  
MASTERS of SCIENCE in  
ENERGY SYSTEMS ENGINEERING**

**US Pakistan Center for Advance Studies in Energy (USPCASE)**

**National University of Sciences and Technology (NUST)**

**H-12, Islamabad 44000, Pakistan**

**November, 2016**

**THESIS ACCEPTANCE CERTIFICATE**

Certified that final copy of MS/MPhil thesis written by Mr. Muhammad Arslan, (Registration No. NUST201463504MCES64114F), of USPCAS-E has been vetted by undersigned, found complete in all respects as per NUST Statues/Regulations, is free of plagiarism, errors, and mistakes and is accepted as partial fulfillment for award of MS/MPhil degree. It is further certified that necessary amendments as pointed out by GEC members of the scholar have also been incorporated in the said thesis.

Signature: \_\_\_\_\_

Name of Supervisor Dr. Naseem Iqbal

Date: \_\_\_\_\_

Signature (HoD): \_\_\_\_\_

Date: \_\_\_\_\_

Signature (Dean/Principal): \_\_\_\_\_

Date: \_\_\_\_\_

# Certificate

This is to certify that work in this thesis has been carried out by **Mr. Muhammad Arslan** and completed under my supervision in US Pakistan Centre for Advance Studies in Energy (USPCAS-E), National University of Sciences and Technology, H-12, Islamabad, Pakistan.

Supervisor:

---

Dr. Naseem Iqbal  
USPCAS-E  
NUST, Islamabad

GEC member # 1:

---

Dr. M. Bilal Khan  
USPCAS-E  
NUST, Islamabad

GEC member # 2:

---

Dr. Nisar Ahmad  
NCP  
Islamabad

GEC member # 3:

---

Dr. Majid Ali  
USPCAS-E  
NUST, Islamabad

HoD-CES

---

Dr. Zuhair S Khan  
USPCAS-E  
NUST, Islamabad

Principal/ Dean

---

Dr. M. Bilal Khan  
USPCAS-E  
NUST, Islamabad

## **Dedication**

*I dedicate this endeavor to my father for his advice, inspiration and faith*

*&*

*To my mother for her love, care and support*

## Abstract

Energy consumption is increasing day by day placing a lot of load on fossil fuels which in turns cause various threats to environment. Among other forms of energy, liquid fuels are most commonly and intensively used in daily life. To match the demand of liquid fuels scientists are working to find new sources to generate relatively clean liquid fuels that poses minimum environmental threat. Fischer Tropsch Synthesis is one of such efforts that generate synthetic hydrocarbons from various sources like coal, biomass, natural gas and environmental carbon dioxide. The Fischer Tropsch Synthesis uses syngas (mixture of carbon monoxide and hydrogen) to generate liquid hydrocarbons at high temperatures of 200 to 350<sup>o</sup>C in the presence of a catalyst at high pressures (upto 20 bars). This study focuses on developing a cobalt based catalyst for Fischer Tropsch Synthesis (FTS) process and to check the effect of promoters on the activity of the prepared catalyst. Zinc and Zirconium promoters are used in this study. Hydrotalcite supported cobalt catalyst is prepared by co-precipitation method and the (Zn and Zr) promoters are added by wetness impregnation method. The qualitative and quantitative analyses of all the prepared samples are done using various characterization techniques. XRD and SEM were performed to gather information about the structure and morphology of the catalyst. EDS was used for elemental analysis of the samples. BET and TGA are two techniques that give information about the properties of catalyst like surface area and thermal stability. FTIR was performed to check the purity of samples. The samples were tested for FTS process in a micro reactor especially to check the C<sub>5+</sub> selectivity. The product obtained from FTS reactor was analyzed using GC-MS. The results showed very high C<sub>5+</sub> selectivity for promoted catalyst as compared to unpromoted catalyst.

**Key Words:** Fischer Tropsch Synthesis; Cobalt Catalyst; Hydrotalcite; Zinc Promoters; Zirconium Promoters

# Table of Contents

Table of Figures .....	IV
List of Tables.....	VI
List of Abbreviations.....	VII
List of Publications.....	VIII
<b>Chapter 1: Introduction .....</b>	<b>1</b>
1.1 Synthetic Fuels .....	3
1.1.1 Coal to Liquids (CTL).....	3
1.1.2 Gas to Liquid (GTL) .....	4
1.1.3 Biomass to Liquid (BTL) .....	5
1.1.4 Recycled Carbon Dioxide to Liquid (RCTL).....	5
1.2 Fischer Tropsch Synthesis Process.....	6
1.3 Brief History of Fischer Tropsch Synthesis .....	7
1.3.1 Development of Technology.....	7
1.3.2 Commercialization .....	7
1.4 Summary.....	10
1.5 References .....	11
<b>Chapter 2: Literature Review .....</b>	<b>12</b>
2.1 Types of FT Reactions.....	12
2.1.1 High Temperature Fischer Tropsch Reaction (HTFT).....	12
2.1.2 Low Temperature Fischer Tropsch Reaction (LTFT).....	12
2.2 Types of Reactors in FTS .....	12
2.2.1 Fixed Bed Reactor .....	12
2.2.2 Slurry Phase Reactor .....	13
2.2.3 Fluidized Bed Reactor .....	13
2.3 Fischer Tropsch Synthesis Catalyst.....	14
2.4 Role of Support.....	16
2.5 Promoters.....	17

2.5.1	Stabilizing Support Oxide .....	17
2.5.2	Glueing Effect .....	17
2.5.3	Increased Active Metal Dispersion .....	17
2.5.4	Decoration of Active Metal.....	18
2.5.5	Metal Alloying .....	18
2.5.6	Synergistic Promotion Effect .....	18
2.5.7	Help Against Poisoning.....	19
2.5.8	Coke Burning during Regeneration.....	19
2.6	Promoters Used in FTS .....	19
2.6.1	Nobel Metal Promoter.....	19
2.6.2	Metal Oxide Promoters .....	20
2.6.3	Transition Metal Promoters.....	20
2.6.4	Alkali Metal Promoters .....	21
2.7	Catalyst Deactivation.....	21
2.7.1	Sulphur Poisoning .....	21
2.7.2	Nitrogen Compounds Poisoning .....	21
2.7.3	Alkali and Alkaline Earth Metals Poisoning.....	21
2.7.4	Sintering of Cobalt Crystallites .....	22
2.7.5	Fouling by Carbon Species .....	22
2.8	Flow Chart of Thesis .....	22
2.9	Summary.....	23
2.10	References .....	24
<b>Chapter 3: Review on Characterization.....</b>		<b>27</b>
3.1	X-ray powder diffraction (XRD).....	27
3.2	Scanning Electron Microscope (SEM).....	28
3.3	Fourier Transform Infrared Spectroscopy (FTIR).....	30
3.4	Brunauer-Emmett-Teller Analysis (BET) .....	31
3.5	Thermogravimetric analysis (TGA) .....	34
3.6	Gas Chromatography - Mass Spectrometry (GC-MS) .....	35
3.7	Summary.....	37
3.8	References .....	38

<b>Chapter 4: Methodology</b> .....	<b>39</b>
4.1 Catalyst Preparation.....	39
4.1.1 List of Catalyst Prepared.....	40
4.2 Characterization of Catalyst .....	40
4.3 FTS Process .....	40
4.4 Summary.....	42
4.5 References .....	43
<b>Chapter 5: Results and Discussion</b> .....	<b>44</b>
5.1 Characterization Results.....	44
5.1.1 SEM.....	44
5.1.2 FTIR .....	49
5.1.3 TGA.....	51
5.1.4 BET .....	52
5.1.5 XRD .....	55
5.2 FTS Product Analysis.....	57
5.2.1 HTCo-Cpt-Unp.....	58
5.2.2 HTCo-Cpt-Zr.....	59
5.2.3 Comparison .....	61
5.3 Summary.....	63
5.4 Reference .....	64
<b>Conclusions and Recommendations</b> .....	<b>65</b>
<b>Acknowledgements</b> .....	<b>66</b>
<b>Annex I</b> .....	<b>67</b>
<b>Annex II</b> .....	<b>73</b>

## List of Figures

Figure 1: Global Energy Mix 2015 .....	1
Figure 2: Pakistan Energy Consumption 2015.....	2
Figure 3: FTS Process Diagram .....	6
Figure 4: FTS Reactor Types .....	13
Figure 5: Pictorial demonstration of Braggs Law .....	28
Figure 6: Emissions after Collision of Source Electron with Sample in SEM .....	29
Figure 7: Scanning Electron Microscope Instrumentation.....	29
Figure 8: Working Principle of FTIR.....	30
Figure 9: Types of Pores .....	32
Figure 10: Types of Adsorption Isotherms .....	33
Figure 11: Thermal Gravimetric Analysis Apparatus.....	34
Figure 12: Schematics of GC-MS Analysis System .....	36
Figure 13: Lab scale FT Plant (NUST) .....	41
Figure 14: SEM Micrographs of HTCo-Unp at (a) X10,000 (b) X5000 (c) X500 .....	45
Figure 15: SEM Micrographs of HTCo-Zn at (a) X10,000 (b) X5000 (c) X500 .....	46
Figure 16: SEM Micrographs of HTCo-Zr at (a) X10,000 (b) X5000 (c) X500 .....	47
Figure 17: EDS Spectrum of HTCo-Unp.....	48
Figure 18: EDS Spectrum of HTCo-Zr.....	49
Figure 19: EDS Spectrum of HTCo-Zn .....	49
Figure 20: FTIR Spectra of HTCo-Zn.....	50
Figure 21: FTIR Spectra of HTCo-Zr .....	50
Figure 22: FTIR Spectra of HTCo-Unp .....	51

Figure 23: TGA Graphs of (a) HTCo-Zn (b) HTCo-Zr .....	52
Figure 24: Adsorption Isotherm of HTCo-Unp.....	53
Figure 25: Adsorption Isotherm of HTCo-Zn.....	54
Figure 26: Adsorption Isotherm of HTCo-Zr.....	54
Figure 27: XRD of HTCo-Unp .....	55
Figure 28: XRD of HTCo-Zr .....	56
Figure 29: XRD of HTCo-Zn.....	56
Figure 30: Collected Samples from FTS.....	57
Figure 31: GCMS Analysis of Product From HTCo-Unp .....	58
Figure 32: Chain Length Distribution of HTCo-Unp Product .....	58
Figure 33: GCMS Analysis of Product from HTCo-Zr .....	61
Figure 34: Chain Length Distribution of HTCo-Zr Product .....	61

## List of Tables

Table 1: Major Plants of Synthetic Liquid Fuels .....	17
Table 2: Properties of Reactor Beds Used in FTS .....	22
Table 3: Effect of Active Metal on Nature of Product .....	24
Table 4: Elemental Analysis Obtained from EDS.....	56
Table 5: Surface Area Analysis .....	61
Table 6: List of Compounds in the Product of HTCo-Unp .....	67
Table 7: List of Compounds in the Product of HTCo-Zr .....	68
Table 8: Comparison of FTS Product .....	70

## List of Abbreviations

MTOE	Million Tonnes Oil Equivalent
GHG	Green House Gasses
CTL	Coal to Liquid
DTL	Direct Coal Liquefaction
ICL	Indirect Coal Liquefaction
DME	Dimethyl Ether
BTL	Biomass to Liquid Technology
GTL	Gas to Liquid Technologies
ATR	Auto-thermal Reforming
SMR	Steam Methane Reforming
FTS	Fischer Tropsch Synthesis
RCTL	Recycled Carbon Dioxide to Liquid
BPD	Barrels per Day
FFB	Fixed Fluidized Bed Reactor
NNPC	Nigerian National Petroleum Corporation
HTFT	High Temperature Fischer Tropsch
LTFT	Low Temperature Fischer Tropsch
CFB	Circulating Fluidized Bed Reactor
IUPAC	International Union of Pure and Applied Chemistry
ICTAC	International Confederation for Thermal Analysis and Calorimetry
EI	Electron Ionization
CI	Chemical Ionization
JCPDS	Joint Committee on Powder Diffraction Standards

## List of Publications

- i. Muhammad Arslan, Muhammad Faizan Sharif, Naseem Iqbal, *Promoted Hydrotalcite Based Cobalt Catalyst for Fischer Tropsch Synthesis Application*, 4<sup>th</sup> International Conference on Energy, Environment and Sustainability (EESD 2016), November 01-03, 2016, organized by Mehran University of Engineering and Technology, Jamshoro, Pakistan. (Accepted)\*
  
- ii. Muhammad Faizan Sharif, Muhammad Arslan, Naseem Iqbal, *Hydrotalcite Based Cobalt Catalyst for Synthesis of Hydrocarbons from Syngas*, 4<sup>th</sup> International Conference on Energy, Environment and Sustainability (EESD 2016), November 01-03, 2016, organized by Mehran University of Engineering and Technology, Jamshoro, Pakistan. (Accepted)\*\*

\* Annex I

\* Annex II

# Chapter 1: Introduction

Fossil fuels had been used as a source of energy for a long time. There are three basic forms of fossil fuels known to us: coal, natural gas and oil. These three types were formed more than 350 million years ago from the remains of living organisms hence named fossil fuels. The sudden boost in the energy utilization demanded in the rapid excavation of the fossil fuels resulting in depletion of the resources. Furthermore, the energy extraction by combustion of fossil fuel is causing serious global and local environmental issues. On a global scale, environmental issues arise mainly due to the emission of greenhouse gases (mainly CO<sub>2</sub>) whereas at local level, emissions like SO<sub>x</sub>, NO<sub>x</sub> and particulates can cause serious environment damage and health issues. Therefore, the ever increasing energy demand and environmental degradation are the major driving forces to find new sustainable energy systems.

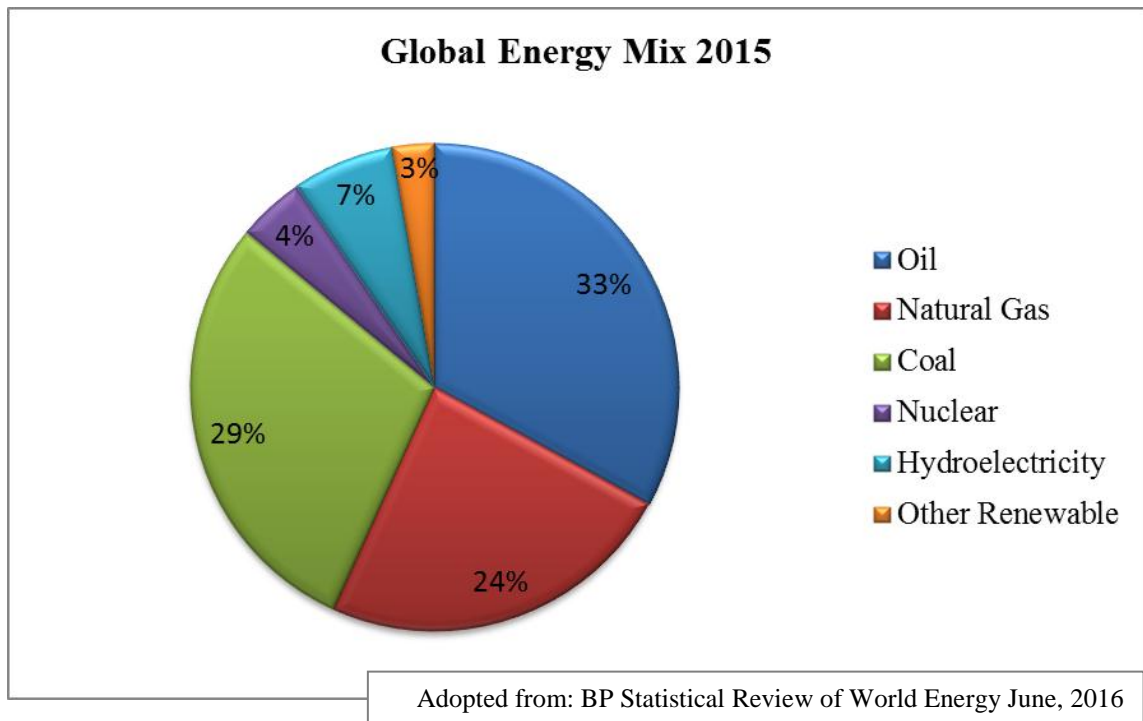


**Figure 1: Global Energy Mix 2015**

The global energy consumption is increasing day by day. In 2015 the net consumption of energy in every sector is more than 13147.3 mtoe. Among this the net oil consumption is 4331.3 mtoe. The net global energy mix is shown in the Figure 1. In

other words we are still fulfilling the 86% of our global energy demand using fossil fuels. Among the vast usage of fossil fuels nearly 33% of the energy consumption is fulfilled by using oil (including biodiesel and synthetic oil).

If we discuss with respect of Pakistan's net consumption of energy, it is more than 78.2 million tones oil equivalent. This energy consumption includes transport, industrial, domestic and every other sector where energy is being consumed. Pakistan is consuming 25.5 mtoe oil which makes up the 32% of Pakistan's net consumption. Apart from that, we are using 39 mtoe natural gas, which is almost 50 % of our net energy consumption. The hydal and renewable collectively makes up for the 11% of our annual consumption. Pakistan's net consumption is shown in the chart below (Figure 2).

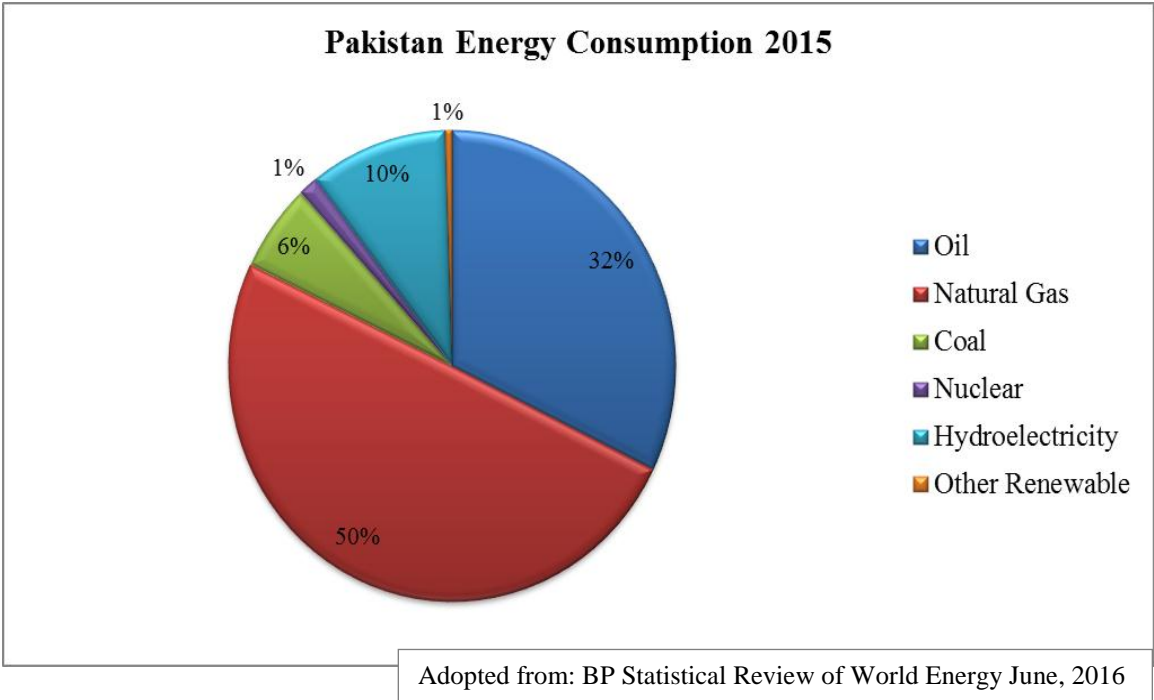


**Figure 2: Pakistan Energy Consumption 2015**

The above trends suggest that we as human beings have a huge dependence on the fossil fuels. On the other hand, we have serious threats of environmental degradation and diminishing resources which is motivating the researchers to move towards finding new resources of fossil fuels to meet the ever rising energy demand. The technological advancements have also helped us in utilizing those resources that were previously considered inaccessible. The main focus of the technology is to improve energy

efficiency, utilize low carbon fuels (like natural gas), carbon capture and storage technologies, utilize abundant resources (such as coal), and the use of renewable energy sources while causing minimum environmental damage at the same time.

## **1.1 Synthetic Fuels**

The massive usage of fossil fuels and their derived compounds in the transport, energy and other sectors are a main cause of greenhouse gas emission (GHG) and on the other hand tie our society to ever shrinking natural fossil reserves. The synthetic fuel is one of such options and can provide an alternative to the natural fossil fuels without damaging environment [1]. The synthetic fuels can be manufactured from various raw material including fossils (like coal and natural gas) and renewable (biomass and atmospheric CO<sub>2</sub>) [2]. The synthetic fuels share the same chemical composition as that of the natural liquid fossil fuels and hence they can easily be incorporated in present fuel infrastructures, like filling stations and power plants, without any unnecessary cost and technical obstacles. There are several methods that can be used for generation of synthetic liquid fuels as mentioned below [3].

### **1.1.1 Coal to Liquids (CTL)**

CTL (coal to liquids) usually indicates the conversion of coal (including lignite) or petroleum coke into liquid fuels also termed as synthetic liquid fuels. Coal to liquid (CTL) is one of the cleaner production techniques because it create fuels that have relatively lower environmental impacts during burning as compared to their precursors and have flexibility in choosing the outputs (more diesel or more naphtha). There are two pathways to achieve liquid fuels from coal. First one is indirect coal liquefaction process (ICL) in which the coal is converted into a gas termed as syngas and further syngas is converted into liquid hydrocarbons. Syngas (a mixture of carbon monoxide and hydrogen) can be used as an input material in different processes:

- Fischer Tropsch Synthesis: Liquid hydrocarbons are synthesized from the reaction of carbon monoxide and hydrogen contained in syngas under certain conditions

- Methanol to Gasoline: Syngas is first converted into methanol under strict conditions of temperature pressure and syngas mixture. In second step, methanol is dehydrated to form dimethyl ether (DME). The third step is to convert DME into light hydrocarbons in the presence of catalyst. In the end, product up-gradation and separation techniques are used to get required fuel fractions.

Second one is direct coal liquefaction method (DCL) in which coal is directly converted into liquid hydrocarbons without any intermediate step. There are two processes that are being used for that purposes.

- Hydrogenation: In this process dry coal is mixed with solvent and catalyst. The mixture is then exposed to hydrogen at temperatures maintained from 400 to 500°C and pressure at 50 to 70 MPa to get liquid hydrocarbons.
- Carbonization Process: Pyrolysis or destructive distillation is used for the production of coal tar, oil and water vapors, syngas and char. The coal tar and oil are further processed to get liquid hydrocarbons.

### **1.1.2 Gas to Liquid (GTL)**

The GTL (gas to liquid) process involves the conversion of (methane) natural gas into syngas (a mixture of carbon monoxide and hydrogen) using processes like autothermal reforming (ATR) and steam methane reforming (SMR). The syngas is then used in the Fischer Tropsch synthesis (FTS) process to convert the syngas into a series of liquid hydrocarbons. The liquid hydrocarbons that are generated form FTS are processed to get fuel that have same burning potential as that of natural fuel. Methane hydrate is another technology that utilizes methane trapped in a cage-like lattice of ice. The methane hydrates can be heated or depressurized, to get natural gas. It is estimated that one meter cube of gas hydrate has a potential to releases 164 meter cube of natural gas. That natural gas can be extracted and used for generation of liquid fuel generations after reforming and Fischer Tropsch synthesis process. The methane extraction from hydrates is still under development but it has the huge potential to unlock the hidden reserves of methane in permafrost (sediments, soil or rock freeze under layer of ice or earth).

### **1.1.3 Biomass to Liquid (BTL)**

BLT (biomass to liquids) is a process which is used to convert needless biomass into variety of high quality liquid fuels offering a significant decline in greenhouse gas emissions. This technology uses a variety of raw material. For example: biomass like woodchips, fallen leaves, corn/sugarcane residue and agricultural or municipal waste. There are two main process that are used in biomass to liquid technology

- Pyrolysis: Pyrolysis is a thermochemical conversion of biomass into liquid fuels. This technique involves the burning of biomass in the absence of oxygen, to accomplish decomposition. Bio-oil and charcoal are two main products of this technology.
- Gasification: Gasification technology involves partial combustion of biomass in limited supply of air to generate synthesis gas (carbon monoxide and hydrogen) which can be subjected to Fischer Tropsch synthesis to generate liquid fuels.

### **1.1.4 Recycled Carbon Dioxide to Liquid (RCTL)**

Recycled carbon monoxide to liquid is one of the rising technologies as it utilizes carbon dioxide for the synthesis of sustainable liquid fuels. The carbon dioxide can be captured either directly from atmosphere or from carbon capture techniques. The main advantage of this technique is that it utilizes carbon dioxide as raw material which is a greenhouse gas and is normally discarded. The advantage of using such fuels in combustion process is that the net carbon dioxide production is zero. The CO<sub>2</sub> emitted during burning process can be recaptured and becomes a part of fuel cycle again. The heat and other process requirements can be achieved using renewable technologies like solar, hydal, wind and tidal energy. Thus this process is considered as the most environmental friendly liquid fuel generation process. There is a lot of research being done for improving the carbon capture and sequestration techniques, making it more economical and safe. The capture of CO<sub>2</sub> from atmosphere is relatively underdeveloped technology and requires extensive effort. Researchers are trying to find new ways to capture carbon dioxide from large point sources (like fossil burning power plants) to utilize it for beneficial purposes.

## 1.2 Fischer Tropsch Synthesis Process

Fischer Tropsch Synthesis is a commercial polymerization process that usually employs a catalyst to convert carbon monoxide and hydrogen into a variety of hydrocarbons having wide range of chain length and functionality [4, 5]. The main process mechanism of the reaction is shown in Figure 3.

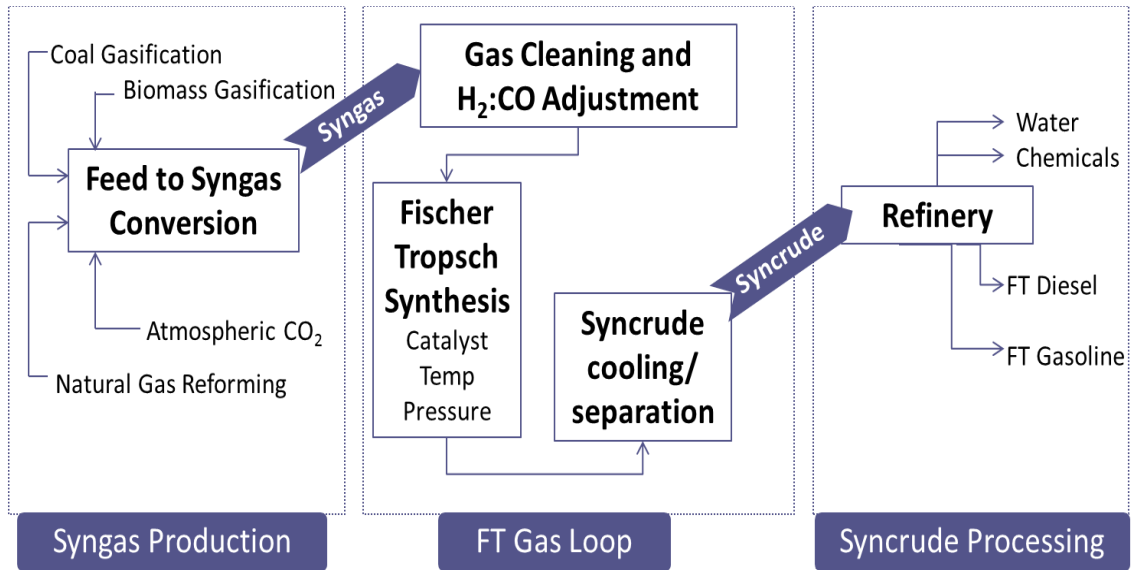


Figure 3: FTS Process Diagram

The usual products of FTS include paraffin, olefins and oxygenates. Depending upon a number of factors like catalyst and reaction conditions either paraffin formation or olefins formation dominates in synthesis process [6]. The product formation of FTS is mainly guided by following reaction



Apart from main reactions there are several side reactions that are being carried out apart from above mentioned reactions. Those side reactions include water-gas shift reaction, carbide formation, alcohols formation, Boudouard reaction, coking and catalyst oxidation and reduction. Water is another important but side product of FTS which can affect the reaction in many ways [7].

### **1.3 Brief History of Fischer Tropsch Synthesis**

Fischer Tropsch Synthesis is a commercial technology that is used mainly for the synthesis of synthetic fuels or hydrocarbons from syngas (mixture of carbon monoxide and hydrogen) [8]. FTS reaction is carried out in the presence of a catalyst at high temperatures and pressure to generate transportation fuel and other petrochemical substitutes [9]. There are two main stages of history and development of Fischer Tropsch synthesis. First stage is discovery and the second one is commercial adaptation of technology.

#### **1.3.1 Development of Technology**

In 1902, Paul Sabatier and J D Senderens produce methane by reacting carbon dioxide and hydrogen at high temperatures and high pressures over finely divided nickel and this reaction is called as Sabatier–Senderens reduction [10]. In 1923 two German scientists Franz Fischer and Hans Tropsch used the work of Sabatier and Senderens to hydrogenate carbon monoxide to produce synthol. Their work is recorded as Fischer Tropsch Synthesis Process and it was used to generate liquid hydrocarbons by reacting syngas over alkalized iron at 400 to 450 °C temperatures and 150 atm pressure [11]. The fuel derived from this process was tested as transportation fuel in a 1922 model NSU motorbike carrying two persons and the results were so good that they opened a way of synthetic fuel in the fuel market [12].

#### **1.3.2 Commercialization**

In 1934 Ruhrchemie AG acquired the patent rights to FT process and started constructing a pilot scale FT synthesis plant in Oberhausen-Holtien, Germany having a capacity of 7240 barrels per annum [13]. By the end of 1935, four commercial scaled FT plants were under construction under the license of Ruhrchemie. They have an annual production capacity of 868,000 barrels of diesel, gasoline, lubricating oil and other petroleum compounds. All these plants use syngas made from reaction of coke and steam. These plants used cobalt based catalyst, developed by Otto Roelen in 1933, and operated at atmospheric (1atm) or medium pressure (15atm). Five more pilot-scale plants were constructed in 1938. At the outbreak of World War II in September 1939,

nine FT plants of Germany had a net production capacity of 5.4 million barrels per annum [14]. During World War II most of the aviation fuel for Luftwaffe was provided by synthetic fuel industry. By 1940, German synthetic fuel production was more than 72,000 BPD (catering for 46% of Germany's war time fuel requirements). By 1943 the synthetic fuel production was doubled and reached 124,000 BPD (57% of total fuel and 92% of aviation fuel supply was done by synthetic fuel). In 1945, due to WW II the Germany was focusing mainly on the new developments and betterment in FTS process [15]. WWII insisted the world to recognize the potential limits natural oil and hence a lot of efforts were directed towards establishment of plants for synthetic fuel generation. Before 1950 a commercial FT plant was established in Brownville Texas, USA using fluidized bed reactors. Apart from that small pilot scale FT plants were established in Louisiana and Kansas, USA in 1950. However the discovery of massive oil reserves in Middle East around 1950 hindered the commercial success of these pilot plants of USA. In 1951 South African based company Sasol started building its first synthetic fuel generation plant based on FTS process. By 1955 the Sasol 1 plant was successfully marketing fuel and other synthetic chemicals using fixed bed Arge reactor technology and iron based catalyst [16]. By 1978 Sasol have over 200,000 BPD production of synthetic fuel.

The 1970s energy crises (Middle East oil embargo) force the US to reconsider the potential of synthetic fuel. Standard oil (now EXXON) started new FT plants and many companies like Mobil, Texaco, Statoil, Sasol and others joined them. In 1970s GULF Oil's research and development center along with Badger Engineering introduced cobalt based catalyst for FT process and process was referred to as "The Gulf-Badger Process". The Chevron purchased the GULF oil in 1980's and sold the "Gulf-Badger Process" to Shell. Shell utilized the knowledge of gulf- badger process in development of a full scale plant running on "Shell Middle Distillate Process" in Bintulu, Malaysia [17]. In 1993 Shell completed its plant having a capacity of 12,500 BPD which was later increased to 15,000BPD in 2000.

In 1987 the South African government started a Moss gas project due to the discovery of natural gas fields. That plant synthesizes liquid fuels from natural gas. The Moss gas

plant is still functional in Mosel Bay, South Africa having a production potential of 47,000 BPD of liquid hydrocarbons from natural gas.

**Table 1: Major Plants of Synthetic Liquid Fuels**

<b>Year</b>	<b>Country</b>	<b>Company</b>	<b>Production Level (bpd)</b>
1936	Germany	Ruhrchemie	2500
1955	South Africa	Sasol	5000
1980	South Africa	Sasol II	20,000
1982	South Africa	Sasol III	20,000
1992	South Africa	Petro SA	20,000
1993	Malaysia	Shell	15,000
2005	Qatar	Sasol, Qatar Petroleum and Chevron	34,000
2007	Nigeria	Sasol Chevron and NNPC	34,000

The spark ignited by Fischer and Tropsch discovery has led the world in further development of this technology. A lot of research is still progress for the betterment of this technology. The FTS technology is working worldwide not only for gas to liquid (GTL) but also for coal to liquid (CTL) and biomass to liquid (BTL) conversions [18]. The 'Table 1' shows some of the major plants working for generation of synthetic liquid fuel by FTS.

## **1.4 Summary**

The energy consumption of the planet earth is rising day by day. Fossil fuels are playing an important role in fulfilling our present energy need. However, the negative environmental impacts and limited resources of fossil fuels forced the researchers to find more reliable and more efficient resources of energy. There are several cleaner energy production techniques that are being used to produce synthetic liquid fuel like CLT, BLT, GLT and RCTL. These resources are not only providing clean fuels but are also helps in utilizing such resources that otherwise are not efficient to use. Fischer Tropsch Synthesis was first introduced by Germany around WWII. It is a process which is used to generate liquid hydrocarbons from various sources like coal, biomass and natural gas. There are several commercial plants that are successfully producing reasonable amount of synthetic fuel using FTS process, in different parts of the world.

## 1.5 References

1. T. Fu, Y. Jiang, J. Lv, and Z. Li, *Fuel Processing Technology*, 2013, 110, 141-149.
2. F. Pöhlmann and A. Jess, *Catalysis Today*, 2015.
3. E. V. Steen, M. Claeys, *Chemical Engineering and Technology*, 2008, 31, 655.
4. Y. T. Tsai, X. Mo, A. Campos, J. G. Goodwin, J. J. Spivey, *Applied Catalysis A: General*, 2011, 396, 91-100.
5. D. O. Uner, *Ind. Eng. Chem. Res.*, 1998, 37, 2239.
6. B. H. Weil, J. C. Lane, *The technology of the Fischer-Tropsch process*; Constable & Co. LTD: London, 1949.
7. W. Ning, N. Koizumi, H. Chang, T. Mochizuki, T. Itoh, M. Yamada, *Applied Catalysis A: General*, 2006, 312, 35.
8. H. Xiong, Y. Zhang, S. Wang, J. Li, *Catalysis Communications*, 2005, 6, 512.
9. B. H. Davis, *Catalysis Today*, 2003, 84, 83.
10. P. Sabatier, J. B. Senderens, *CR Acad. Sci. Paris*, 1902, 134, 514.
11. F. Fischer, H. Tropsch, *Brennst. Chem.* 1923, 4, 276.
12. J. L. Casci, C. M. Lok, M.D. Shannon, *Catalysis Today*, 2009, 145, 38.
13. A. Steynberg, M. Dry, *Studies in Surface Science and Catalysis*, 2004, 152, 69-74.
14. B. H. Davis, M. L. Occelli, *Studies in Surface Science and Catalysis*, 2007, 163, 6-8.
15. B. H. Davis, *Topics in Catalysis*, 2005, 32, 3-4.
16. M. E. Dry, *Chem. Tech.*, 1982, 12, 744.
17. F. Morales, B. M. Weckhuysen, *Catalysis*, 2006, 19, 1.
18. X. Hao, G. Dong, Y. Xu, Y. Li, *Chemical Engineering & Technology*, 2007, 30, 1157-1165.

# Chapter 2: Literature Review

## 2.1 Types of FT Reactions

### 2.1.1 High Temperature Fischer Tropsch Reaction (HTFT)

HTFT reaction operates at temperature around 330°C to 350°C. Fused iron based catalyst is commercially used in HTFT process. The HTFT process yields larger quantities of olefins and gasoline fractions. Fluidized bed reactors are more optimized to be used for HTFT process. Sasol is a CTL-FT plant located in South Africa and it operated using HTFT reaction conditions.

### 2.1.2 Low Temperature Fischer Tropsch Reaction (LTFT)

LTFT are such FT reactions in which reaction temperature is around 230°C to 250°C. Both cobalt or iron based catalyst is commercially used in LTFT process. The LTFT process yields larger quantities linear waxes and diesel fractions. Slurry and fixed bed reactors are more commonly used in LTFT. Shell has an integrated GTL (gas to liquid) plant in Bintulu, Malaysia, which is operating using LTFT process.

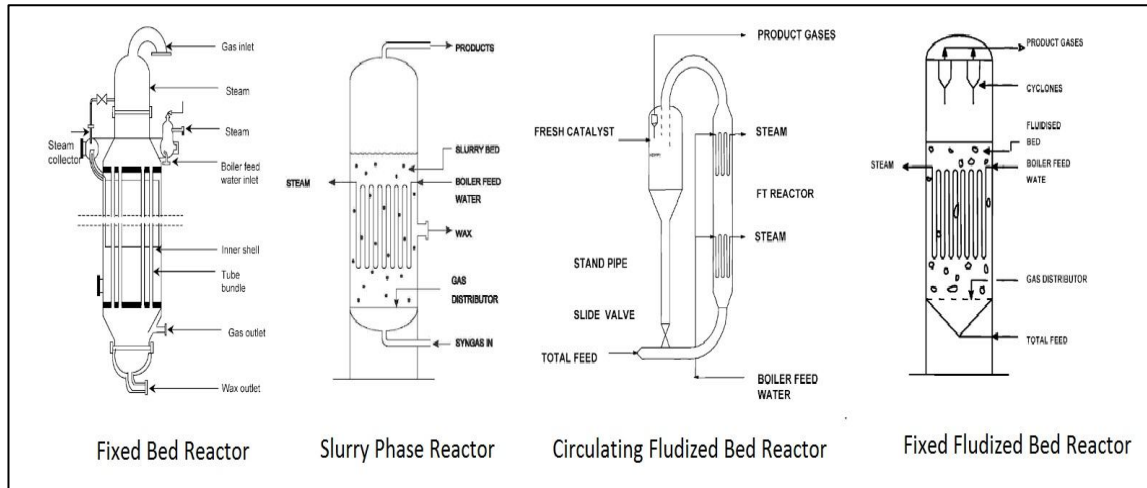
## 2.2 Types of Reactors in FTS

There are three main types of reactors used in FTS: fixed bed reactor, slurry bed reactor and fluidized bed reactor. The reactor type selection requires a comprehensive study of requirement and raw material of plant. However, the main differences in three reactors are mentioned below.

### 2.2.1 Fixed Bed Reactor

The catalyst is loaded in double concentric tubes surrounded by cooling water. The syngas is passed at high flow rates and in turbulent conditions through the reactor. The main function of water is to avoid rapid heat changes and to minimize axial and radial temperature differences. The main disadvantages of using such reactors include high capital cost, difficulty in mechanical upgradation and impossibility of catalyst removal during operation. The tubular fixed bed reactor are simple to operate at wide range of

temperature. Sasol had installed Arge for first time to generate liquid hydrocarbons commercially [2]. Shell is using multi tublar fixed bed reactor in Bintulu plant, Malaysia [3].



Adopted from [1] : Fischer-Tropsch Technology edited by André Steynberg, Mark Dry p 69-74

**Figure 4: FTS Reactor Types**

### 2.2.2 Slurry Phase Reactor

As the name suggests the catalyst is present in slurry phase in this type of reactors. The particle size of catalyst is much smaller as compared to the fixed bed reactor. The catalyst particles are suspended in liquid wax medium. The main advantages of this type of reactor is easy upgradation by increasing size and diameter of the reactor, easy online catalyst removal, high activity per unit mass of catalyst during to smaller particle size and controlled product selectivity at high conversion. The slurry phase reactor gives efficient control of temperature as it works in isothermal conditions [4]. The main disadvantages of using such reactors include high development and difficulty in wax separation. The major oil companies like ExxonMobil and Sasol has installed plant using slurry bed reactor and having a capacity of thousands of barrels per day.

### 2.2.3 Fluidized Bed Reactor

There are two main types of fluidized bed reactors that are used commonly. First one is fixed fluidized bed reactor (FFB) and the second one is circulating fluidized bed reactor (CFB). The fluidized bed reactors are excellent choice in case of high temperature

fischer tropsch synthesis due to production of gasoline and/or light alkenes. The FFB are preferred over CFB due to low capital cost, better temperature regulation and less recycling requirements of catalyst fines in outlet gasses. The only large scale CFB is operational at Mossgas GLT facility at South Africa. The Sasol has widely adopted the fluidized bed reactor technology in their production plans. The following table shows the main differences between different types of reactors used in FTS.

**Table 2: Properties of Reactor Beds Used in FTS**

<b>Feature</b>	<b>Fixed Bed</b>	<b>Slurry Phase</b>	<b>Fluidized Bed</b>
<b>Catalyst Type</b>	Precipitated	Precipitated/Fused	Fused
<b>Catalyst Activity</b> (Standard Catalyst for each type)	Low	Medium	High
<b>Online Catalyst Removal</b>	Not possible	Easy	Possible
<b>Flexibility</b>	Intermediate	High	Medium
<b>Temperature Control</b>	Poor	Good	Good
<b>Reactor Diameter</b>	<0.08m	Large	Large
<b>Conversion % (CO+H<sub>2</sub>)</b>	46	49-79	93
<b>CH<sub>4</sub> Formation</b>	Low	As fixed bed or lower	High
<b>High Selectivity for</b>	Waxes	Waxes and Gasoline	Gasoline & Light

### 2.3 Fischer Tropsch Synthesis Catalyst

The choice of catalyst plays a critical role in Fischer Tropsch Synthesis. There are three main properties of Fischer Tropsch catalyst i.e. catalytic activity, product selectivity and life time of catalyst that are viewed while selecting a catalyst [5]. Fischer Tropsch Synthesis usually works in the presence of a catalyst and the elements of Group VIII (transition metals) of the periodic table are used for that purpose. However, only those catalyst are discussed here which have high carbon monoxide hydrogenation rate to be used commercially. Among transition metals (Group VIII), cobalt (Co), iron (Fe),

ruthenium (Ru) and nickel (Ni) shows high catalytic ability. The choice of catalyst depends upon various parameters like source of syngas, price of active metal and end product needed.

The carbon rich syngas (such as obtained from coal) usually requires iron based catalyst. As iron promotes water gas shift activity so less hydrogen is required and the unwanted carbon monoxide escapes in the form of carbon dioxide [6]. In case of hydrogen rich syngas (as obtained from natural gas) we usually use cobalt or ruthenium based catalyst. This choice is made because both Co and Ru have less water gas activity. Nickel catalyst offers easy dissociation of carbon monoxide and hence promotes too much hydrogenation activity which results in high methane formation. Increase in reaction temperature while using nickel catalyst results in high methane formation and this tendency is also observed in Ru and Co based catalyst. However, Fe based catalyst show low methane formation even at elevated reaction temperatures. The Ru based catalyst can work even at very low temperatures. Even at 150 °C the Ru based catalyst show formation of higher chained compounds [7]. The high price and less availability is a huge hindrance in the application of Ru in FTS commercially.

Cobalt is three folds more active than iron catalyst but its cost is two hundred times more than the iron. Because of low price of iron it is usually loaded (fresh catalyst material) on line in the fluidized bed reactors as compared to its expensive counterparts that are usually employed to maximize the use of active metal. Cobalt based catalyst is preferred usually due to high production of paraffins as they can give high fractions of heavier hydrocarbons producing much less oxygenates. Iron based catalyst is used when olefins are needed in the product because of less hydrogenation of primary formed olefins. Iron based catalyst also produce fractions of aromatics and oxygenates as by products. Iron based catalyst are more sulfur resistant than cobalt. That is why it is recommended to use sulfur free syngas while using cobalt based catalyst. Following given 'Table 3' shows the effect of active metal on the product nature and operating parameters.

**Table 3: Effect of Active Metal on the Nature of Product**

<b>Metal</b>	<b>Pressure (bars)</b>	<b>Temperature (°C)</b>	<b>Nature of Product</b>
Iron (Fe)	10 – 30	200-250	Alkanes, Alkenes, Oxygenates
	10 – 30	300-350	Alkanes, Alkenes, Aromatics, Oxygenates
Cobalt (Co)	5 – 30	170 - 250	Alkanes, Some Alkenes, Oxygenates
Ruthenium (Ru)	100 - 1000	150 - 250	Paraffin Waxes
Nikle (Ni)	10	170 - 210	Alkanes, Some Alkenes

Adopted From [8]: Catalysis in the Refining of Fischer-Tropsch Synchrude By A. D. Klerk. E. Furimsky

## 2.4 Role of Support

Support material provides mechanical strength, increase in surface area, high metal dispersion and high thermal stability. There are several types of support materials which can be used in Fischer Tropsch catalysis. The choice of support material has enormous effect on the activity and efficiency of catalyst [9]. The number of active cobalt metal sites are greatly affected by the choice of the support material after reduction. A strong cobalt and support interaction can greatly increase the dispersion of cobalt metal as occurs in case of alumina and titania but at the same time can decrease the reducibility leading to less active metal sites. However, less interaction can also lead to the decrease in reducibility due to agglomeration of active metal component on the surface during thermal activation treatment. High melting point oxides are mainly used as support. Metal oxides such as titanium oxide [10], aluminium oxide [11] and silicon dioxide are commonly used as support material [12].

Hydrotalcites are hydroxides having manifold layered structure and have the potential to be utilized as support material for catalyst in Fischer Tropsch synthesis. Hydrotalcites are widely used as a support material for cobalt catalysts used for Auto thermal reforming [13], carbon monoxide methanation [14] and CO Hydrogenation [15] etc. Beside this some studies also focused on the effect of change of aluminium and

magnesium molar ratio in hydrotalcite and suggested that lower Mg/Al leads to improved dispersion of cobalt in the crystal [16].

## **2.5 Promoters**

Promoters are third agents that are deliberately added along with active metal to modify the net rate of a catalytic reaction. Promoters can improve the activity, selectivity or stability of a catalyst. There are three main types of promoters depending upon their mode of action. Structural promoters can influence the dispersion of active metal by effecting the active metal – support interaction [17]. The chemical or electronic promoters change the electronic environment of active metal by electronic donation or withdrawal [18]. Some promoters alters the side reaction that can effect the whole reaction. The effects of the promoters on FTS are mentioned below.

### **2.5.1 Stabilizing Support Oxide**

Promoter addition can stabilize active metal component by preventing the reaction of active metal with the support oxide. The promoters can prevent the formation of Co compounds with support such as cobalt titanate, cobalt silicate or cobalt aluminate. Such cobalt compounds are formed due to diffusion of cobalt species in the subsurface areas of the support oxide. It is reported that lanthanum doping on Co/Al<sub>2</sub>O<sub>3</sub> can reduce the formation of cobalt aluminate by forming lanthanum-aluminium compounds, which imparts structural integrity and helps in increasing catalytic activity and selectivity [19].

### **2.5.2 Glueing Effect**

Promoters can act as an interface (oxidic layer) between active metal and support material. This layer formation can lead to increased stability against sintering during reduction. To decrease this effect transition metal promoters are used. If zirconia (ZrO<sub>2</sub>) is used as a promoter in Co/SiO<sub>2</sub> catalyst it can decrease Co-SiO<sub>2</sub> interaction by increasing the Co-Zr interactions which helps in increasing stability of catalyst [20].

### **2.5.3 Increased Active Metal Dispersion**

Promoter addition can increase the dispersion of active metal in the catalyst. If promoters are not present some active metals can form relatively large cobalt crystals.

However when you add promoters small supported active metal particles can be formed. When small groups of active metal having promoters are formed, they can dissociate hydrogen in the neighbourhood and form atomic hydrogen which may spill over active metal by diffusion. This leads to more reduction of active metal oxides to expose more active metal. In other words the effect of this promotion is increase in number of active sites and ultimately more catalytic activity. Cobalt catalyst show such effect when promoted with noble metal promoters like Rhenium (Re) or Platinum (Pt). It is reported that platinum (Pt) promoter can increase the cobalt dispersion in Co/Al<sub>2</sub>O<sub>3</sub> (cobalt supported on aluminium oxide) due to hydrogen spillover effect [21].

#### **2.5.4 Decoration of Active Metal**

When active metal surface is decorated by these promoters they can alter the surface properties of the catalyst and result in improved selectivity and activity. This type of promotion can also increase the tolerance of cobalt catalyst against some poisoning element in uncleaned syngas. Active metal oxide promoters can act in this manner. This type of promotion is beneficial if the deposited metal oxide does not block all the active metal site. The magnesium promoters can increase the carburization process of Fe/Cu/K/SiO<sub>2</sub> catalyst which can decrease reduction temperatures and it also increases the activity of catalyst [22].

#### **2.5.5 Metal Alloying**

Sometimes the deposited promoter forms alloy with the active metal by altering its electronic properties. This alloy formation can be beneficial in terms of increased activity, selectivity and stability depending upon the properties of promoter and alloy formed. Rhenium (Re) promoted cobalt catalyst show increase in the catalytic activity due to formation of bimetallic alloyed particles of rhenium and cobalt [23].

#### **2.5.6 Synergistic Promotion Effect**

Some promoters doesnot effect the main reactions of the process for which the catalyst is used. Instead, they alter the side reactions which ultimately effect the whole dynamics of the reaction. Some transition metal promoters effect the water gas shift reation in the FT reaction. This leads to change the net CO/H<sub>2</sub> ratio in the process which ultimately

affects the end product of the whole FTS process. It is reported that addition of La, Ca promoters can affect the WGS reaction which can increase the catalytic behaviour of Fe/Cu/SiO<sub>2</sub> during FT Reaction [24].

### **2.5.7 Help Against Poisoning**

The cobalt catalysts are susceptible to sulfur poisoning in FTS. The promoters like zinc (Zn) and boron (B) can form stable surface compounds with the sulfur and hence reduce the poisoning effect of sulfur in case of cobalt catalyst. Boron (B) is reported to have retarded the poisoning of Co/TiO<sub>2</sub> by sulfur during FTS [25].

### **2.5.8 Coke Burning during Regeneration**

Coke is formed during FTS process and it is highly unwanted as it blocks the active sites by depositing on the catalyst surface. The coke can be removed by oxidative treatment. The addition of promoter can decrease the temperature of oxidation during regeneration process and ultimately helps in reducing the overall cost of the process. For example, the addition of Gadolinium (Gd) to Co/SiO<sub>2</sub> catalyst can help in carbon deposition at lower temperatures as compared to unpromoted catalyst [26]. Apart from that, some promoter also helps in reducing coke formation.

## **2.6 Promoters Used in FTS**

There is a wide range of compounds that can be used as promoters in FTS. These promoters are divided into four groups depending on the state in which they operate. As we used cobalt-based catalyst in our study, so only those promoters are discussed here which have an effect on the cobalt-based catalyst in FTS.

### **2.6.1 Nobel Metal Promoter**

Among noble metals, Ruthenium (Ru), Rhenium (Re) and Platinum (Pt) are extensively used as promoters in cobalt-based FT reactions. Apart from that, some studies also showed the use of Rh, Pd, osmium (Os) and iridium (Ir) as promoters. Ru plays an important role in both structural and electronic promotion [27]. The addition of Ru promoter leads to a drastic increase in the activity of the catalyst without altering the selectivity [28]. It also helps in the reduction of cobalt by hydrogen spillover from Ru to

Co resulting in an increase of number of reduced cobalt species ultimately increasing the reaction rate. Re acts as structural promoter and increase the reduction of cobalt by hydrogen spillover effect. Some authors suggest that Re does not require a direct contact with cobalt to show its promotion effect so there is no electronic change in the structure of active metal when we use Re [29]. However some authors suggests that Re forms alloy with the cobalt which helps in increase FT activity [30]. Pt is another nobel metal promoter which is considered to act as structural promoter and it can increase the cobalt dispersion [31]. This promoter can also reduce the reduction temperature of the cobalt and also helps in the CO hydrogeneration.

### **2.6.2 Metal Oxide Promoters**

Several metal oxides like MnO, ZrO<sub>2</sub>, ZnO, Al<sub>2</sub>O<sub>3</sub> are added in this group. There are several promotion effects that are attributed to metal oxide promoters but mostly they acts as electronic promoter for Co based FT catalyst. This effect can be explained as the direct interaction of transition metal oxide with the active metal oxides. Zirconium oxide promoters can influence reduction of cobalt oxide phase and higher growth probability of higher alkanes [32]. ZnO promoters can increase cobalt surface and also helps in the increase in C<sub>5+</sub> selectivity [33]. TiO<sub>2</sub> promoter can increase cobalt dispersion and also enhances the activity of catalyst [34].

### **2.6.3 Transition Metal Promoters**

Several metals like chromium (Cr), molybdenum (Mi), tantalum (Ta), vanadium (V) and zirconium (Zr) are included in this group. This group of promoters mostly acts as electronic promoters and can mostly helps in increasing selectivity and activity of catalyst. It is reported that addition of V promoters on cobalt based catalyst can increase catalyst activity and selectivity towards higher hydrocarbons [35]. Similarly the addition of Cr as promoter can shift the selectivity from methane to higher and more olefinic hydrocarbons [36]. This promoter can also reduces the hydrogenation rate during FT process hence can be beneficial in carbon rich syngas. Another study states that addition of Cr (Chromium), Ta (Tantalum), Mo (Molybdenum) and Mn (Manganese) promoters can enhance the catalyst selectivity towards C<sub>5+</sub> compounds and decreases methane formation [37].

#### **2.6.4 Alkali Metal Promoters**

Alkali metals like Na, K, are used as promoters in various cobalt catalysed FT reactions. It is reported that the addition of small quantity of  $K^+$  can increase the selectivity of  $C_{5+}$  hydrocarbons, decreased methane formation and avoid immediate catalyst deactivation. Similarly, the addition of  $Na^+$  enhances the activity and stability of catalyst in FTS [38]. Some alkali metal promoters like  $Cs^+$  (Caesium ion),  $Rb^+$  (Rubidium ion) and  $Li^+$  (Lithium ion) act as poisons for catalyst used in FTS and also decrease CO conversions.

### **2.7 Catalyst Deactivation**

There are several different causes that can cause possible deactivation of FTS catalyst. The main causes include poisoning due to undesired components of syngas, sintering effects and effects of carbon species [39]. These effects are mentioned below in detail.

#### **2.7.1 Sulphur Poisoning**

Sulphur acts as poison for the FT catalyst by adsorbing on the active metal sites and possibly cause the electronic modification of the surrounding atoms. It is reported that one sulfur atom adsorption can effect two cobalt atoms. Sulfur is usually present in biomass derived syngas and in corrosion resistant chemicals added.

#### **2.7.2 Nitrogen Compounds Poisoning**

Nitrogen compounds have an immediate effect on the cobalt activity. It has been reported that a direct relationship has been found in the nitrogen compound concentration and the deactivation of the catalyst. However the deactivation can be reversed by insitu hydrogen treatment. The nitrogenous compounds are added in the syngas during the downstream syngas generation process.

#### **2.7.3 Alkali and Alkaline Earth Metals Poisoning**

The alkali metal promoters have a positive effect on the chain growth probability and catalyst activity but if their concentration is very high this can lead to the less activity. It has been reported that alkali metal does not trigger operational deactivation but the reduces activity when added in surplus amount.

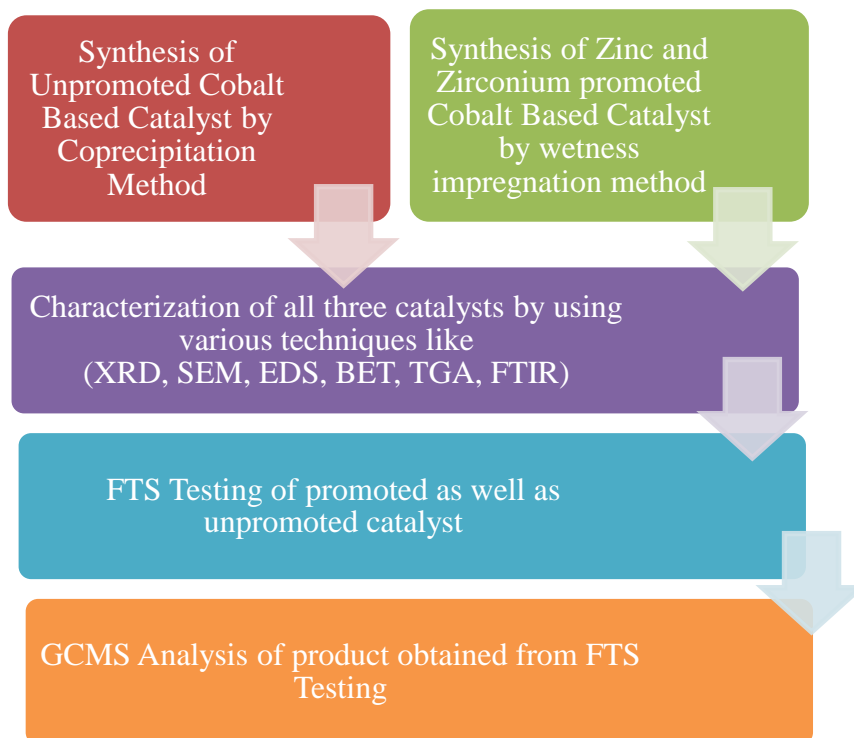
#### 2.7.4 Sintering of Cobalt Crystallites

Sintering effects the active surface area due to collapse of pores at high temperature conditions. Water vapours, high temperature and the nature of support material are the main factors that directly effect the sintering process. Sintering is an irreversible process however reduction-oxidation-reduction sequence at certain conditions can regain the cobalt dispersion.

#### 2.7.5 Fouling by Carbon Species

Carbon species may form as a by product and seriously effect the FTS process. They can either get deposited on the active metal site or react with the cobalt species. The cobalt crystallites are more resistant to carbide formation as compared to iron based FT catalyst

### 2.8 Flow Chart of Thesis



## **2.9 Summary**

There are two main types of Fischer Tropsch Synthesis (FTS) process; High Temperature Fischer Tropsch Process and Low Temperature Fischer Tropsch Process. The FTS process is carried out in a reactor, under certain conditions of temperature and pressure, in the presence of catalyst. There are four basic types of reactors that we use in FTS process: Fixed bed reactor, circulating fluidized bed reactor, fixed fluidized bed reactor and slurry bed reactor. The reaction conditions and nature of product required decides the catalyst that is used in FTS process. Promoters are used to enhance the activity, selectivity and stability of catalyst. Promoters can alter the properties of catalyst to better the whole dynamics of the reaction. Choice of promoter is made based on the type of promotion effect that is required in the reaction. There are several factors that can deactivate a catalyst and these factors can be controlled by using promoters.

## 2.10 References

1. A. Steynberg, M. Dry, *Studies in Surface Science and Catalysis*, 2004, 152, 69-74.
2. M. E. Dry, *Applied Catalysis A: General*, 1996, 138, 319.
3. S. T. Sie, *Reviews in Chemical Engineering*, 1998, 14, 109.
4. B. Jager, R. C. Kelfkens, A. P. Steynberg, *A Slurry Bed Reactor for Low Temperature Fischer-Tropsch*; Elsevier Science, 1994.
5. A. Y. Khodakov, W. Chu, and P. Fongarland, *Chemical Reviews*, 2007, 107, 1692-1744.
6. M. Luo, H. Hamdeh, B. H. Davis, *Catalysis Today*, 2009, 140, 127.
7. F. Morales, B. M. Weckhuysen, *Catalysis*, 2006, 19, 1.
8. A. D. Klerk, E. Furimsky, *Catalysis in the Refining of Fischer-Tropsch Syncrude*, 2010, 13.
9. E. Iglesia, *Applied Catalysis A: General*, 1997, 161, 59-78.
10. A. Khodakov, A. Griboval-Constant, R. Bechara, V. L. Zholobenko, *Journal of Catalysis*, 2002, 206, 230.
11. D. Schanke, A. M. Hillmen, E. Bergene, K. Kinnari, E. Rytter, E. Adnanes, A. Holmen, *Energy and Fuels*, 1996, 10, 867.
12. M. Kraun, M. Baerns, *Applied Catalysis A: General*, 1999, 186, 189.
13. K. Takehira, T. Shishido, P. Wang, T. Kosaka, K. Takaki, *Journal of Catalysis*, 2004, 221, 43-54.
14. L. He, Q. Lin, Y. Liu, Y. Huang, *Journal of Energy Chemistry*, 2014, 23, 587-592.
15. A. Di Fronzo, C. Pirola, A. Comazzi, F. Galli, C. Bianchi, A. Di Michele, A. Vivani, R. Nocchetti, M. Bastianini, D. C. Boffito, *Fuel*, 2014, 119, 62-69.
16. A. Forgionny, J. Fierro, F. Mondragón, and A. Moreno, *Topics in Catalysis*, 2016, 59, 230-240.
17. B. Cornilis, W. A. Herrmann, R. Schlogl, C. H. Wong, *Catalysis from A to Z, A Concise encyclopedia*, Wiley-VCH, Weinheim, 2000.
18. E. Iglesia, S. L. Soed, R. A. Fiato, *Journal of Catalysis*, 1993, 143, 345.
19. M. R. Hemmati, M. Kazemeini, J. Zarkesh, F. Khorasheh, *Journal of the Taiwan Institute of Chemical Engineers*, 2012, 43, 704-710.

20. G.R. Moradi, M. M. Basir, A. Taeb, A. Kiennemann, *Catalysis Communications*, 2003, 4, 27–32.
21. G. Jacobs, Y. Ji, B. H. Davis, D. Cronauer, A. J. Kropf, C. L. Marshall, *Applied Catalysis A: General*, 2007, 333, 177–191.
22. J. Yang, Y. Sun, Y. Tang, Y. Liu, H. Wang, L. Tian, H. Wang, Zhixin Zhang, H. Xiang, Y. Li, *Journal of Molecular Catalysis A: Chemical*, 2006, 245, 26–36.
23. M. Rønning, D. G. Nicholson, A. Holmen, *Catalysis Letters*, 2001, 72, 3-4.
24. A. N. Pour, S. M. K. Shahri, H. R. Bozorgzadeh, Y. Zamani, A. Tavasoli, M. A. Marvast, *Applied Catalysis A: General*, 2008, 348, 201–208.
25. J. Li, N. J. Coville, *Applied Catalysis A: General*, 2001, 208, 177–184.
26. J. Huang, W. Qian, H. Zhang, W. Ying, *International Journal of Chemical, Molecular, Nuclear, Materials and Metallurgical Engineering*, 2016, 10, 8.
27. D. Schanke, A. M. Hilmen, E. Bergene K. Kinnari, E. Rytter, E. Adnanes, A. Holmen, *Catalysis Letters*, 1995, 34, 269.
28. L. A. Bruce, M. Hoang, A. E. Huges, T. W. Turney, *Applied Catalysis A: General*, 1993, 100, 51-67.
29. A. M. Hilmen, D. Schanke, A. Holmen, *Catalysis Letters*, 1996, 38, 143.
30. D. Bazin, L. Borko Z. Koppány, I. Kovacs, G. Stefler, L.I. Sajo, Z. Schay, L. Guzzi, *Catalysis Letters*, 2002, 84, 169.
31. D. Schanke, S. Vada, E.A. Blekkan, A. M. Hilmen, A. Hoff, A. Holmen, *Journal of Catalysis*, 1995, 156, 85.
32. P. Kangvansura, H. Schulz, A. Suramitr, Y. Poo-arporn P. Viravathana, A. Worayingyong, *Materials Science and Engineering*, 2014, 190, 82–89.
33. R. P. Marin, S. A. Kondrat T. E. Davies, D. J. Morgan D. I. Enache G. B. Combes, S. H. Taylor, J. K. Bartleya, G. J. Hutchings, *Catalysis Science & Technology*, 2014, 4, 1970.
34. C. H. Bartholomew, R. C. Reuel, *Industrial & Engineering Chemistry Product Research and Development*, 1985, 24, 56.
35. A. G. Ruiz, A. S. Escribano, I. R. Ramos, *Applied Catalysis A: General*, 1994, 120, 71.
36. S. Bessell, *Studies in Surface Science and Catalysis*, 1994, 81, 479.

37. E. Kikuchi, R. Sorita, H. Takahashi, T. Matsuda, *Applied Catalysis A: General*, 1999, 186, 121.
38. M. K. Gnanamani, G. Jacobs, W. D. Shafer, D. E. Sparks, S. Hopps, G. A. Thomas, B. H. Davis, *Topics in Catalysis*, 2014, 57, 612–618.
39. N. E. Tsakoumis, M. Rønning, O. Borg, E. Rytter, A. Holmen, *Catalysis Today*, 2010, 154, 162–182.

# Chapter 3: Review on Characterization

Several characterization techniques are used for the qualitative analysis of the sample of catalyst prepared. The basic working conditions and the principle of the techniques are mentioned below

## 3.1 X-ray powder diffraction (XRD)

X-ray powder diffraction (XRD) is a commonly used analytical method primarily used for identification of phase of a crystalline material and information on unit cell dimensions. X-rays are electromagnetic waves of shorter wavelength having energy between 200 eV to 1 MeV [1]. X-ray Diffraction method uses the constructive interference of crystalline sample with monochromatic X-rays. Bragg's law is the main operating principle that is used in this technique. When radiation, having wavelength similar to atomic spacings of the crystal, is scattered by the atoms of a crystalline solid, and experiences constructive interference. Consider X-rays strikes a crystalline solid having interplanar distance 'd'. Some of the X-rays got scattered from the crystal atoms. If the scattered waves interfere constructively, they stay in phase as the variation between the path lengths of the two waves is equivalent to an integer multiple of the wavelength. The variation in the path length of two waves experiencing interference is given by  $2d\sin\theta$ , as  $\theta$  is the scattering angle. The Bragg's law describes the relation of  $\theta$  with wavelength and interplaner spacing 'd' for the constructive interference to be at its greatest by following equation

$$2d\sin\theta = n\lambda$$

The material sample is finely pulverized and average bulk composition is defined using this technique. The high speed electrons are generated from filament, which strikes a metal plate (Cu) to give X-Rays. The generated x-rays are allowed to pass through a collimator which absorbs all X-rays except a narrow beam. Filters or crystal monochromators are used for monochromatization of X-rays. After that the X-rays fall on sample and the scattered X-rays are recorded by a photographic film or counter

methods. The result obtained from this technique are called diffractogram. The diffractogram can be obtained in either intensity vs transmittance or reflectivity format.

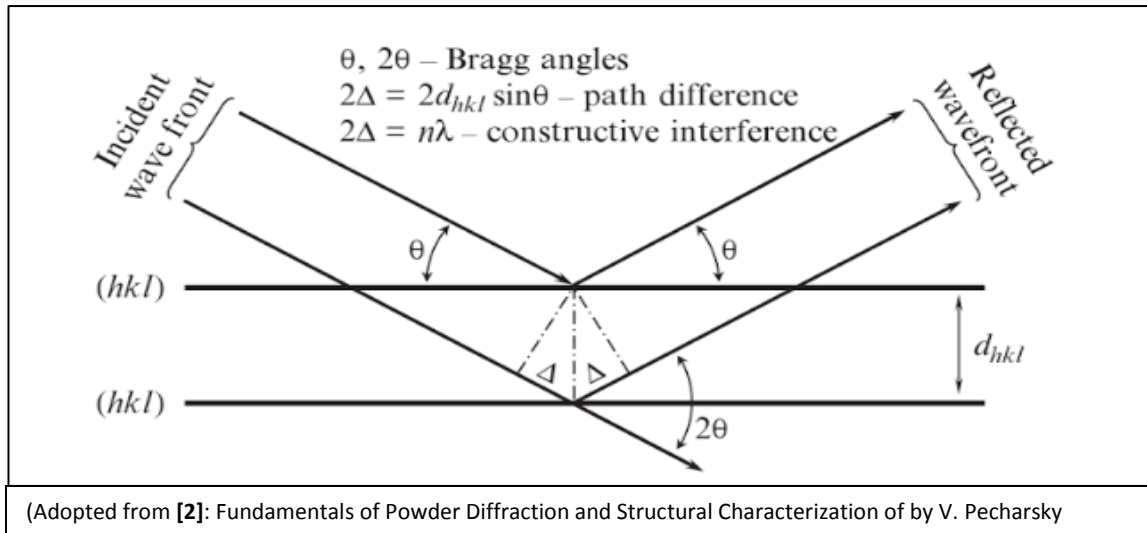


**Figure 5: Pictorial demonstration of Bragg's Law**

### 3.2 Scanning Electron Microscope (SEM)

Scanning Electron Microscope is a technique that informs about the structural properties of the crystal. The SEM coupled with EDS is most commonly used technique because it can give more information about the sample. EDS stands for energy-dispersive X-ray spectroscopy also denoted as (EDX, or XEDS). It is also known as energy dispersive X-ray analysis (EDXA) or energy dispersive X-ray microanalysis (EDXMA). SEM is an analytical technique which can be used for the elemental analysis of a sample to determine its chemical composition. This technique used a focused beam of high energy electrons. The electron when interacts with the sample surface it produces signals carrying information about the topography, chemical structure and orientation of the material making up the sample. The beam of electron is generated by electron gun and it is directed on the specimen with the help of several lenses and a vacuum chamber. The beam when falls on the sample it produces primary electron, secondary electron, auger electrons and x-rays [3]. 'Figure 6' shows all possible emissions when source electron collides with the sample.

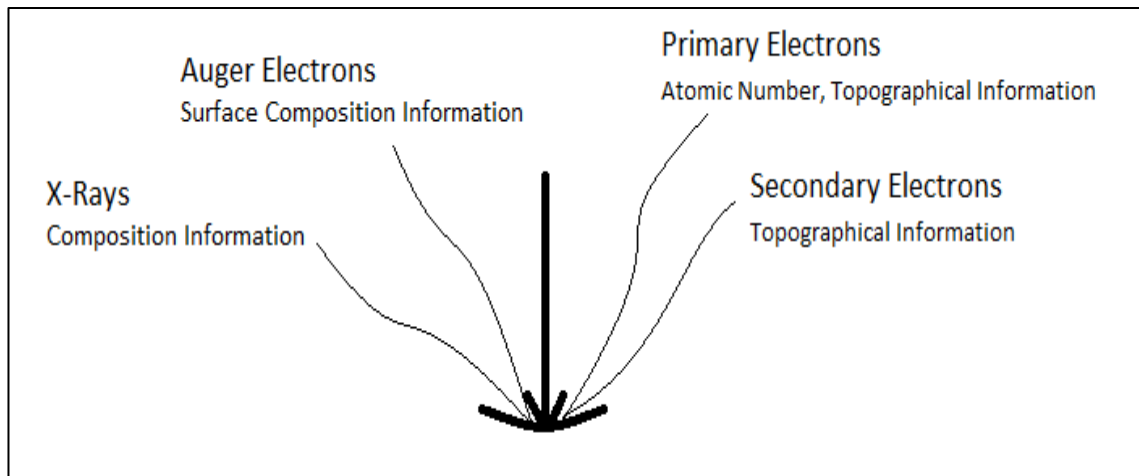
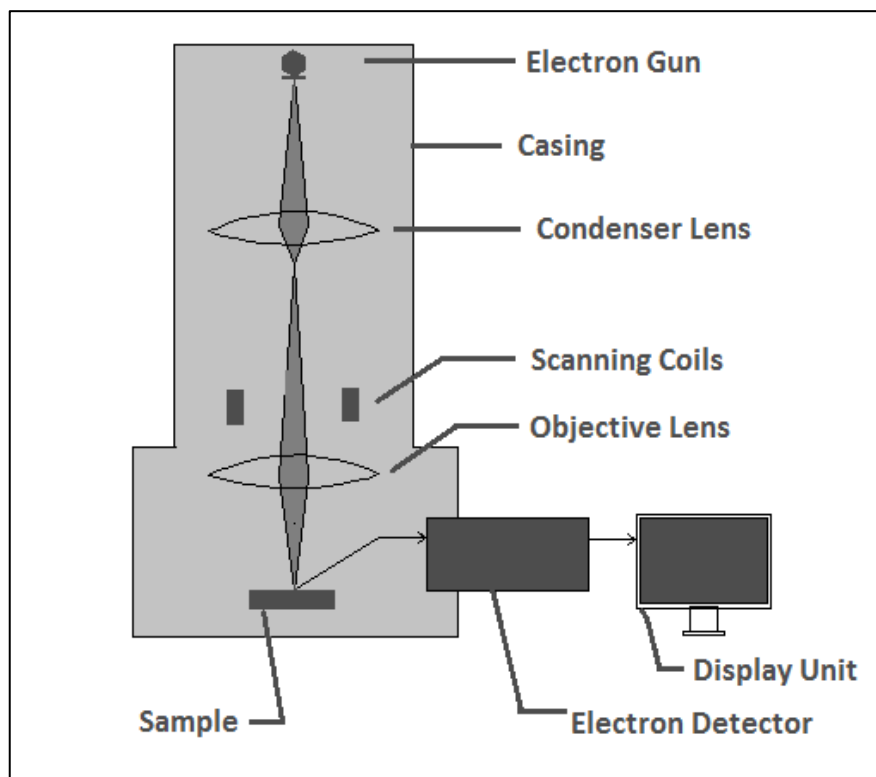


**Figure 6: Possible Emissions after Collision of Source Electron with Sample in SEM**

The secondary electron are mainly used in the SEM analysis. The electron recorder is used to record the imprints of these electrons. This information is recorded on the screen as micrographs of the specimen. ‘Figure 7’ shows the basic working principle of SEM coupled with EDS.



Adopted from [5]: Scanning Electron Microscopy: Physics of Image Formation and Microanalysis by L. Reimer

**Figure 7: Scanning Electron Microscope Instrumentation**

The SEM coupled with EDS is most commonly used technique because it can give more information about the sample. The EDS uses the back scattered electrons and x-rays generated by the sample and uses them to perform an elemental analysis of the sample. The back scattered electrons correspond with the atomic number of the elements in the sample [4]. Hence EDS coupled SEM gives a precise qualitative as well as quantitative analysis of the sample at the elemental level.

### 3.3 Fourier Transform Infrared Spectroscopy (FTIR)

Fourier Transform Infrared Spectroscopy (FTIR) is an analytical technique, commonly used to obtain an infrared spectrum of a gas, solid or liquid samples due to absorption or emission. This technology can also be used to study the purity of the sample by analyzing the unique absorption band of each sample [6]. The working of this machine is quite simple as shown in 'Figure 8'.

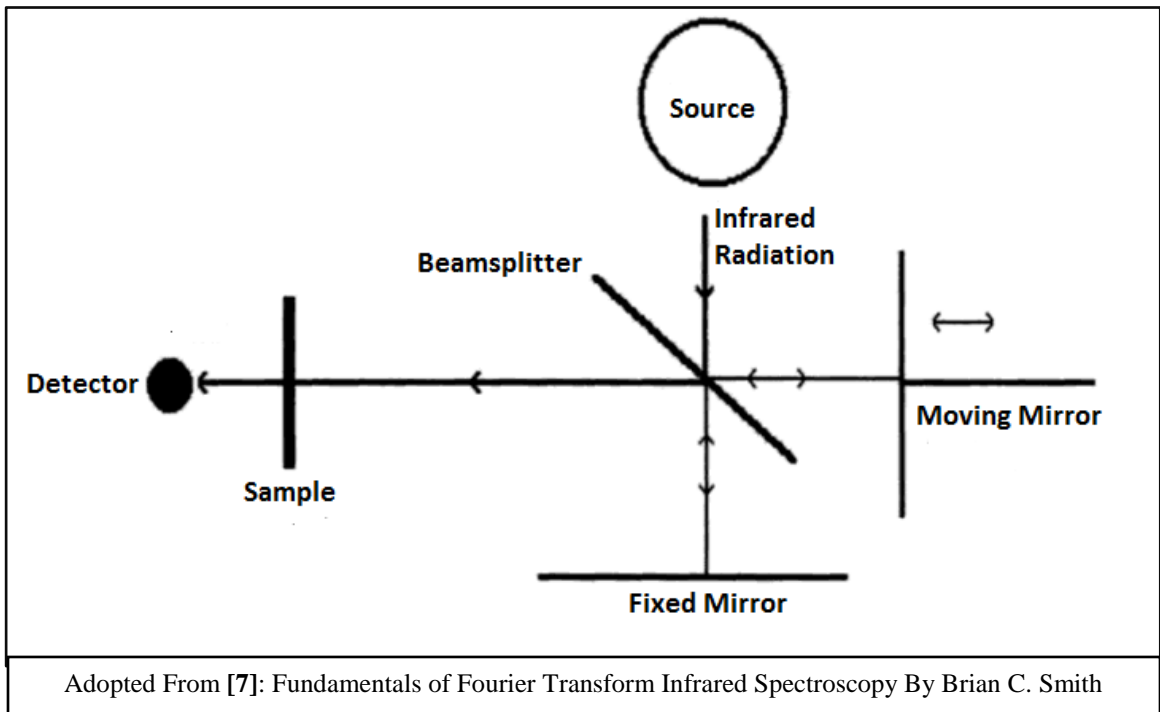


**Figure 8: Working Principle of FTIR**

A source is used to generate a broad range of radiations in the infrared region which enters the interferometer. In the interferometer, a beam splitter divides the beam into two similar

radiations. One half is sent to a fixed mirror and other is sent towards moving mirror. The radiations after reflection from mirrors are reunited by beam splitter and the interference occurs either constructive or destructive. The modulated radiations from interferometer strike the sample. A detector detects the radiations coming out of sample chamber having all the information about the sample properties and a digital signal is transmitted to the computer. The detector reports the energy versus time variations for all the wavelengths instantaneously. Intensity versus time formatted graphs are not reported generally. Computer software is used to convert intensity versus time graphs into wavelength versus transmittance or absorbance graphs.

### **3.4 Brunauer-Emmett-Teller Analysis (BET)**

BET is named after the first names of its inventors Brunauer-Emmett-Teller. This technique is used for the external surface area evaluation and pore area measurements yielding important information about the effects of porosity and particle size on the material properties [8]. The heterogeneous catalysts have one or more group of pores whose size and volume are influenced by the method of preparation of catalyst. The pores are differentiated in different classes depending on their size.

- Micropores : Size < 2nm
- Mesopores : 2nm < Size < 50nm
- Macropores : Size > 50nm

Pores can further be divided in different categories depending upon their geometry. Pores can be cylindrical or slit shaped or more commonly irregular shaped. The irregular shaped pores can be bottleneck shaped or funnel shaped. Apart from that the pores can be divided into various categories depending upon their connectivity. Some pores are connected with each other to form a porous network whereas some pores are 'closed' which means they have no access from any sides. Some pores are 'through' which means they can be accessed from two or more sides where some pores are termed as 'open pores' because they can be accessed from only one side. These attributes of pores can greatly affect the catalytic behavior of the porous solid. Sometimes these pores can

greatly enhance the activity of a catalyst whereas sometimes their limitations of coke deposition and diffusion can greatly hinder the catalytic activity of the catalyst.

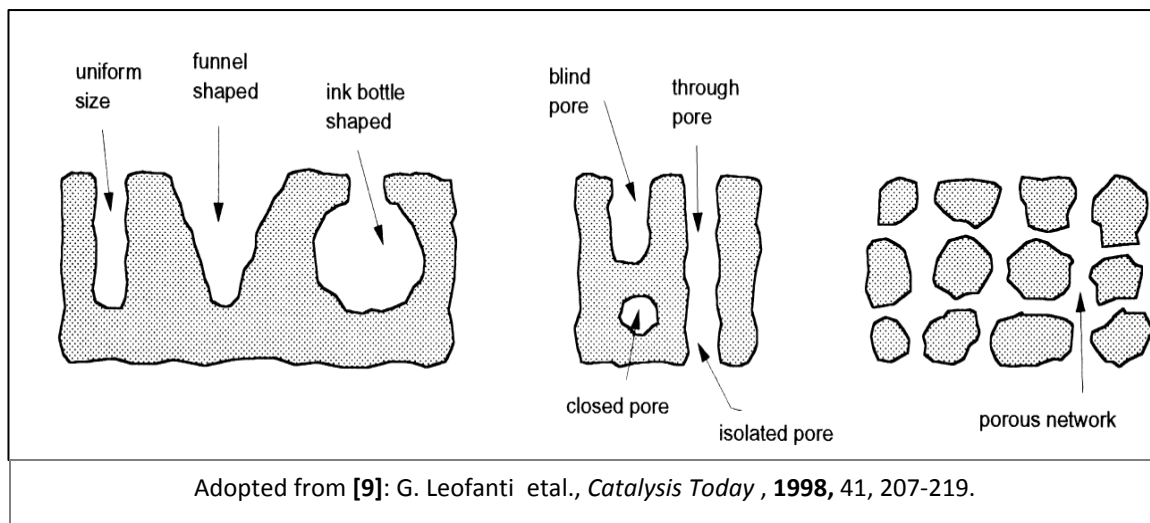


**Figure 9: Types of Pores**

Nitrogen Adsorption at 77K is the most widely used technique for surface area analysis and characterization of porous texture. This analysis method uses the nitrogen multilayer physical adsorption studied against change of pressure. First step is the determination of adsorption isotherm; nitrogen adsorbed volume against its relative pressure. The adsorption isotherm depends upon the porous texture of the solid. IUPAC suggests that there are six types of adsorption curves but only six are mentioned here because they are more commonly found in the catalysts used for FTS.

- **TYPE I (Microporous Solids):** There is strong interaction between pore walls and the adsorbate because of which adsorption takes place at very low relative pressure. First the pores are filled at low relative pressures without capillary condensation. Once the pores got filled the adsorption is continued at external surface as in case of mesoporous solid.
- **TYPE II (Macroporous Solids):** At low pressure adsorption takes place due to formation of monolayer whereas at higher relative pressures multilayer adsorption takes place. The monolayer and multilayer formation processes always overlaps.

- TYPE IV (Mesoporous Solid): At low relative pressures monolayer formation takes place. At higher relative pressures multilayer formation occurs until a condensation pressure is achieved which gives a sharp rise in adsorbed volume.
- TYPE VI (Ultramicroporous Solids): The relative pressure at which adsorption occurs depends on the adsorbate-surface interaction. If the solid is energetically uniform the whole process takes place at a well-defined pressure. Whereas if the surface have energetically non uniform groups, a stepped isotherm is achieved.

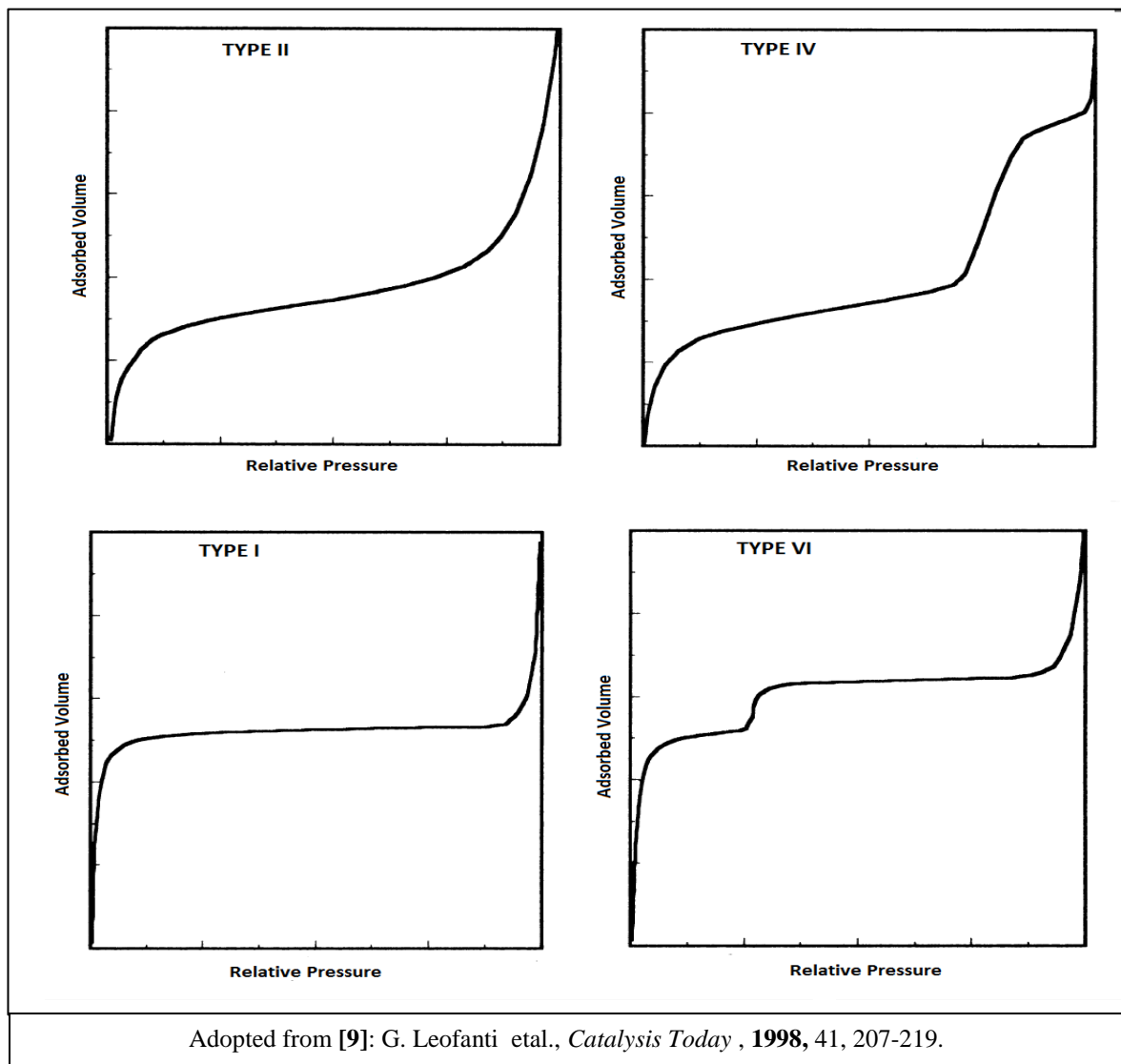


**Figure 10: Types of Adsorption Isotherms**

### 3.5 Thermogravimetric analysis (TGA)

Thermal analysis is a technique used to study the changes in weight of a substance when subjected to the temperature change. When any material is subjected to heating under controlled environment it undergoes several changes due to reduction, oxidation, or decomposition. Such weight changes can be used to study the thermal stability and kinetics of any sample under temperature [10]. The basic apparatus used for thermal analysis is mentioned in the 'Figure 11'.

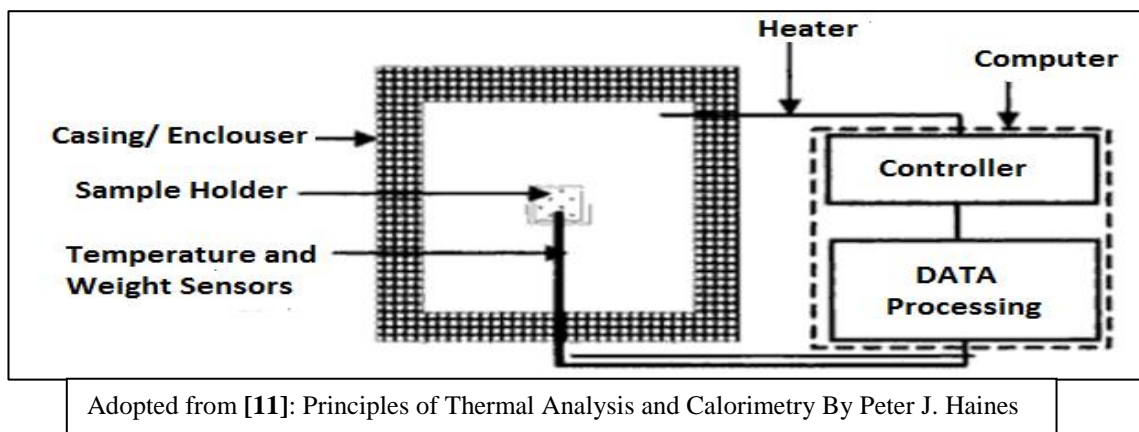


**Figure 11: Thermal Gravimetric Analysis Apparatus**

Thermo-gravimetric analysis also termed as thermal gravimetric analysis (TGA) is a type of thermal analysis. It is defined by ICTAC (International Confederation for Thermal Analysis and Calorimetry) as a technique in which the change in the mass of a sample is observed as it is subjected to a controlled temperature programme. In this technique we observe the variations in physical or chemical properties of sample by with constant heating rate, or as a function of time (with constant temperature and/or constant mass loss). There are three types of thermal gravimetric analysis used as mentioned below

- Dynamic TGA: Weight change is examined while temperature rise is linear with time.
- Static TGA: Weight change is recorded against time while providing constant temperature.

- Quasistatic TGA: A series of temperature increase is provided and sample weight remains constant for each series.

The dynamic thermal gravimetric analysis is performed in this study. The constant rise in temperature is provided and the weight changes are studied. The apparatus used for analysis is Mettler TGA/SDTA 851e.

### **3.6 Gas Chromatography - Mass Spectrometry (GC-MS)**

GC-MS was performed to analyse the product obtained from FTS testing. GC-MS analysis as the name suggests, is a combination of two analysis techniques in sequence. Gas chromatography (GC) is used to separate multiple components of the sample whereas Mass spectrometer is used to analyze each component individually. GC separates the component of a sample based on their volatility. The sample is introduced into the GC injection port which is heated to around 300 °C to keep the sample in vaporized state. A carrier gas (usually helium) is used to move the sample in the chromatographic column. The column is 30 meter thin tube having inner coating (stationary phase). The column is placed inside a specialized oven, which can operate at 40 to 400 °C temperature range. The sample moves across the column and the components of sample are separated due to their relative interaction with the coating of the column (stationary phase) and the carrier gas (mobile phase).

The sample exiting the GC column, enters the ionization chamber of the MS. Two types of ionization techniques are used. In electron ionization (EI) electron beam is bombarded to the sample molecules to remove an electron, hence making it positively charged molecular ion or sometimes fragments of positively charged ions. Second method used for ionization is CI (chemical Ionization). CI ionizes methane first to generate a positive ion which further ionizes the sample molecule. The next part is (filter) mass analyzer which separates the charged ions based on various mass related properties. There are several types of analyzers that are being used commercially: quadrupoles, ion traps, time of flight to name a few. After separation of charged species in filters, a detector is placed which counts the number of ions with specific mass. When single charged particle collides with the surface of detector it generates multiple

electrons depending upon its mass. Each electron collides with secondary surface to create more electrons. Hence multiple electrons collisions with multiple surfaces give a cascade of electrons emitting the final surface. The output of the detector is amplified and sent to a computer to be displayed in the form of peaks called 'mass spectrum'. The height of the peak increases with number of counts detected with one particular mass. Figure 13 shows basic components of GC-MS analysis systems

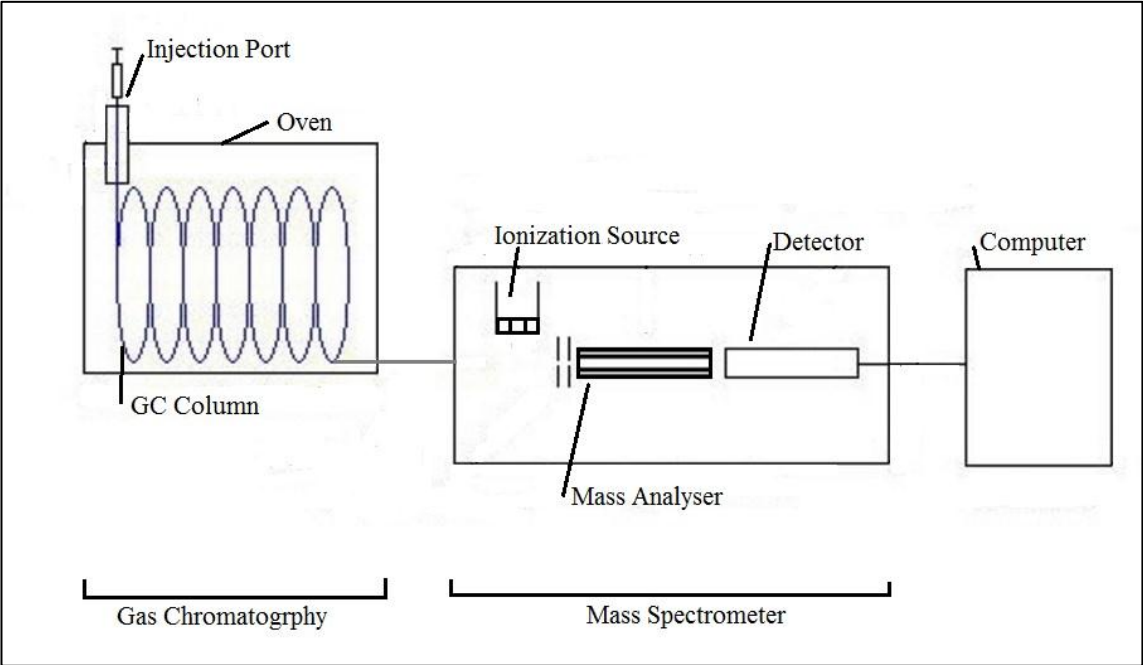


**Figure 12: Schematics of GC-MS Analysis System**

### **3.7 Summary**

Several characterization techniques are used for the qualitative as well as quantitative analysis of the catalysts prepared. These techniques give information about various aspects of the sample. Hence, brief introduction about basic working principle of each technique is given in this chapter. XRD is a technique commonly used for identification of phase of a crystalline material and to get information on unit cell dimensions. SEM is used for topographical imaging of the samples whereas EDS is performed for elemental analysis. The surface area analysis is performed using BET analysis in which nitrogen physisorption is used. Those materials that operate at high temperatures require thermal stability tests which is performed using thermogravimetric analysis (TGA). FTIR is a spectroscopic technique which is used for determining unknown components of a sample as well as to check the purity of the solid sample. The GC-MS is another technique that is used to analyse the various components in the liquid and gaseous product of FTS process.

### 3.8 References

1. C. Suryanarayana, M. G. Norton, X-ray Diffraction: A Practical Approach, Plenum , New York, 1998.
2. V. K. Pecharsky, P. Y. Zavalij, Fundamentals of Powder Diffraction and Structural Characterization of Materials, Kluwer Academic Publishers, London, 2009.
3. L. Reimer, Scanning Electron Microscopy: Physics of Image Formation and Microanalysis, Second Ed., Springer Newyork, 1998.
4. A. Khursheed, Scanning Electron Microscope Optics and Spectrometers , World Scientific Publications, Singapore, 2011.
5. J. Goldstein, D. E. Newbury, P. Echlin, D. C. Joy, A. D. Romig Jr., C. E. Lyman, C. Fiori, E. Lifshin, Scanning Electron Microscopy and X-Ray Microanalysis: A Text for Biologists, Material Scientists and Geologists, Second Ed., Plenum , New York, 1992.
6. P. R. Griffiths, J. A. De Haseth, Fourier Transform Infrared Spectrometry, John Wiley and Sons Inc., USA, 2007.
7. B. C. Smith, Fundamentals of Fourier Transform Infrared Spectroscopy, Second Ed., CRC Press, USA, 2001.
8. S. Lowell, J. E. Shields, M. A. Thomas, M. Thommes, Characterization of Porous Solids and Powders: Surface Area, Pore Size and Density, Kluwer Academic Publishers, London, 2009.
9. G. Leofanti, M. Padovan, G. Tozzola, B. Venturelli, Catalysis Today , 1998, 41, 207-219.
10. P. Gabbott, Principles and Applications of Thermal Analysis, Blackwell Publications, UK, 2011.
11. P. J. Haines, Principles of Thermal Analysis and Calorimetry, The Royal Society of Chemistry, UK, 2002.

# Chapter 4: Methodology

There are three main catalyst synthesized in this study using co-precipitation method. The cobalt is used as active metal of the catalyst supported on aluminium-magnesium hydrotalcite. First the unpromoted catalyst is prepared by coprecipitation method and then both zinc and zirconium promoters were added by using wetness impregnation method. The prepared catalyst are characterized by using various analytical techniques to determine their properties. In the end the catalysts were tested in a fixed bed reactor for Fischer Tropsch Synthesis. The product collected from FTS was analysed by using GC-MS. The detailed description of each step is mentioned below.

## 4.1 Catalyst Preparation

The first unpromoted catalyst (HTCo-Unp) is prepared by coprecipitation method. First precipitating agent solution was prepared by adding 8.99g sodium hydroxide pellets [NaOH] and 1.49g sodium carbonate [Na<sub>2</sub>CO<sub>3</sub>] in 100ml deionized water to get clear solution. The metal nitrate solution was prepared by adding 7.03g aluminium nitrate [Al(NO<sub>3</sub>)<sub>3</sub>.9H<sub>2</sub>O], 7.27g cobalt nitrate [Co(NO<sub>3</sub>)<sub>2</sub>.6H<sub>2</sub>O] and 8.01g magnesium nitrate [Mg(NO<sub>3</sub>)<sub>2</sub>.6H<sub>2</sub>O] in 100 ml deionized water to get a purplish red colour. The metal nitrate solution was added drop wise to the precipitating agent solution provided with constant stirring. After mixing, pH of the solution was adjusted around 9 by careful addition of nitric acid [HNO<sub>3</sub>]. The solution was heated at 80<sup>o</sup>C for 16 hours provided with constant stirring. After 16 hours the solution was filtered and precipitates were washed thoroughly with distilled water and oven dried at 80<sup>o</sup>C overnight. The calcination at 600<sup>o</sup>C gives the unpromoted catalyst notified as sample name HTCo-Unp.

For preparation of promoted catalyst the above method is repeated. Both zinc and zirconium promoters were added by wet impregnation method separately. Zinc nitrate or zirconium nitrate solution (5% by weight as that of cobalt) was added drop wise on the dried sample from oven. The sample was dried again at 80<sup>o</sup>C for 5 hours. In the end the sample was calcined at 600<sup>o</sup>C for 5 h in an airtight furnace. Zinc promoted catalysts are reported here as HTCo- Zn whereas zirconium promoted as HTCo-Zr.

### 4.1.1 List of Catalyst Prepared

Name of Catalyst	Method of Preparation	Promoter
<sup>1</sup> HTCo-Unp	Co-precipitation	Un-promoted
<sup>2</sup> HTCo-Zr	Co-precipitation	Zirconium
<sup>3</sup> HTCo-Zn	Co-precipitation	Zinc

<sup>1</sup> Un-promoted Hydrotalcite based Cobalt catalyst prepared using coprecipitation method

<sup>2</sup> Zirconium Promoted Hydrotalcite based Cobalt catalyst prepared using coprecipitation method

<sup>3</sup> Zinc Promoted Hydrotalcite based Cobalt catalyst prepared using coprecipitation method

## 4.2 Characterization of Catalyst

Various analysis techniques are used for the characterization of prepared catalysts like SEM, EDS, XRD, FTIR, TGA, and BET

## 4.3 FTS Process

The catalyst was tested in a fixed bed micro reactor having length of 10 cm with a diameter of 3.3 cm. The complete diagram of the reactor is shown in 'Figure 13'. The nitrogen, carbon monoxide and hydrogen are provided to synthesize syngas artificially on lab scale. The flow of the gasses is controlled by flow controllers. The required composition of the syngas can be synthesized by controlling the flow through flow controllers. There is a pressure gauge that is used for the pressure measurements. A pressure safety valve is also installed for the safety purposes so that it releases excess pressure avoiding the reactor or the tubing to burst. After flow controllers the gasses passed down to reactor. An electric heater is placed around the reactor in spiral form to heat the reactor to desired temperatures. The Fischer Tropsch synthesis reaction usually takes place at higher temperatures; therefore an insulation casing was installed to avoid heat losses. After the reactor the unreacted gasses passed to an escape pipe whereas the

product is condensed in separators. Separator 1 is used for the collection of heavier products whereas the lighter products move down to separator 2, due to difference in their boiling point. After separators a back pressure valve is installed that ensures the high pressure between flow controllers and the back pressure valve. 1 grams of freshly prepared catalyst was mixed with 5gm of ceramic balls and loaded in the reactor. Glass wool plugs are inserted at the top and bottom of the reactor for packing purposes. The inert ceramic balls act a diluting material and have no effect on the activity and selectivity of catalyst [1]. They were used for increasing the surface area of catalyst.

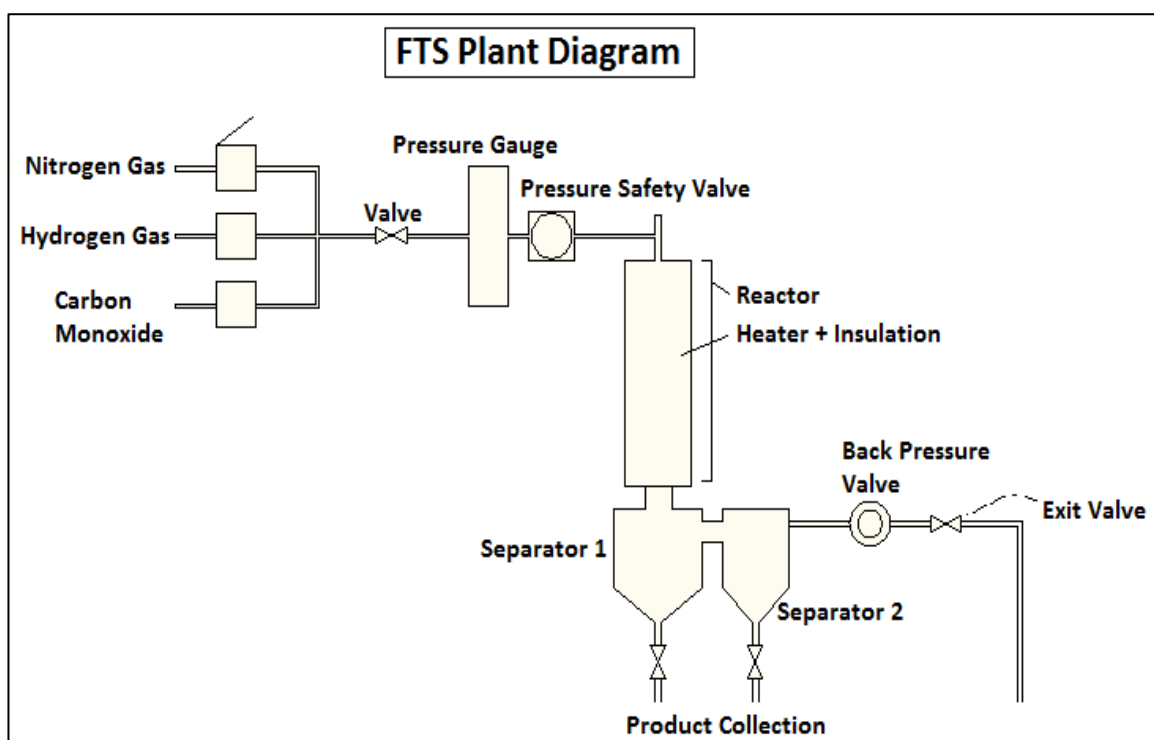


Figure 13: Lab scale FT Plant (NUST)

The loaded catalyst was initially reduced at 400°C for 16 h using hydrogen gas at a flow rate of 50 sccm and nitrogen at flow rate of 10 sccm. Reaction was carried out at 250°C with hydrogen to carbon monoxide ratio of 2:1 which is a standard ratio to test FT catalyst [2, 3]. Flow rates were maintained at 50 sccm of hydrogen, 25 sccm of carbon monoxide and 10 sccm of nitrogen. The pressure of the reactor was maintained at 20 bars (0.20 MPa). The product was collected in the separator 1 (Hot Trap) at 150 °C and Separator 2 (Cold Trap) at room temperature.

#### **4.4 Summary**

This study focused on the comparison of promoted and unpromoted cobalt based catalyst in FTS process. Three catalysts were prepared using coprecipitation method. First catalyst prepared was hydrotalcite based unpromoted cobalt catalyst denoted in this study as HTCo-Unp. Zinc and Zirconium promoted cobalt catalysts were also prepared using coprecipitation method, denoted in this study as HTCo-Zn and HTCo-Zr respectively. These catalysts were tested for FTS in a micro reactor at 250°C temperature and 20 bars pressure. The detailed description of the FT plant and the process is given in this chapter.

## 4.5 References

1. C. L. Bianchi, C. Pirola, and V. Ragaini, *Catalysis Communications*, 2006, 7, 669-672.
2. V. S. Ermolaev, K. O. Gryaznov, E. B. Mitberg, V. Z. Mordkovich, V. F. Tretyakov, *Chemical Engineering Science*, 2015, 138, 1-8.
3. A. Irankhah, A. Haghtalab, E. V. Farahani, K. Sadaghianizadeh, *Journal of Natural Gas Chemistry*, 2007, 16, 115-120.

# Chapter 5: Results and Discussion

## 5.1 Characterization Results

### 5.1.1 SEM

Scanning Electron Microscope is a technique that informs about the structural properties of the crystal. SEM modal JEOL, JED 2300 is used for the analysis of specimen in this study. Scanning electron micrographs are shown in Figure 14, 15 and 16. 'Figure 14' shows the SEM images of un-promoted catalyst prepared by coprecipitation method (HTCo-Unp). The image shows micrographs at different resolution. The images are given at three different resolution. High resolution image (Figure 14a) is marked as X10,000 which means that the image is taken when subject is enlarged 10,000 times its original size. Similarly X5000 means subject is magnified 5000 times its original size whereas X500 means the subject is magnified only 500 times. The images (Figure 14a, 14b, 14c) suggests that there are aggregations or stacking of relatively flat platy particles having random sizes and shapes. The high resolution image (Figure 14a) suggests the formation of needle like structures.

The 'Figure 15' shows the SEM micrographs of (HTCo-Zn). 'Figure 15a' shows images at X10,000 whereas 'Figure 15b' and 'Figure 15c' at X5000 and X500 respectively. It can be seen from 'Figure 15a' that the zinc promoted catalyst show relatively smooth surface without formation of large agglomerates. The SEM micrographs shown in 'Figure 16' are of zirconium promoted catalyst (HTCo-Zr). It can be seen in 'Figure 16a' that zirconium promoted catalyst show platy particles that are stacked over each other. The particles are either half embedded in the surface or laying in the form of stacks on the surface of particles.

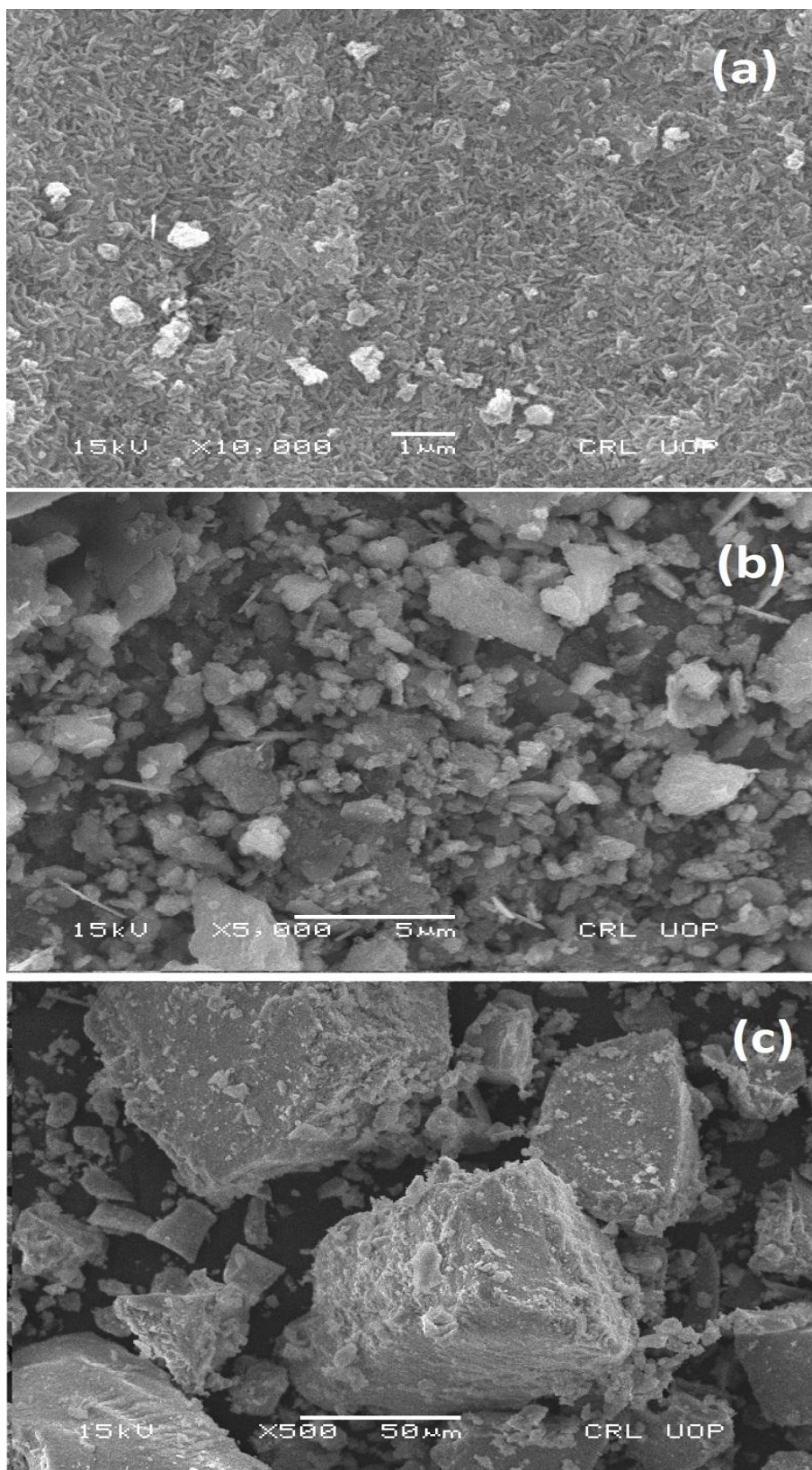


**Figure 14: SEM Micrographs of HTCo-Unp at  
(a) X10,000 (b) X5000 (c) X500**

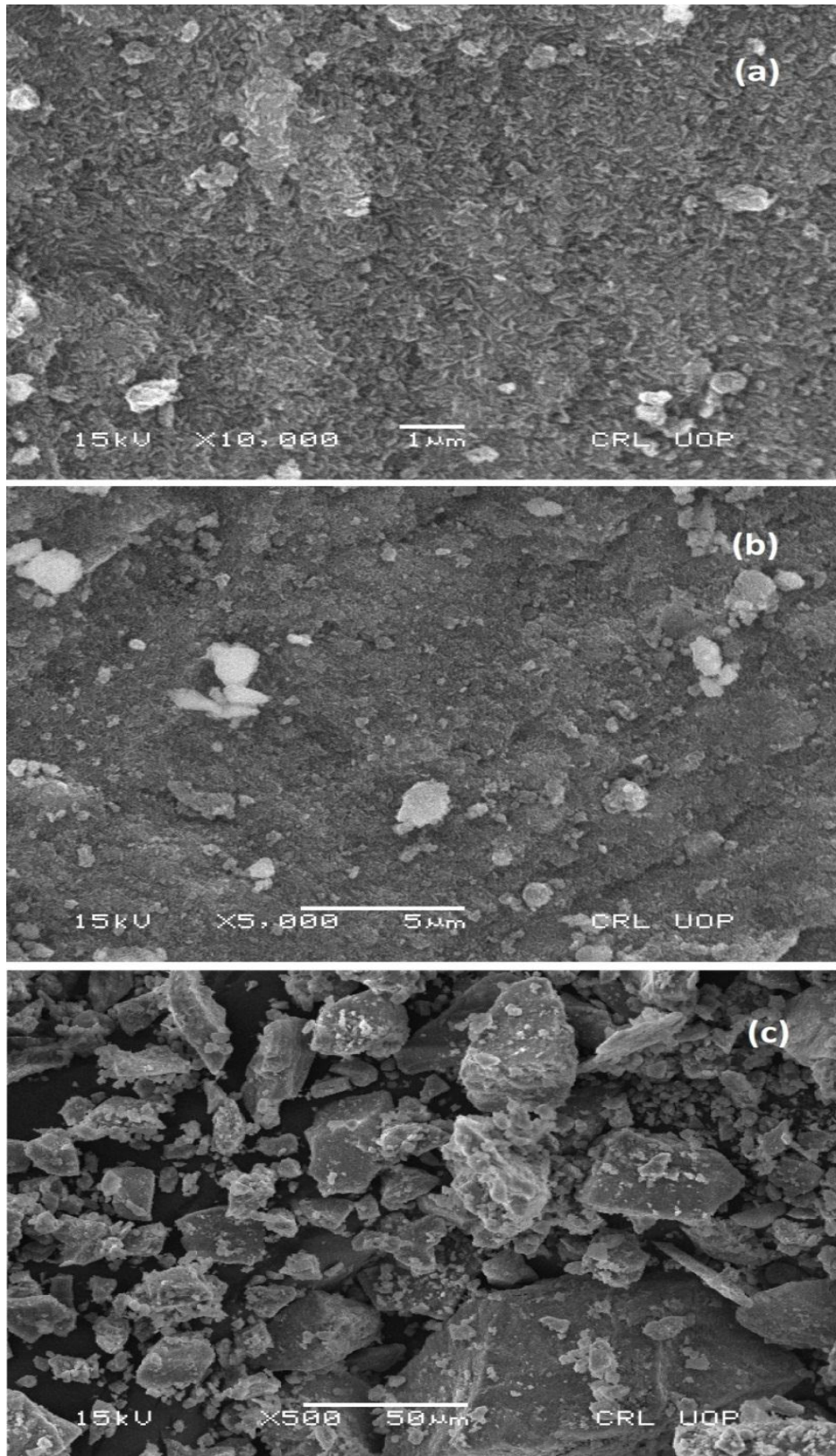


**Figure 15: SEM Micrographs of HTCo-Zn at  
(a) X10,000 (b) X5000 (c) X500**

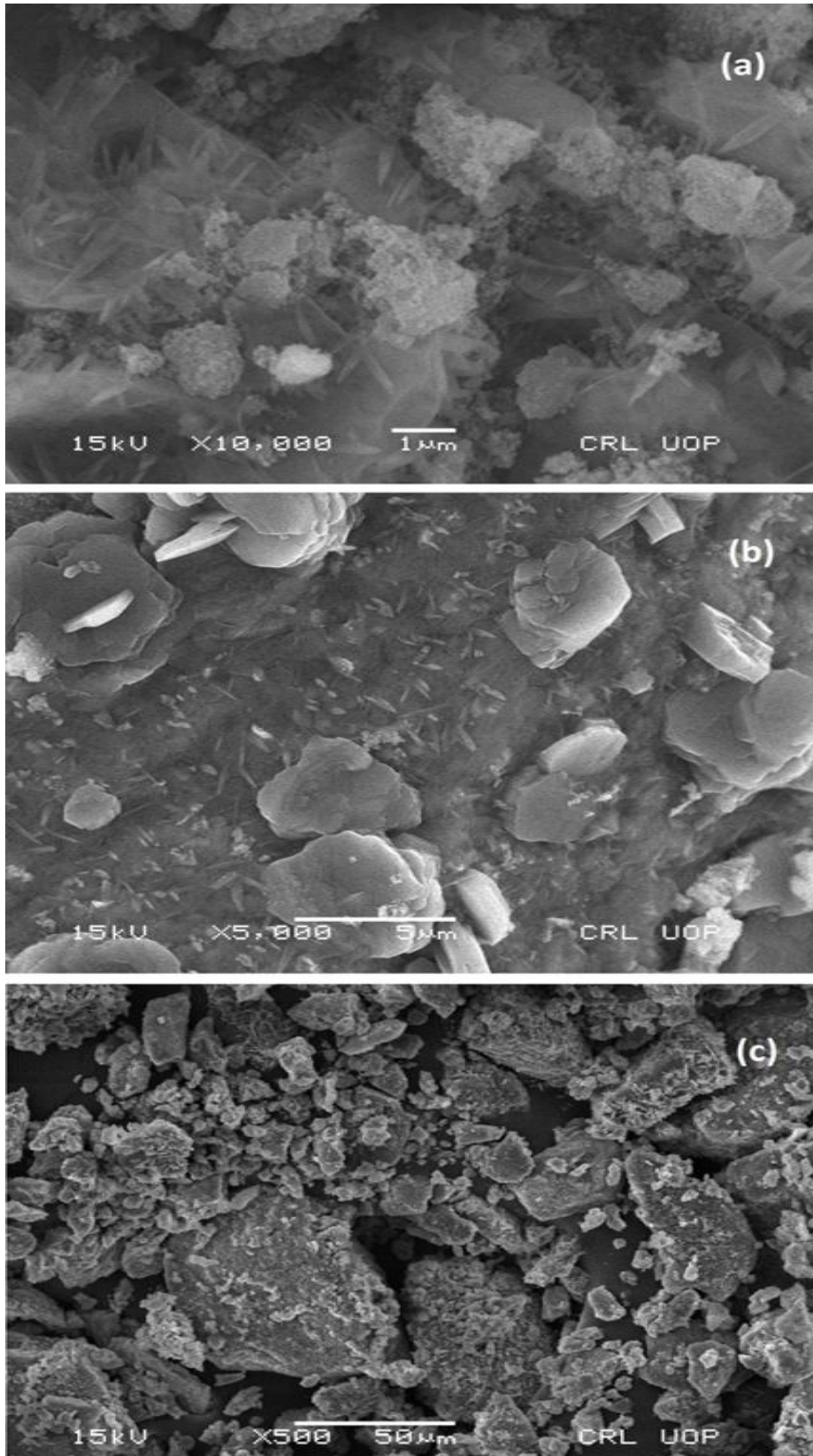


**Figure 16: SEM Micrographs of HTCo-Zr at (a) X10,000 (b) X5000 (c) X500**

The EDS data is shown in the ‘Table 4’ the table suggests that both promoted and the unpromoted catalyst have almost same cobalt loading of around 32 %. There is small difference in the percentages of magnesium, aluminium and sodium. This difference in the percentages is in the support part of catalyst and hence this difference does not affect the working of the catalyst. The zirconium promoted catalyst 6.29% zirconium loading whereas the zinc promoted catalyst show 3.15% zinc loading. The presence of oxygen in all three catalyst show formation of oxides on surface of catalyst. Those oxides are removed during reduction phase of FTS reaction. The EDS images of HTCo-Unp, HTCo-Zr and HTCo-Zn are shown in Figure 17, Figure 18 and Figure 19 respectively.

**Table 4: Elemental Analysis Obtained from EDS**

Sample ID	Co (%)	Zr (%)	Zn (%)	Mg (%)	Al (%)	Na (%)	O (%)
HTCo-Zn	32.20		3.15	11.79	8.07	4.25	40.55
HTCo-Zr	32.33	6.29	----	9.09	7.30	7.75	37.25
HTCo-Unp	32.22	--	--	12.15	8.46	4.35	42.81

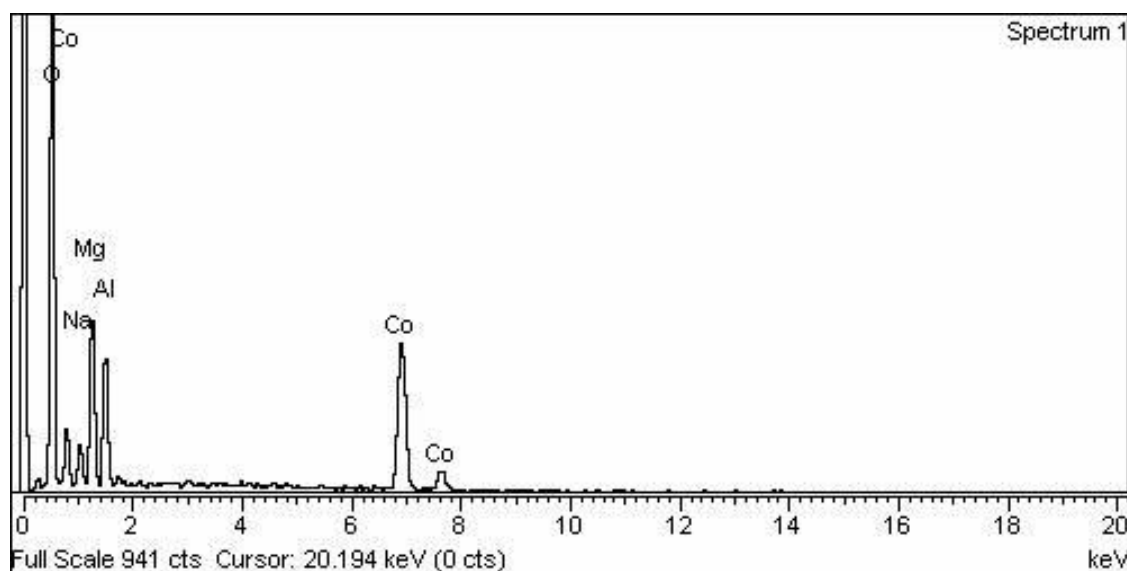


**Figure 17: EDS Spectrum of HTCo-Unp**

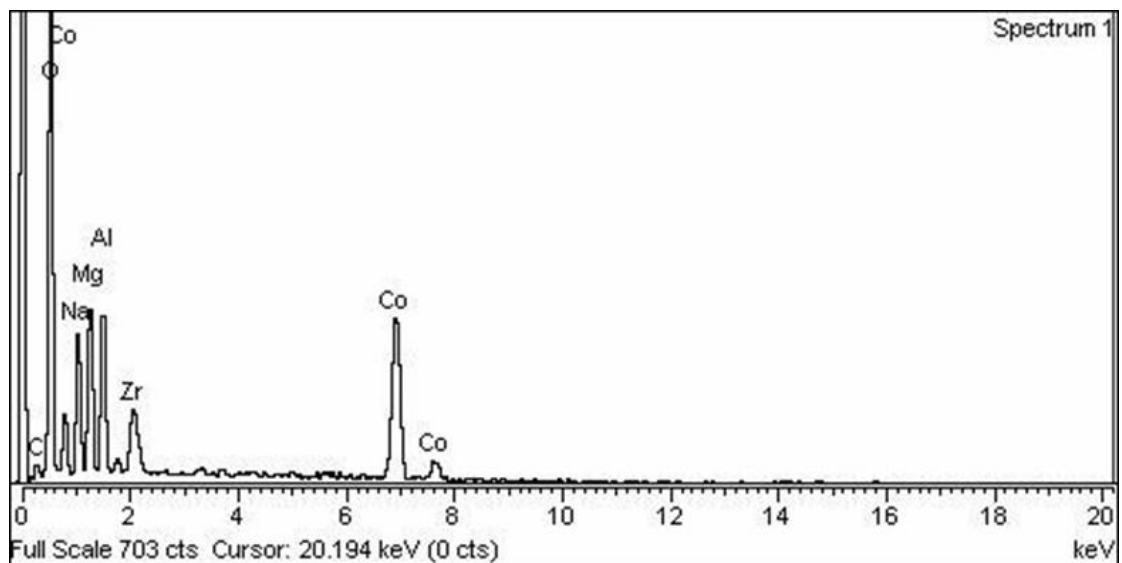


Figure 18: EDS Spectrum of HTCo-Zr

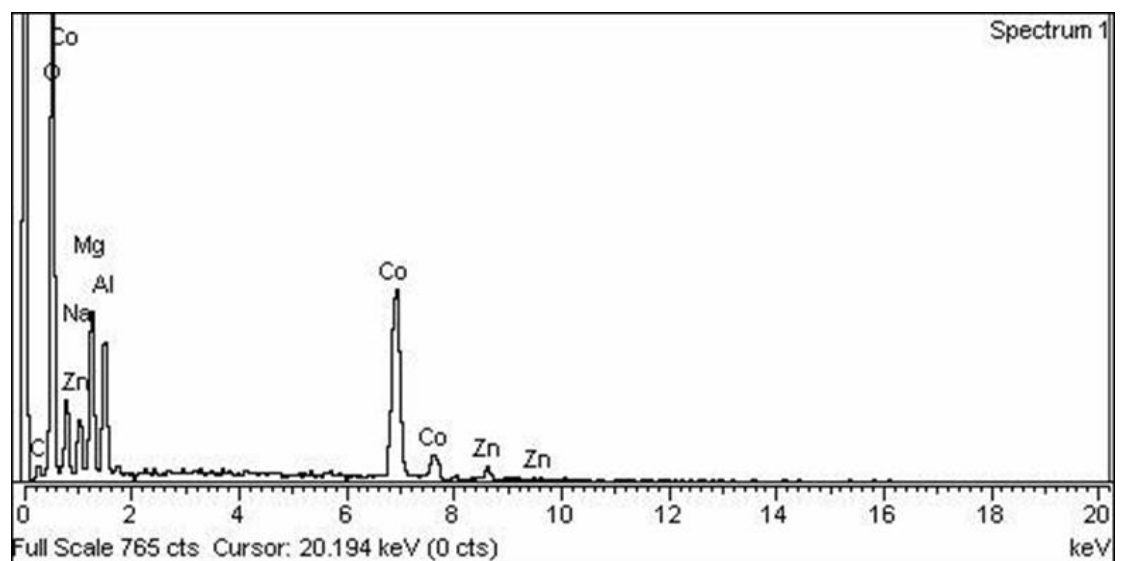
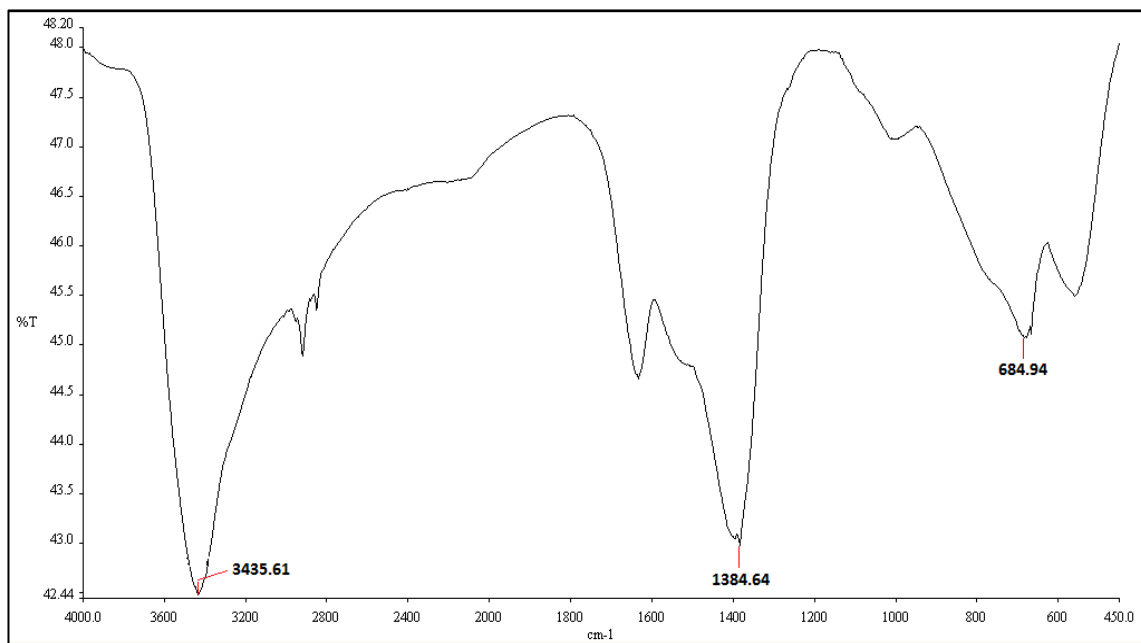


Figure 19: EDS Spectrum of HTCo-Zn

### 5.1.2 FTIR

Fourier Transform Infrared Spectroscopy is a technique used to study presence of certain functional groups in a molecule. FTIR was performed using PerkinElmer Spectrum 100 Spectrometers. The FTIR spectra of Zinc promoted (HTCo-Zn), zirconium promoted (HTCo-Zr) and unpromoted (HTCo-Unp) is shown in Figure 20, 21 and 22 respectively. It is evident from the spectra that there exists an absorption around  $3430\text{ cm}^{-1}$  in case of HTCo-Zn and correspond to the OH-stretching between  $2500\text{ cm}^{-1}$

to  $3900\text{ cm}^{-1}$  [1]. The absorption at  $1383\text{ cm}^{-1}$  corresponds to H-OH bending vibration. The Co-O stretching for the characteristic absorption of  $\text{Co}_3\text{O}_4$  can be observed at  $679\text{ cm}^{-1}$  is evident from the spectra. The absorption around  $550\text{ cm}^{-1}$  represents the  $\text{Al}_2\text{O}_3$  stretching.



**Figure 20: FTIR Spectra of HTCo-Zn**

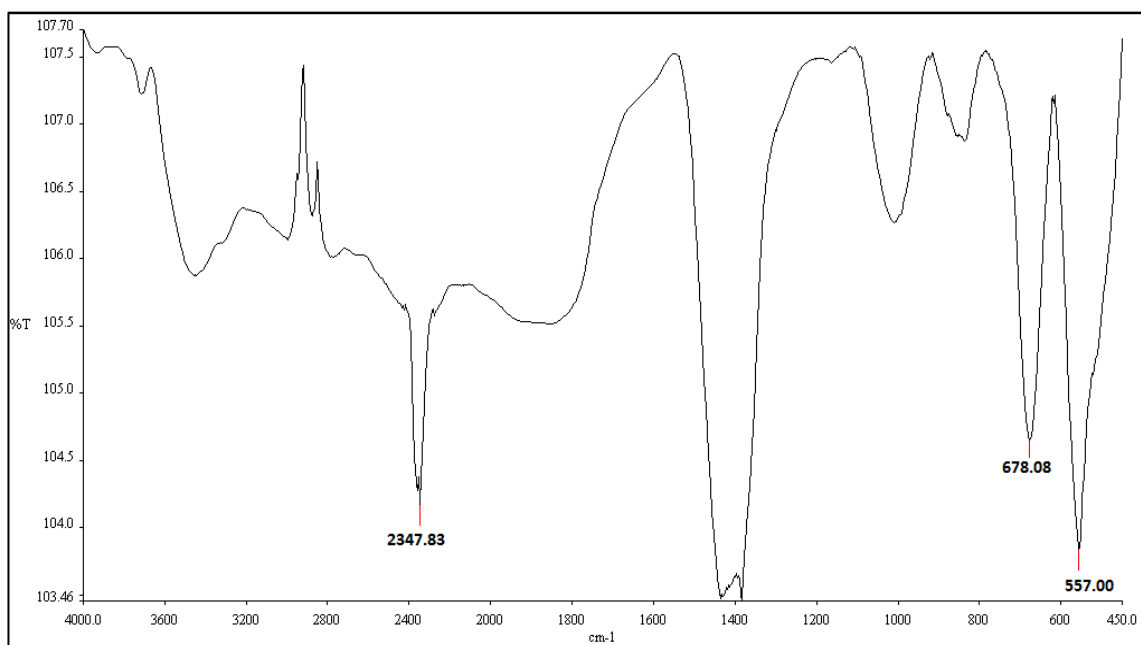


**Figure 21: FTIR Spectra of HTCo-Zr**

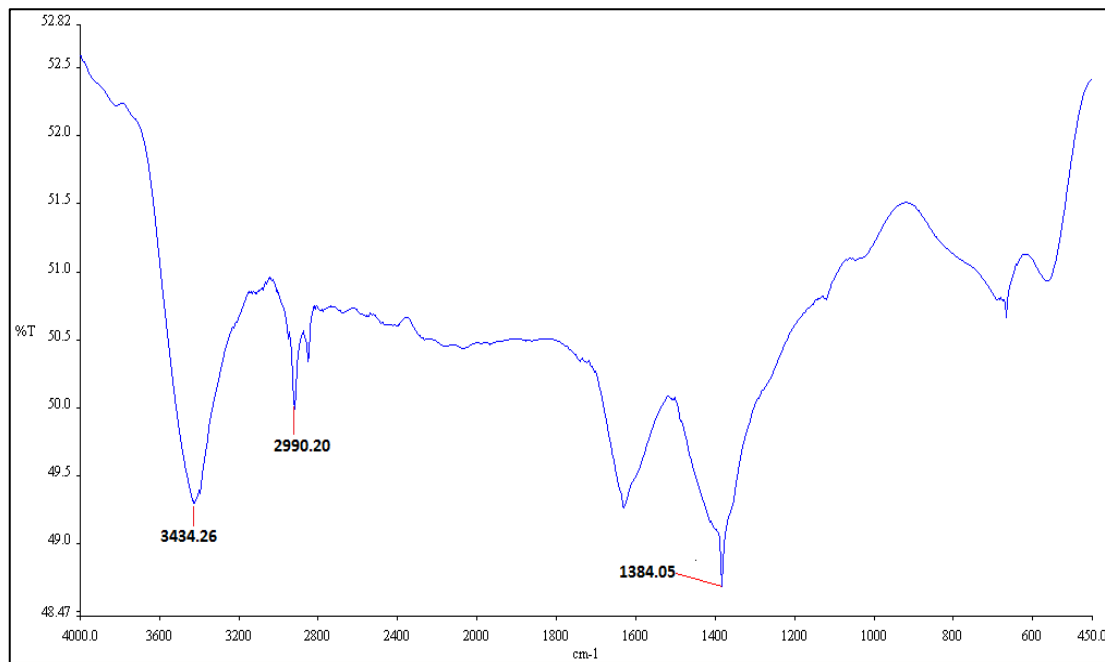


**Figure 22: FTIR Spectra of HTCo-Unp**

### 5.1.3 TGA

The apparatus used for analysis is Mettler TGA/SDTA 851e. The TGA graph is shown in 'Figure 23'. 'Figure 23' shows two curves (a) shown the weight loss of zinc promoted catalyst (HTCo-Zn) whereas weight loss of zirconium promoted catalyst (HTCo-Zr) is shown by curve (b). Both curves show the characteristic decomposition behaviour of hydrotalcite materials.

The typical TGA decomposition profile of all catalysts show similarity and two weight loss events can be observed. First weight loss in the range of 110 °C to 250 °C is due to the loss of water molecules from the interlayer space [2]. Second weight loss occurs around 250 to 380 °C due to de-hydroxylation of the hydroxide layer together with the loss of interlayer anions, inducing the layered structure collapse in order to generate a mixed oxide [3].

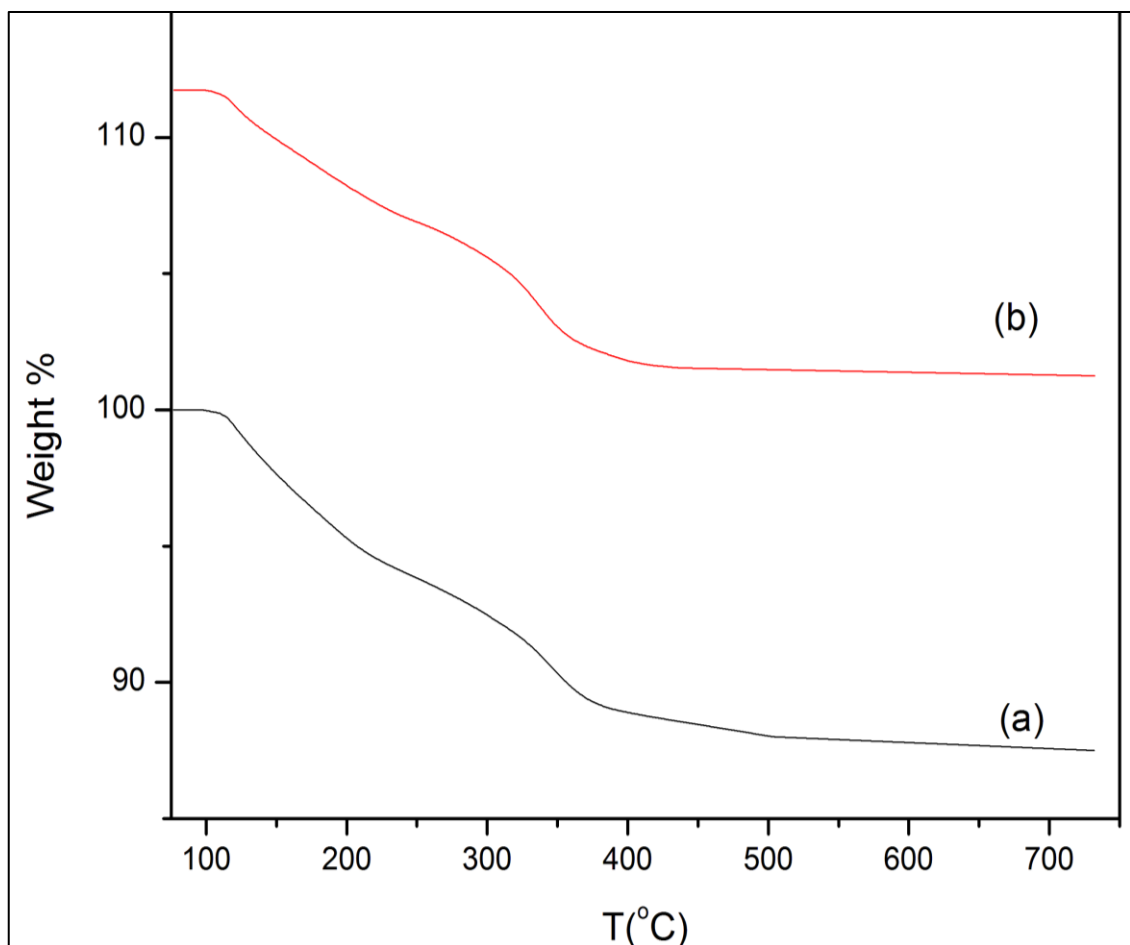


Figure 23: TGA Graphs of (a) HTCo-Zn (b) HTCo-Zr

#### 5.1.4 BET

The surface area analysis was performed using Tri-Star II 3020 apparatus. Surface area analysis is shown in Table 5. The isotherm gives the information about the porous texture of solids. The isotherm obtained in this study suggests that at low relative pressures the formation of monolayer of adsorbate is the prevailing process. However when the relative pressure increases the multilayer adsorption takes place. The thickness of adsorbate increases progressively as the relative pressure increase until the condensation point reaches. There appears to be a minor hysteresis which can occur due to the difference between pore body and pore mouth (ink bottle shaped pore) or due to cylindrical channel crossings in solid. The result from the analysis suggests that the surface area of the catalyst prepared by co-precipitation method and using zinc as promoter (HTCo-Zn) have the largest surface area. However the pore volume, pore

width and the particle size is smallest. However zirconium promoted cobalt catalyst prepared by coprecipitation method (HTCo-Zr) has the smallest surface area but larger pore size. This data suggests that for HTCo-Zn there is larger distribution of pores (porosity) across the surface of solid but the pores have small mouth sizes and small volume as compared to HTCo-Zn. The larger surface area and small pores volume and size suggest that solid have small sized pores but the number of pores is very large. The smaller average particle size and larger surface area of the samples promoted with zinc confirms its advantages over zirconium promoted and unpromoted catalyst [4, 5].

**Table 5: Surface Area Analysis**

Catalyst	BET Surface Area (m <sup>2</sup> /g)	Pore volume (cm <sup>3</sup> /g)	Pore Width (nm)	Avg. particle size (nm)
HTCo-Cpt-Zn	78.978	0.1425	7.22	75.70
HTCo-Cpt-Zr	47.28	0.1229	10.40	126.79
HTCo-Unp	37.88	0.064	7.67	158.36

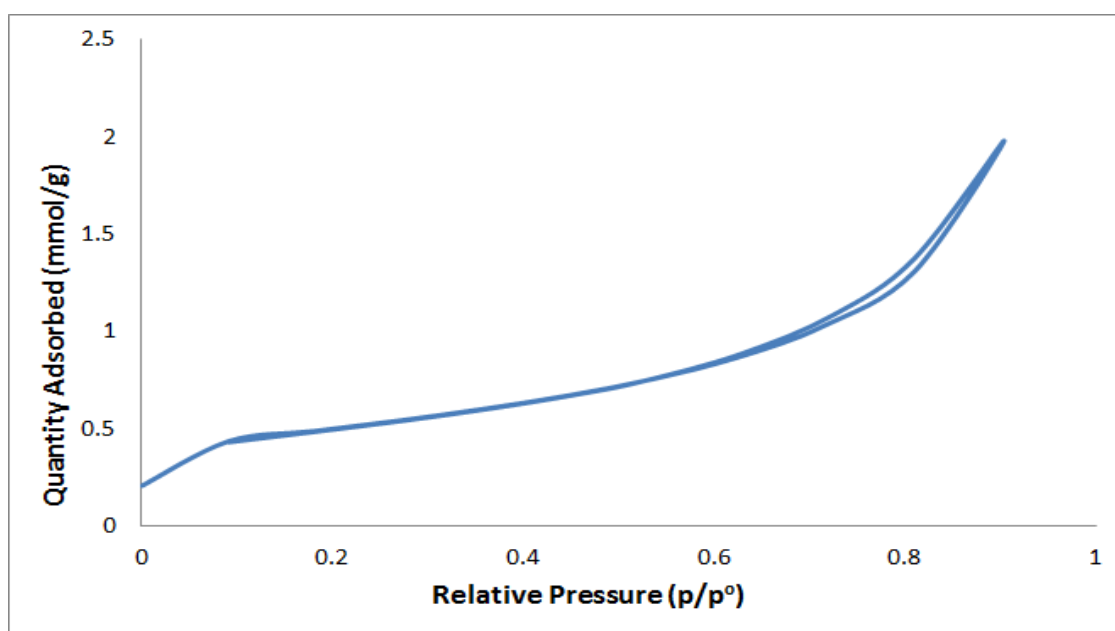


**Figure 24: Adsorption Isotherm of HTCo-Unp**

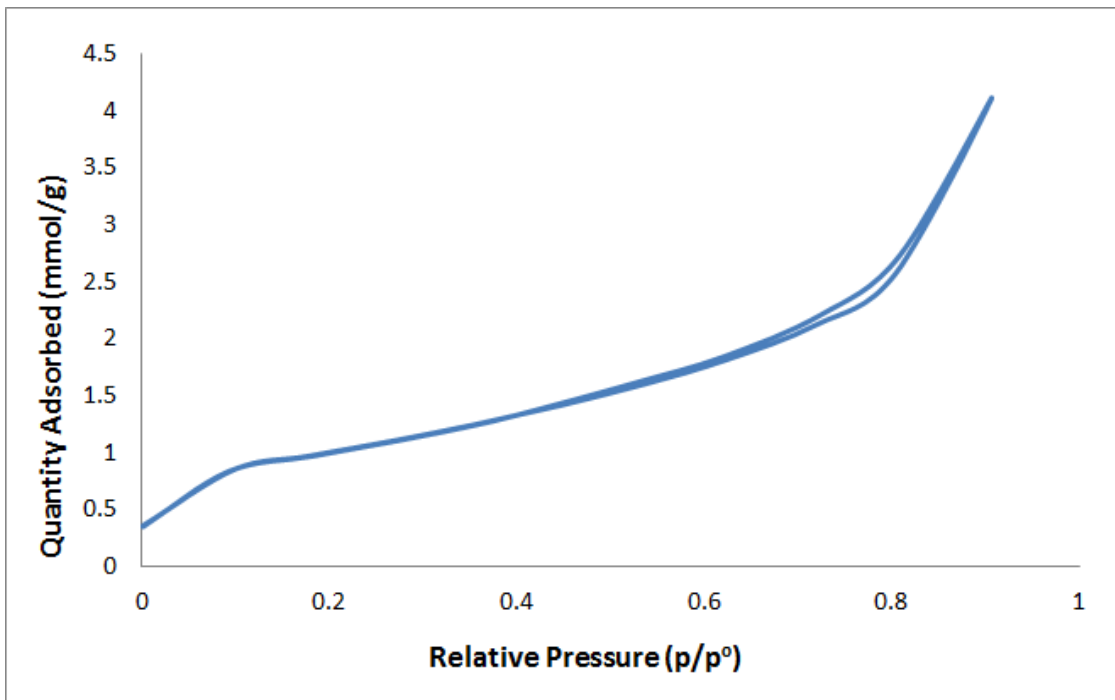


Figure 25: Adsorption Isotherm of HTCo-Zn

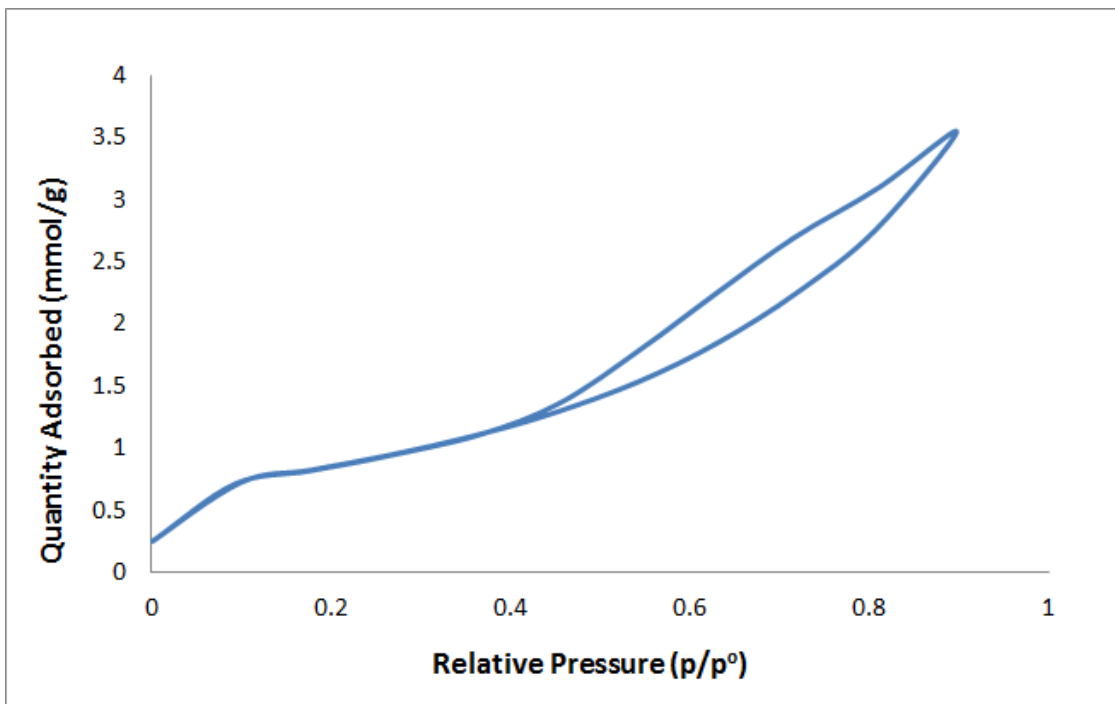


Figure 26: Adsorption Isotherm of HTCo-Zr

### 5.1.5 XRD

X-Ray powder Diffraction denoted as XRD is a fast technique used for the identification of the phase of an unknown crystalline material. It can provide information on the crystal shape and sizes, unit size dimensions and unit cell spacing. The STOE Powder Diffraction system is used for the analysis of the samples in this study. The system was operating at 20 kV and 5 mA, step size 0.04, scan angle 20 to 80 and 0.5 sec per scan

'Figure 27' shows XRD pattern of unpromoted catalyst (HTCO-Unp). Cobalt develops into a ferromagnetic hcp (hexagonal close packed structures) structure whereas at higher pressure where the magnetism is adequately suppressed, we expect a shift from hcp to fcc (face centered cubic structure) [6]. Peaks appear at  $31^{\circ}$ ,  $37^{\circ}$ ,  $45^{\circ}$  which are characteristic peaks of cobalt oxides ( $\text{Co}_3\text{O}_4$ ) matched with pdf card number (JCPDS ref. code 00-043-1004) [7, 8]. Similarly peaks appear at  $59^{\circ}$ ,  $77^{\circ}$ ,  $79^{\circ}$  due to formation of Mg-Al-HT structure matched with pdf card number (JCPDS ref. code 00-076-0306).

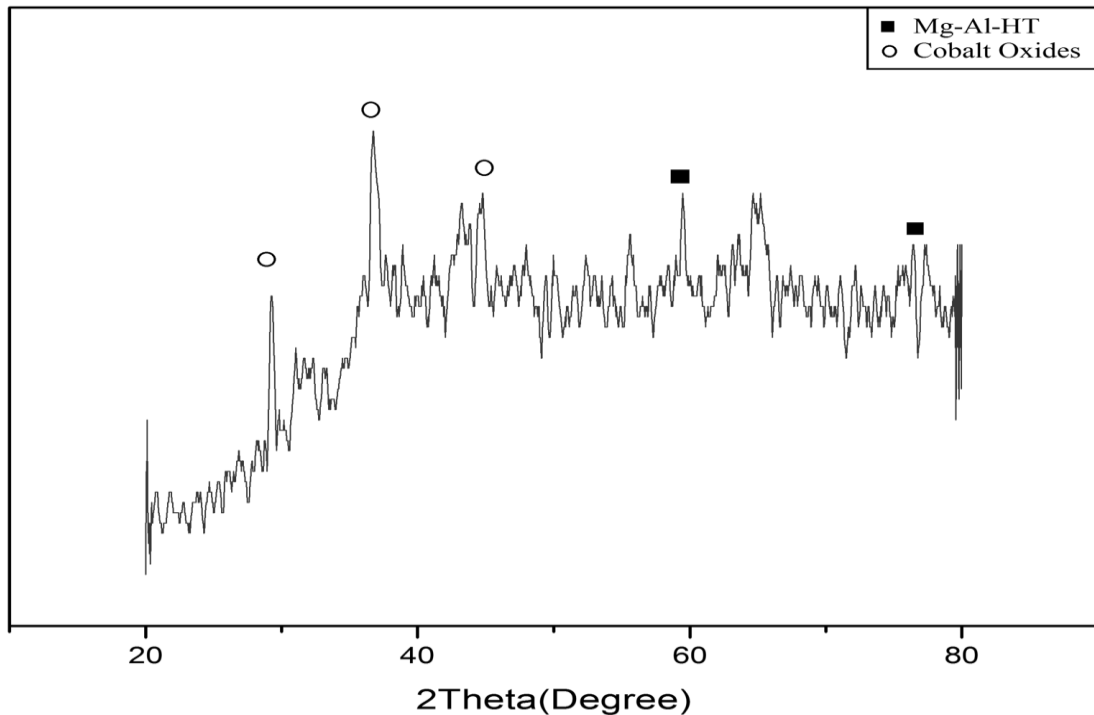


Figure 27: XRD of HTCo-Unp

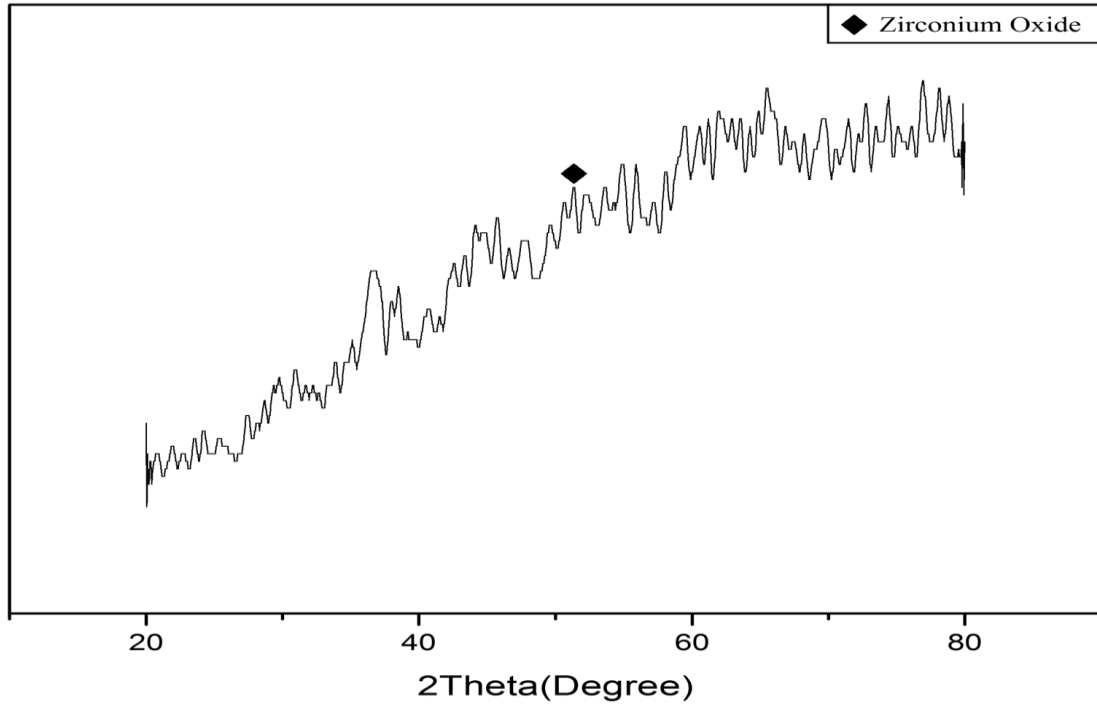


Figure 28: XRD of HTC Co-Zr

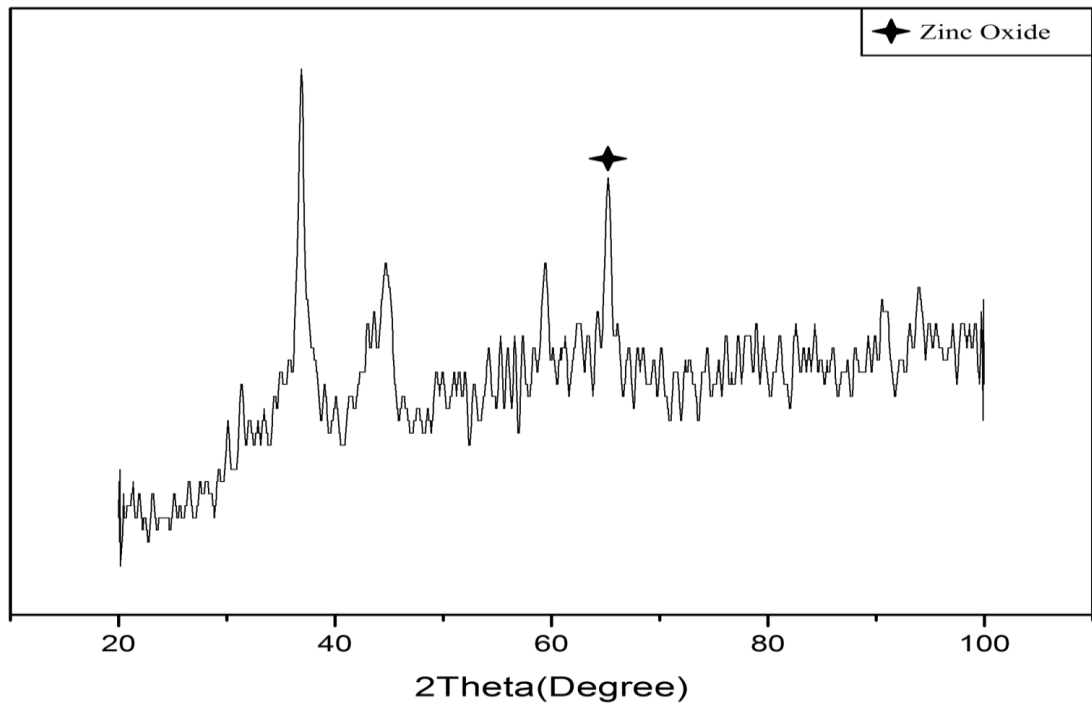


Figure 29: XRD of HTC Co-Zn

The  $\text{Mg}^{2+}$  and  $\text{Al}^{3+}$  have an ion radius of  $0.65\text{\AA}$  and  $0.60\text{\AA}$  which is slightly less than ion radius of cobalt ( $\text{Co}^{2+}$  ion radius of  $0.74\text{\AA}$ ) hence the incorporation of larger cobalt ions in the HT structure makes the structure less crystalline [9]. The 'Figure 29' shows the XRD pattern of zinc promoted cobalt catalyst prepared by hydrothermal method (HTCo-Zn). Peak at  $65^\circ$  is due to the zinc oxide matched with pdf card number (JCPDS ref. code 00-087-0713). XRD pattern of zirconium promoted catalyst (HTCo-Zr) is shown in the 'Figure 28'. There is a peak visible at  $52^\circ$  is the characteristic peak of zirconium oxide in the crystal matched with pdf card number (JCPDS ref. code 00-088-2329). It can be observed that the XRD pattern of zinc promoted catalyst does not show sharp peaks which indicated that the catalyst prepared using zinc promoter have relatively amorphous structure.

## 5.2 FTS Product Analysis

The Fischer Tropsch Synthesis was performed by using both promoted and unpromoted catalyst. The product was collected from Separator 1 and Separator 2 in glass vials. The glass vials are sealed to avoid evaporation of any component of product. The Picture of collected samples in sealed glass vials are shown in 'Figure 30'. The 'Shimadzu QP2010 Ultra' system is used for GC-MS analysis of product obtained from both separators. Injection temperature was set at  $120^\circ\text{C}$ . Helium was used as carrier gas at pressure of  $89.3\text{KPa}$  and column flow rate of  $1.44\text{mL}/\text{min}$ . The total flow was  $158.9\text{mL}/\text{min}$  and total time of process is 25mins.

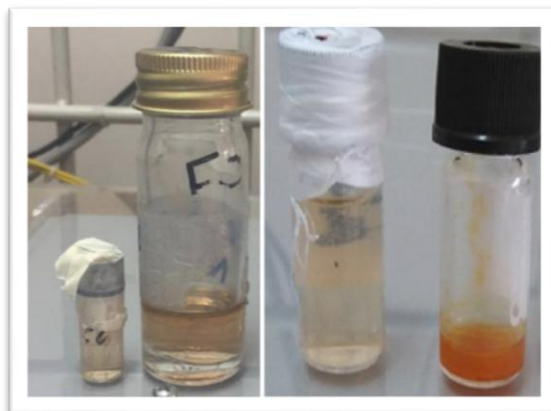


Figure 30: Collected Samples from FTS

### 5.2.1 HTCo-Cpt-Unp

The unpromoted catalyst was tested for FTS and the GCMS analysis was shown in the 'Figure 31'. From the 'Figure 31' it can be concluded that there are 20 peaks which shows the probable existence of 20 different fractions in our product. 'Table 6' stated below shows all the possible compounds present in the product. The data suggests that the highest quantity is of C<sub>3</sub> compounds. The C<sub>4</sub> compounds are also in abundance. In other words when we use unpromoted catalyst there are higher fractions of lower chain oxygenated in the product. There is a net percentage of 62.81% of less than C<sub>5</sub> compounds in the product. The net C<sub>5+</sub> compounds are 37.19% of the whole product. If we talk about the C<sub>5+</sub> compounds the C<sub>14</sub> C<sub>11</sub> and C<sub>5</sub> are relatively in abundance.

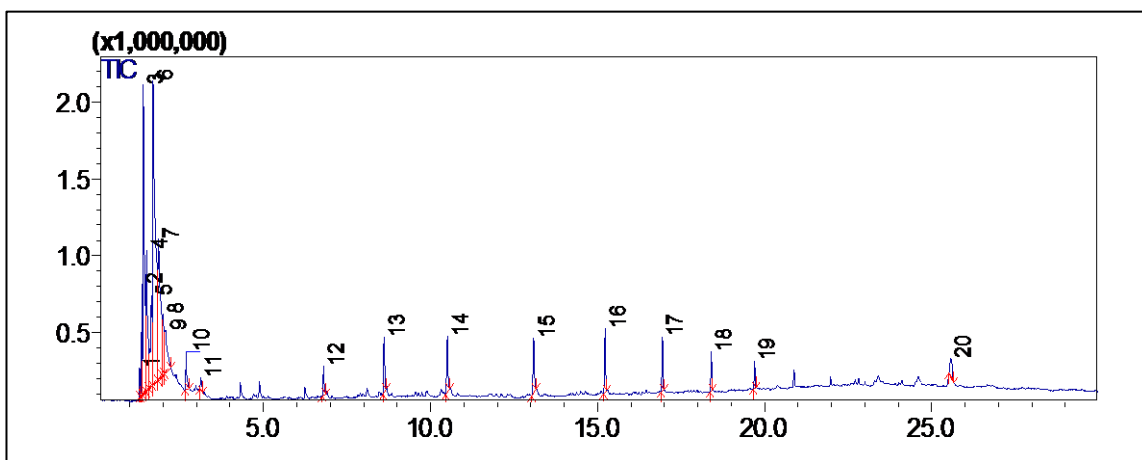


Figure 31: GCMS Analysis of Product From HTCo-Unp

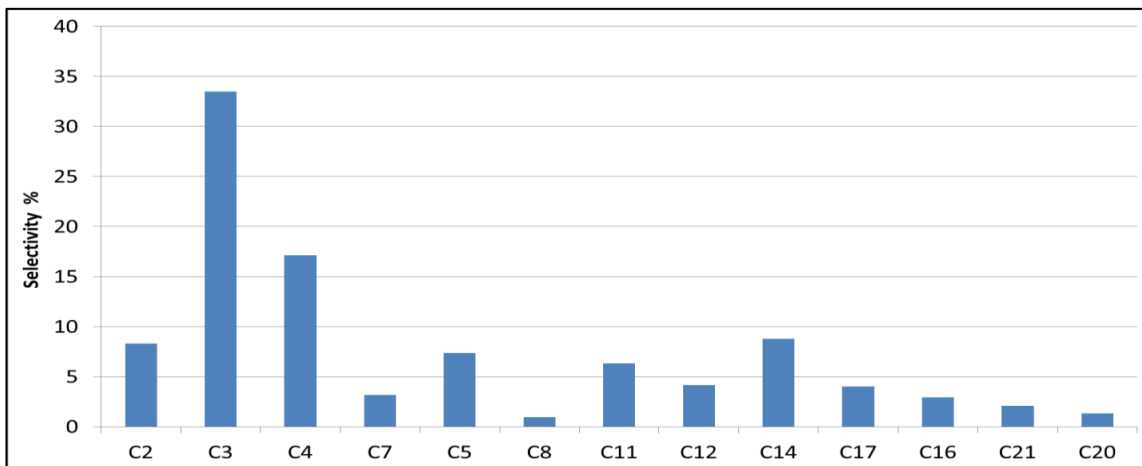


Figure 32: Chain Length Distribution of HTCo-Unp Product

**Table 6: List of Compounds in the Product of HTCo-Unp**

Compound Name	Mol. wt.	Similarity	Formula	Area %	Height %
Ethanol	46	94	C <sub>2</sub> H <sub>6</sub> O	6.65	2.75
Acetone	58	95	C <sub>3</sub> H <sub>6</sub> O	18.44	15.73
Propanol	60	96	C <sub>3</sub> H <sub>8</sub> O	8.38	7.46
Butanone	72	90	C <sub>4</sub> H <sub>8</sub> O	5.37	5.49
Butanol	74	97	C <sub>4</sub> H <sub>10</sub> O	8.36	12.68
Pentanone	86	95	C <sub>5</sub> H <sub>10</sub> O	3.63	3.14
2-Hexanol	116	88	C <sub>7</sub> H <sub>16</sub> O	2.52	3.93
1-Pentanol	88	97	C <sub>5</sub> H <sub>12</sub> O	2.26	1.51
Octane	114	87	C <sub>8</sub> H <sub>18</sub>	0.74	0.55
Undecane	156	95	C <sub>11</sub> H <sub>24</sub>	1.75	1.09
Dodecane	170	97	C <sub>12</sub> H <sub>26</sub>	3.31	1.94
Tetradecane	198	96	C <sub>14</sub> H <sub>30</sub>	3.34	2.53
Heptdecane	240	95	C <sub>17</sub> H <sub>36</sub>	3.25	2.55
Hexadecane	226	96	C <sub>16</sub> H <sub>34</sub>	3.77	2.53
Heneicosane	296	95	C <sub>21</sub> H <sub>44</sub>	3.22	1.90
Cyclopropanoicacid	310	89	C <sub>20</sub> H <sub>38</sub> O <sub>2</sub>	2.35	1.24

### 5.2.2 HTCo-Cpt-Zr

The zirconium promoted catalyst tested for FTS and the GCMS analysis was shown in the 'Figure 33'. From the 'Figure 33' it can be concluded that there are 30 peaks which shows the probable existence of 30 different fractions in our product. 'Table 7' stated below shows all the possible compounds present in the product. The data suggests that the highest quantity is of C<sub>12</sub> compounds. The C<sub>8</sub>, C<sub>9</sub>, C<sub>11</sub>, C<sub>16</sub> and C<sub>17</sub> compounds are also in abundance. In other words when we use zirconium promoted catalyst we get higher fractions of straight chain hydrocarbons having higher chain length in the

product. There is a net percentage of 8.75% of less than C<sub>5</sub> compounds in the product. The net C<sub>5+</sub> compounds are 91.25% of the whole product.

**Table 7: List of Compounds in the Product of HTCo-Zr**

Compound Name	Mol. Wt.	Similarity	Formula	Area %	Height %
1-Propanol	60	95	C <sub>3</sub> H <sub>8</sub> O	1.55	2.56
1-Butanol	74	94	C <sub>4</sub> H <sub>10</sub> O	1.85	3.03
1-Pentanol	88	93	C <sub>5</sub> H <sub>12</sub> O	3.58	3.31
n-Hexane	86	92	C <sub>6</sub> H <sub>14</sub>	3.74	3.71
1-Hexanol	102	96	C <sub>6</sub> H <sub>14</sub> O	3.76	2.57
Heptane	100	93	C <sub>7</sub> H <sub>16</sub>	3.15	5.09
2-Heptene	98	89	C <sub>7</sub> H <sub>14</sub>	1.54	3.08
1-Heptanol	116	92	C <sub>7</sub> H <sub>16</sub> O	2.07	1.83
1-Octene	112	91	C <sub>8</sub> H <sub>16</sub>	2.49	2.98
Octane	114	92	C <sub>8</sub> H <sub>18</sub>	4.98	6.08
4-Octene	112	89	C <sub>8</sub> H <sub>16</sub>	2.69	3.49
Nonane	142	92	C <sub>9</sub> H <sub>20</sub>	6.65	6.09
4-Nonene	126	88	C <sub>9</sub> H <sub>18</sub>	2.73	3.42
2-Nonene	126	93	C <sub>9</sub> H <sub>18</sub>	1.72	2.08
4-Decene	140	89	C <sub>10</sub> H <sub>20</sub>	2.45	3.15
1-Undecene	154	92	C <sub>11</sub> H <sub>22</sub>	3.29	1.97
5-Undecene	154	87	C <sub>11</sub> H <sub>22</sub>	8.05	8.04
1-Dodecene	168	90	C <sub>12</sub> H <sub>24</sub>	2.63	2.26
Dodecane	170	94	C <sub>12</sub> H <sub>26</sub>	18.38	16.29
Cyclododecane	168	88	C <sub>12</sub> H <sub>24</sub>	3.96	3.59
Tetradecane	198	95	C <sub>14</sub> H <sub>30</sub>	3.75	2.87
Hexadecane	226	93	C <sub>16</sub> H <sub>34</sub>	7.48	6.88
Heptadecane	240	94	C <sub>17</sub> H <sub>36</sub>	7.53	5.63

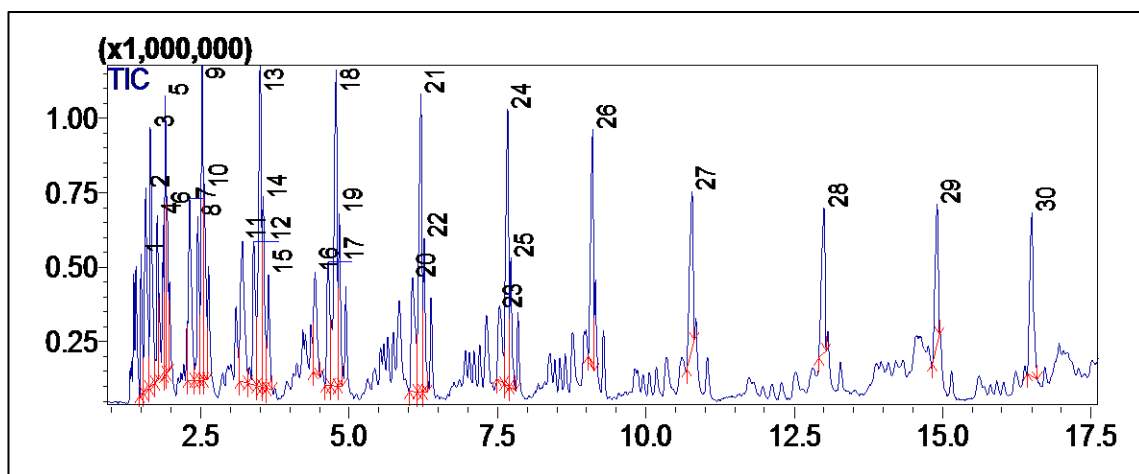


Figure 33: GCMS Analysis of Product from HTCo-Zr

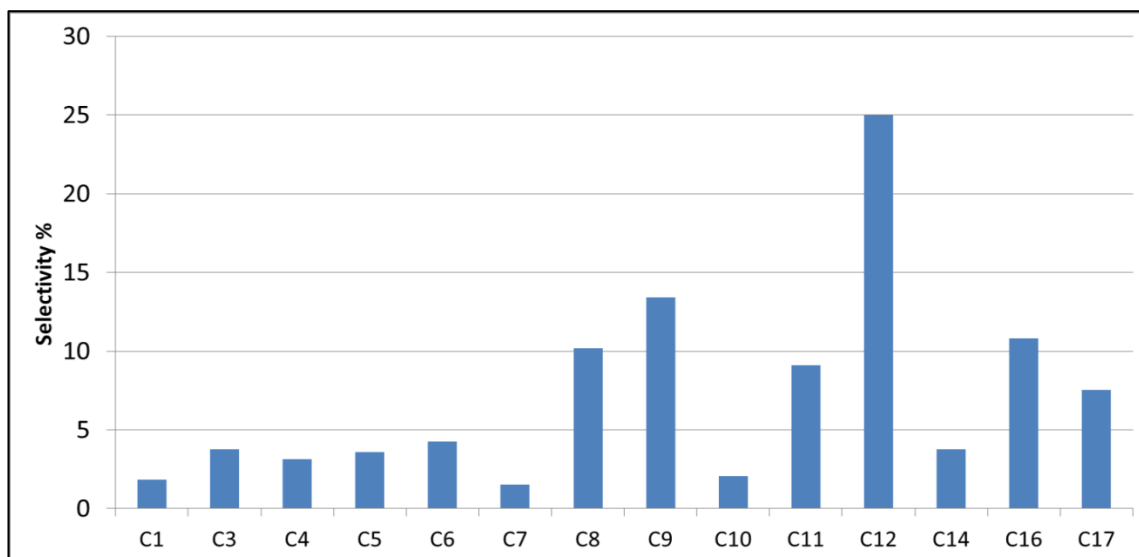


Figure 34: Chain Length Distribution of HTCo-Zr Product

### 5.2.3 Comparison

The comparison show that when unpromoted catalyst was used we get large fractions of lower chain oxygenates. Whereas when zirconium promoted catalyst was used, higher fractions of straight chain hydrocarbons having higher molecular weight are obtained. Similarly, the use of unpromoted cobalt based catalyst can give greater fractions of oxygenates whereas while using zirconium promoted catalyst less oxygenates and more fractions of straight chain hydrocarbons are obtained.

**Table 8: Comparison of FTS Product**

Catalyst	Temperature	Pressure	H <sub>2</sub> :CO	C <sub>1</sub> -C <sub>4</sub>	C <sub>5+</sub>	Oxygenates %
HTCo- Unp	250 °C	20 bar	2:1	62.81	37.19	74.18
HTCo-Zr	250 °C	20 bar	2:1	8.75	91.25	12.81

### 5.3 Summary

The characterization results as well as FTS product analysis is given in this chapter. The characterization reveals that zirconium promoted catalyst (HTCo-Zr) has more stable crystal structure and more promoters loading as compared to zinc promoted (HTCo-Zn). It is quite evident from the results of BET that the zinc promoted (HTCo-Zn) catalyst show the largest surface area as compared to both unpromoted (HTCo-Unp) and zirconium promoted (HTCo-Zr). C<sub>5+</sub> selectivity of unpromoted catalyst (HTCo-Unp) is tested against the selectivity of zirconium promoted catalyst (HTCo-Zr). Catalyst testing for FTS gives very promising results in case of zirconium promoted catalyst as compared to un-promoted catalyst.

## 5.4 Reference

1. J. T. Kloprogge, R. L. Frost, *Journal of Solid State Chemistry*, 1999, 146, 506-515.
2. Z. Jiang, J. Yu, J. Cheng, T. Xiao, M. O. Jones, Z. Hao, P. P. Edwards, *Fuel Processing Technology*, 2010, 91, 97-102.
3. J. Perez-Ramirez, G. Mul, F. Kapteijn, J. Moulijn, *Journal of Materials Chemistry*, 2001, 11, 2529-2536.
4. J. Tantirungrotechai, P. Chotmongkolsap, M. Pohmakotr, *Microporous and Mesoporous Materials*, 2010, 128, 41-47.
5. R. Bastiani, I. Zonno, I. Santos, C. Henriques, J. Monteiro, *Brazilian Journal of Chemical Engineering*, 2004, 21, 193-202.
6. C.-S. Yoo, P. Söderlind, H. Cynn, *Journal of Physics: Condensed Matter*, 1998, 10, 311.
7. M. Trépanier, A. K. Dalai, N. Abatzoglou, *Applied Catalysis A: General*, 2010, 374, 79-86.
8. A. Tavasoli, R. M. M. Abbaslou, A. K. Dalai, *Applied Catalysis A: General*, 2008, 346, 58-64.
9. L. He, H. Berntsen, E. Ochoa-Fernández, J. C. Walmsley, E. A. Blekkan, and D. Chen, *Topics in Catalysis*, 2009, 52, 206-217.

## Conclusions and Recommendations

Hydrotalcite supported cobalt catalysts were synthesized using co precipitation method and two promoters, zinc and zirconium were added by wetness impregnation method. The characterization reveals that zirconium promoted catalyst (HTCo-Zr) has more stable crystal structure and more promoters loading as compared to zinc promoted (HTCo-Zn). It is quite evident from the results of BET that the zinc promoted (HTCo-Zn) catalyst show the largest surface area as compared to both unpromoted (HTCo-Unp) and zirconium promoted (HTCo-Zr). The less surface area of HTCo-Zr can be explained due to tendency of zirconium promoter to modify the surface of the catalyst due to electronic promotion. HTCo-Zr and HTCo-Unp were tested for Fischer Tropsch Synthesis Reaction. Catalyst testing for Fischer-Tropsch synthesis suggests a very intense rise in the formation of gasoline and diesel fractions when we use zirconium promoted catalyst as compared to un-promoted catalyst. Apart from that the promoter addition also demotes the formation of oxygenated in the FTS process as oxygenates are not desired in FTS product. In short this study concludes that use of zirconium promoter is beneficial for increasing the C<sub>5+</sub> selectivity of cobalt based FTS catalyst.

# Acknowledgements

*Most of all I am thankful to Allah who gave me the will and determination to accomplish this task in this manner.*

*I owe my sincere gratitude to Dr. Bilal Khan (Principal USPCAS-E), Dr. Zuhair S Khan (HoD USPCAS-E) and USPCAS-E Administration for their inspiration, guidance and support.*

*Writing this thesis and accomplishing this task so appreciably is only due to the unrelenting support and critical comments of my supervisor Dr. Naseem Iqbal and other GEC Members. My supervisor and aides put in a lot of effort and time giving me critical comments and guidance at the times of need.*

*I am greatly indebted to the Dr. Nisar Ahmad (NCP, Islamabad) along with NCP administration, who offered their guidance and much needed expertise and without whom this would not have been possible. I would also like to offer my gratitude to Mr. Saeed Iqbal (In-charge FT apparatus) and Mr. Amin Durrani (FT Lab Engineer) for their sincere support and technical assistance.*

*Sincerely,*

*Muhammad Arslan*

## Promoted Hydrotalcite Based Cobalt Catalyst for Fischer Tropsch Synthesis Application

Muhammad Arslan<sup>a</sup>, Muhammad Faizan Sharif<sup>a</sup>, Naseem Iqbal<sup>a</sup>

<sup>a</sup>US Pakistan Centre for Advanced Studies in Energy (USPCAS-E), National University of Sciences and Technology, Islamabad (44000), Pakistan

---

### Abstract

The effects of using different promoters on hydrotalcite based cobalt (HT-Co) catalyst for Fischer-Tropsch Synthesis was studied in this paper. The HT-Co catalysts were synthesized by using hydrothermal method whereas zinc and zirconium were added separately as promoters, by wetness impregnation method. The main aim of the study is to see the difference in properties of both zinc and zirconium promoted catalysts. The catalysts were characterized by using several characterization techniques like scanning electron microscope, X-ray diffraction, thermal gravimetric analysis, Brunauer-Emmett-Teller analysis and Fourier-transform infrared spectroscopy. The results showed the differences in the properties of both catalysts

© 2016 "Muhammad Arslan, Muhammad Faizan Sharif, Naseem Iqbal" Selection and/or peer-review under responsibility of Energy and Environmental Engineering Research Group (EEERG), Mehran University of Engineering and Technology, Jamshoro, Pakistan.

**Keywords:** "Zinc Promoted; Zirconium Promoted; Hydrotalcite Cobalt Catalyst; Hydrothermal Method"

---

### 1. Introduction

The inclination in demand of liquid fuels and concern of public towards green fuels has enormously affected the fuel industry. Fuel industry is moving towards finding new sources of liquid fuels that would have minimum environmental impacts. Fischer Tropsch is one of such efforts, as it not only helps in the generation of liquid fuels from various sources but also produces liquid fuels that are relatively more environmentally friendly as compared to their originator [1]. Fischer Tropsch is a commercially used polymerization process and its main purpose is to convert hydrogen and carbon monoxide into a series of hydrocarbons [2]. The mixture of carbon monoxide and hydrogen is termed as syngas and can be manufactured from various sources like methane reforming, coal stream reforming, and biomass gasification [3]. The hydrocarbons obtained from Fischer Tropsch synthesis have a broad range of chain length and utility[4].

The main reaction of hydrocarbons generation in Fischer Tropsch synthesis employs a catalyst. There are several different metals that can serve as active component of catalyst but cobalt and iron are most commonly used commercially. The iron based catalyst usually produces oxygenates and branched hydrocarbons whereas cobalt based catalyst usually produces straight chain compounds including lighter

---

\* Corresponding author. Tel.:+9251-90855281; fax: +0-000-000-0000 .  
E-mail address: naseem@casen.nust.edu.pk

olefins and heavier paraffin [5]. Iron is preferred while using syngas having lower H<sub>2</sub>/CO ratio and it has relatively more resistance for sulfur of syngas than cobalt [6]. In case of higher H<sub>2</sub>/CO ratio cobalt is preferred because of it has high activity, better stability and very low inclination towards water-gas shift (WGS) reaction [7]. Hydrotalcites are hydroxides having double or triple layered structure and can be used as support material for catalyst in FTS. They are widely used as a support material for catalysts used for CO Hydrogenation [2], CO Methanation [2] and Auto thermal reforming [8]. In hydrotalcite supported catalysts the active metal is embedded in the core structure of catalyst instead of adsorbing on the surface of support [3].

Recently a lot of different promoters were added to the cobalt based catalyst for increasing selectivity and activity of the catalyst. La and P were added to the cobalt manganese oxide and increased hydrocarbon selectivity whereas a decreased CH<sub>4</sub> and CO<sub>2</sub> selectivity was reported [9]. Similarly another study reported that Pt promoted cobalt catalyst prepared by co-deposition method is more active than unpromoted catalyst as compared to Ru and Re promoted [4].

Zirconium promotes the activity of the catalyst by enhancing the carbon monoxide hydrogenation and water gas shift activity. On the other hand, the addition of zirconium oxide also increases the reduction temperature of cobalt [10]. During the preparation of catalyst, addition of the small quantities of promoters increases the reducibility of the cobalt catalyst [5]. Zinc promoter has good CO conversion and high selectivity towards C<sub>5</sub>+ product. Moreover the addition of zinc promoter prevents the oxidation of metallic cobalt [4]. The main purpose of the study is to see the effect of adding promoters on the functionality of hydrotalcite based cobalt catalyst. The HT-Co catalyst is prepared by co-precipitation method and the promoters are added by wet impregnation method. Zinc and zirconium were two different promoters that were added.

## **2. Experimentation**

### **2.1. Catalyst Preparation**

Catalysts are prepared by using hydrothermal method. First precipitating agent solution was prepared by adding 8.99g sodium hydroxide pellets (NaOH) and 1.49g sodium carbonate (Na<sub>2</sub>CO<sub>3</sub>) in 100ml deionized water to get clear solution. The metal nitrate solution was prepared by adding 7.03g aluminium nitrate (Al(NO<sub>3</sub>)<sub>3</sub>·9H<sub>2</sub>O), 7.27g cobalt nitrate (Co(NO<sub>3</sub>)<sub>2</sub>·6H<sub>2</sub>O) and 8.01g magnesium nitrate (Mg(NO<sub>3</sub>)<sub>2</sub>·6H<sub>2</sub>O) in 100 ml deionized water to get a purplish red hue. The metal nitrate solution was added drop wise to the precipitating agent solution provided with constant stirring. After mixing, pH of the solution was adjusted around 9 by careful addition of nitric acid (HNO<sub>3</sub>). The solution was transferred to a hydrothermal autoclave and heated at 80°C for 16 h. After 16 h the solution was filtered and precipitates were washed thoroughly with distilled water and oven dried at 80°C overnight. Both zinc and zirconium promoters were added by wet impregnation method separately. Add zinc nitrate or zirconium nitrate solution drop wise on the dried sample from oven. The sample was dried again at 80°C for 5 hours. In the end the sample was calcined at 600°C for 7 h in an airtight furnace. Zinc promoted catalysts is reported in this paper as HTCo-Zn whereas zirconium promoted as HTCo-Zr.

### **2.2. Catalyst Characterization**

The prepared sample of catalyst was characterized by using several techniques like XRD (X-ray Diffraction), SEM (Scanning Electron Microscopy), EDS (Energy Dispersive Spectrometry), BET (Brunauer–Emmett–Teller), and FTIR (Fourier Transform Infrared Spectroscopy). STOE Powder Diffraction System was used for XRD which was operating at 20 kV. FT-IR spectra of the prepared samples were recorded using PerkinElmer Spectrum 100 Spectrometers. SEM and EDS were done with a JEOL, JED 2300 Analysis Station. BET analysis was done by using Tristar II 3020 apparatus whereas nitrogen was used as adsorbate.

## **3. Results and Discussion**

### 3.1. X-Ray Diffraction

The Figure 1 shows the XRD patterns of both HTCo-Zn and HTCo-Zr. There appears to be some peaks around  $37^\circ$ ,  $44^\circ$ ,  $65^\circ$  which are the characteristic behaviors of cobalt oxide ( $\text{Co}_3\text{O}_4$ ) and represents different crystal planes of cobalt oxide. Cobalt have slightly larger radius of ( $\text{Co}^{2+}$  ion radius of  $0.74 \text{ \AA}$ ) than the  $\text{Mg}^{2+}$  and  $\text{Al}^{3+}$  which have an ion radius of  $0.65 \text{ \AA}$  and  $0.60 \text{ \AA}$  hence the incorporation of larger cobalt ions in the HT structure makes the structure less crystalline[11] .

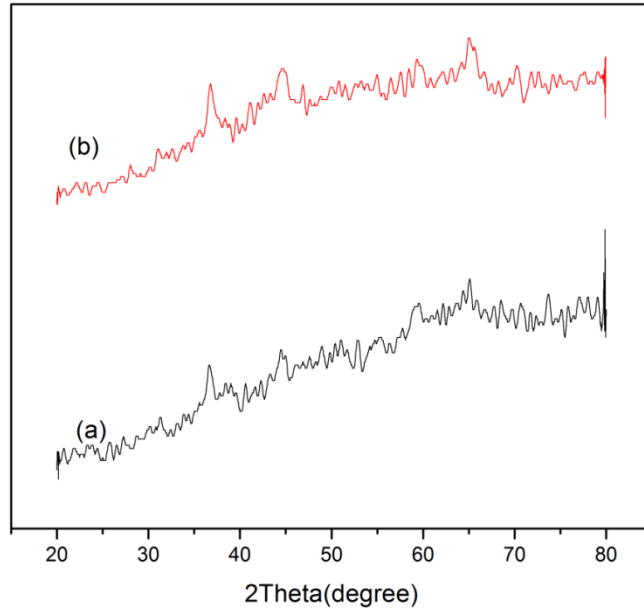
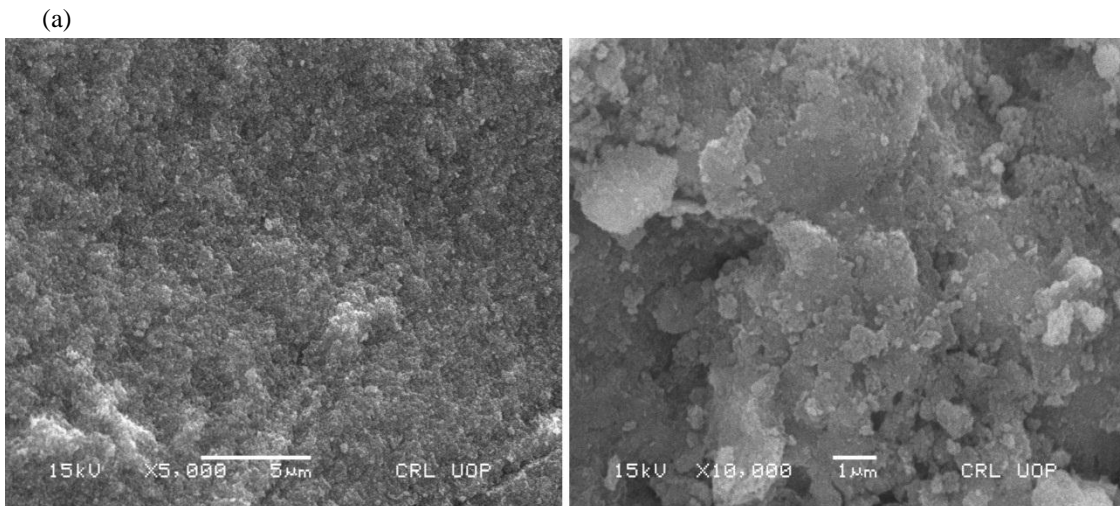


Fig. 1. XRD Pattern of (a) HTCo-Zr (b) HTCo-Zn..

### 3.2. Scanning Electron Microscope

The Figure 2 (a,b) shows the SEM images of the samples prepared at different resolutions of 5000 and 10000. The image shows that the prepared catalysts have rough particles of various shapes and sizes. The particle sizes on average varies from few micrometers up to 50 micrometers or even larger. The hexagonal, relatively shiny particles at the side of Figure 2b, shows the probable presence of zirconium on the surface of hydrotalcite based cobalt catalyst. The SEM images also show that zinc oxide and cobalt oxide are strongly in contact to form the interface in the composite. The addition of zirconium oxide on the catalyst surface prevents the formation of aluminates on cobalt surface hence improves the reducibility



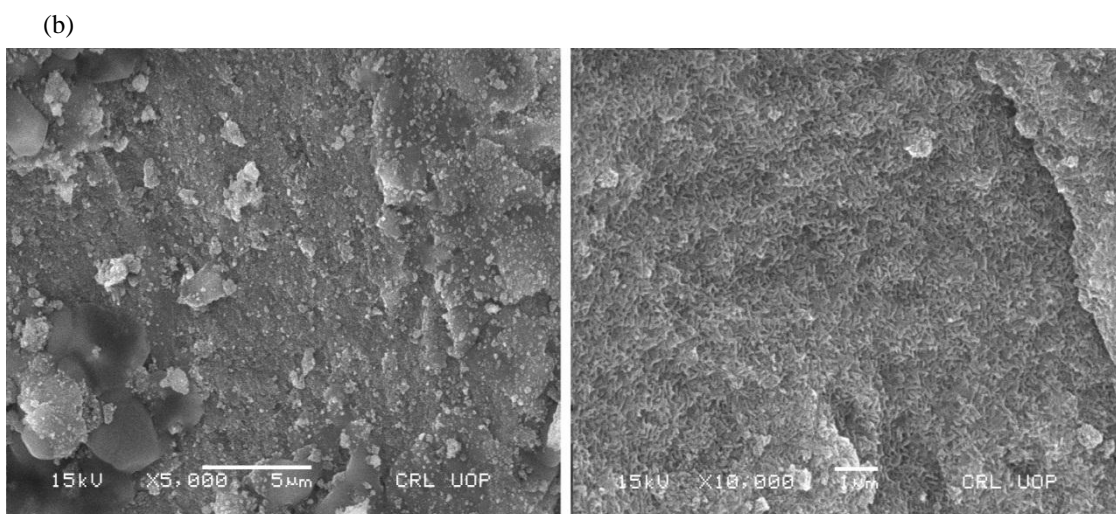


Fig. 2. SEM Images of (a) HTCo-Zn at X5000 and X 10000 (b) HTCo-Zr at X5000 and X 10000.

### 3.3. Energy Dispersive Spectroscopy

Table 1 shows the elemental analysis of prepared catalyst obtained by energy dispersive spectroscopy. The table shows that there is approximately 30 to 31% cobalt loading in our catalyst. There is 3.24 % zinc that is retained on the surface of the crystal. In zirconium promoted 5.32 % zirconium is retained which ensures more promoting effecting than zinc promoted. The carbon percentage points towards another important characteristic feature of hydrotalcite which is existence of carbonates in the layered structure of material.

Table 1. Elemental Analysis of HTCo-Zn and HTCo-Zr

Catalyst	C (%)	O (%)	Na (%)	Mg (%)	Al (%)	Co (%)	Zn (%)	Zr (%)
HTCo-Zn	4.22	38.85	2.90	11.92	7.54	31.32	3.24	-----
HTCo-Zr	5.04	38.60	4.02	9.63	6.76	30.62	-----	5.32

### 3.4. Brunauer–Emmett–Teller

The samples of prepared catalysts were outgassed for 5 hours under vacuum at 300<sup>o</sup>C and nitrogen physisorption measurements were performed. Table 2 gives the details of BET surface area, pore volume, pore size and average particle size. The zinc promoted samples has large surface area around 74.912m<sup>2</sup>/g. The larger pore volume contributes in the reaction due to availability of the pore walls. If pore size is very small that will inhibit rapid transfer of molecules and ultimately limits the reaction rate. The addition of small quantities of promoters like zinc and zirconium does not affect the surface area of the hydrotalcite material.

Table 2. BET Analysis of HTCo-Zn

Catalyst	BET Surface Area (m <sup>2</sup> /g)	Pore volume (cm <sup>3</sup> /g)	Pore size (nm)	Avg. particle size (nm)
HTCo-Zn	74.912	0.1472	7.86	80.09

### 3.5. Fourier Transform Infrared Spectroscopy

FTIR spectra of both zinc and zirconium promoted catalyst are shown in figure. The FTIR spectra of the catalyst suggest that there exists a depression around  $3500\text{ cm}^{-1}$  in both HTCo-Zn and HTCo-Zr, which belongs to the hydroxyl-stretching sector between  $2500$  and  $3900\text{ cm}^{-1}$  [12]. Depression around  $668\text{ cm}^{-1}$  shows the characteristic absorption of  $\text{Co}_3\text{O}_4$  spinel phase (Co-O stretching) [13].  $\text{Al}_2\text{O}_3$  stretching is shown by the depression around  $550\text{ cm}^{-1}$ . [14]The larger depression around  $1400\text{ cm}^{-1}$  shows the possibility of carbonates that is the characteristics of hydrotalcite material[15].

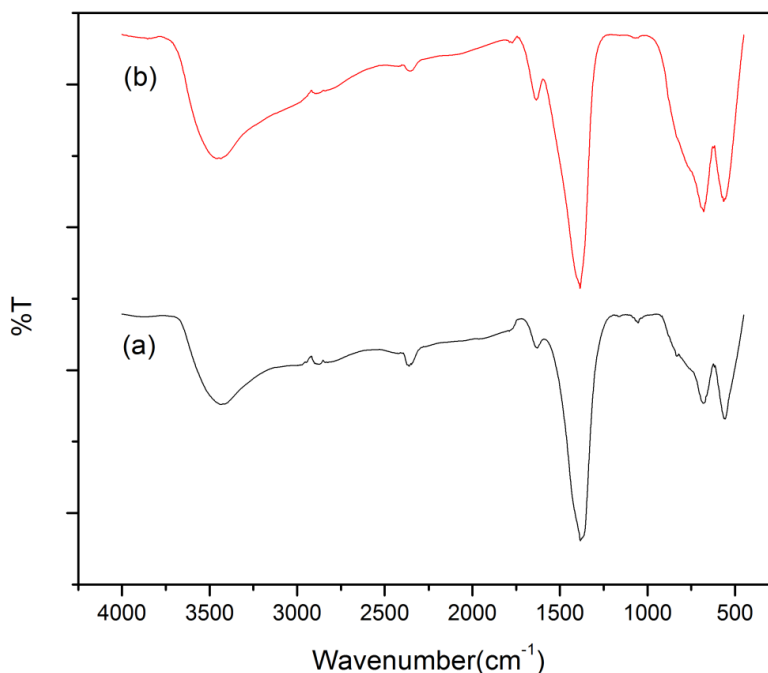


Fig. 1. FTIR Spectra of (a) HTCo-Zr (b) HTCo-Zn.

### 4. Conclusion

Zinc and zirconium are added to the hydrotalcite based cobalt catalyst as promoters. The characterization suggests that HTCo-Zr (Zirconium promoted) have the high promoter loading and more stable crystal structure as compared to zinc promoted catalyst. Surface area analysis suggests that zirconium promoted catalyst have sufficiently large surface area that can further increase its catalytic ability. Hence it points toward the fact that zirconium promoted catalyst can enhances the reaction rate and C5+ selectivity of the cobalt catalyst.

### Acknowledgements

- Dr. Naseem Iqbal
- Dr. Nisar Ahmad
- Dr. Tayabba Noor
- Muhammad Faizan Sharif
- Saeed Iqbal
- Amin Durrani

## References

- [1] T. Fu, Y. Jiang, J. Lv, and Z. Li, "Effect of carbon support on Fischer–Tropsch synthesis activity and product distribution over Co-based catalysts," *Fuel processing technology*, vol. 110, pp. 141-149, 2013.
- [2] Y.-T. Tsai, X. Mo, A. Campos, J. G. Goodwin, and J. J. Spivey, "Hydrotalcite supported Co catalysts for CO hydrogenation," *Applied Catalysis A: General*, vol. 396, pp. 91-100, 2011.
- [3] A. Di Fronzo, C. Pirola, A. Comazzi, F. Galli, C. Bianchi, A. Di Michele, *et al.*, "Co-based hydrotalcites as new catalysts for the Fischer–Tropsch synthesis process," *Fuel*, vol. 119, pp. 62-69, 2014.
- [4] K. M. Cook, H. D. Perez, C. H. Bartholomew, and W. C. Hecker, "Effect of promoter deposition order on platinum-, ruthenium-, or rhenium-promoted cobalt Fischer–Tropsch catalysts," *Applied Catalysis A: General*, vol. 482, pp. 275-286, 2014.
- [5] E. Iglesia, "Design, synthesis, and use of cobalt-based Fischer-Tropsch synthesis catalysts," *Applied Catalysis A: General*, vol. 161, pp. 59-78, 1997.
- [6] A. Y. Khodakov, W. Chu, and P. Fongarland, "Advances in the development of novel cobalt Fischer-Tropsch catalysts for synthesis of long-chain hydrocarbons and clean fuels," *Chemical Reviews*, vol. 107, pp. 1692-1744, 2007.
- [7] M. Trépanier, A. K. Dalai, and N. Abatzoglou, "Synthesis of CNT-supported cobalt nanoparticle catalysts using a microemulsion technique: role of nanoparticle size on reducibility, activity and selectivity in Fischer–Tropsch reactions," *Applied Catalysis A: General*, vol. 374, pp. 79-86, 2010.
- [8] L. He, Q. Lin, Y. Liu, and Y. Huang, "Unique catalysis of Ni-Al hydrotalcite derived catalyst in CO<sub>2</sub> methanation: cooperative effect between Ni nanoparticles and a basic support," *Journal of Energy Chemistry*, vol. 23, pp. 587-592, 2014.
- [9] K. Takehira, T. Shishido, P. Wang, T. Kosaka, and K. Takaki, "Autothermal reforming of CH<sub>4</sub> over supported Ni catalysts prepared from Mg–Al hydrotalcite-like anionic clay," *Journal of Catalysis*, vol. 221, pp. 43-54, 2004.
- [10] S. Iqbal, T. E. Davies, J. S. Hayward, D. J. Morgan, K. Karim, J. K. Bartley, *et al.*, "Fischer Tropsch Synthesis using promoted cobalt-based catalysts," *Catalysis Today*, vol. 272, pp. 74-79, 2016.
- [11] H. Jahangiri, J. Bennett, P. Mahjoubi, K. Wilson, and S. Gu, "A review of advanced catalyst development for Fischer–Tropsch synthesis of hydrocarbons from biomass derived syn-gas," *Catalysis Science & Technology*, vol. 4, pp. 2210-2229, 2014.
- [12] F. Rong, J. Zhao, P. Su, Y. Yao, M. Li, Q. Yang, *et al.*, "Zinc–cobalt oxides as efficient water oxidation catalysts: the promotion effect of ZnO," *Journal of Materials Chemistry A*, vol. 3, pp. 4010-4017, 2015.
- [13] V. M. Lebarbier, A. M. Karim, M. H. Engelhard, Y. Wu, B. Q. Xu, E. J. Petersen, *et al.*, "The effect of zinc addition on the oxidation state of cobalt in Co/ZrO<sub>2</sub> catalysts," *ChemSusChem*, vol. 4, pp. 1679-1684, 2011.
- [14] L. He, H. Berntsen, E. Ochoa-Fernández, J. C. Walmsley, E. A. Blekkan, and D. Chen, "Co–Ni catalysts derived from hydrotalcite-like materials for hydrogen production by ethanol steam reforming," *Topics in Catalysis*, vol. 52, pp. 206-217, 2009.
- [15] J. T. Klopogge and R. L. Frost, "Fourier transform infrared and Raman spectroscopic study of the local structure of Mg-, Ni-, and Co-hydrotalcites," *Journal of Solid State Chemistry*, vol. 146, pp. 506-515, 1999.

## Hydrotalcite Based Cobalt Catalyst for Synthesis of Hydrocarbons from Syngas

Muhammad Faizan Sharif <sup>a</sup>, Muhammad Arslan <sup>a</sup>, Naseem Iqbal <sup>a</sup>

<sup>a</sup>US Pakistan Centre for Advanced Studies in Energy (USPCAS-E), National University of Sciences and Technology, Islamabad 44000, Pakistan

---

### Abstract

The potential of using hydrotalcite based cobalt catalyst for Fischer Tropsch Synthesis application was studied in this paper. The hydrotalcite based cobalt (HT-Co) catalysts were prepared by using two different methods, co-precipitation and hydrothermal method. The main focus of the study is to see the effect of method of preparation on the activity and selectivity of catalyst. The catalysts were characterized by using various techniques like X- ray diffraction, scanning electron microscope, Brunauer-Emmett-Teller analysis, thermal gravimetric analysis, and Fourier-transform infrared spectroscopy. The difference between the properties and behavior of the two catalysts are shown in this study.

© 2016 "Muhammad Faizan Sharif, Muhammad Arslan, Naseem Iqbal" Selection and/or peer-review under responsibility of Energy and Environmental Engineering Research Group (EEERG), Mehran University of Engineering and Technology, Jamshoro, Pakistan.

**Keywords:** "Cobalt Catalyst; Hydrotalcite; Coprecipitation Method; Hydrothermal Method"

---

### 1. Introduction

Fischer Tropsch synthesis is a commercial technology that was first developed during second world war . The main purpose of this technology is to generate liquid fuels from various sources. As the world is moving towards the depletion of the oil resources and on the other hand the demand for the liquid fuel is increasing which have moved the researchers towards finding new sources that are either plenty and environmental friendly[1] . The Fischer Tropsch is one of such technology and is used for producing liquid fuels from various different sources like coal, methane gas, methane hydrates and biomass. These material are passed through gasification or steam reforming process to produce syngas which is the input material for FTS process. The FTS process used a catalyst to convert syngas into a series of hydrocarbons that can further be used as fuels[2]. Iron and Cobalt are two main active components of the catalyst used in FTS. The cobalt based catalyst usually produces lighter olefins and heavier paraffin whereas iron based catalyst produces oxygenates and branched hydrocarbons [3]. Iron is chosen while using syngas having low H<sub>2</sub>/CO ratio whereas if that ratio is relatively high cobalt catalyst is favored [4]. Cobalt is favored because of its high activity for FTS, more stability and high selectivity for C<sub>5</sub>+ [5].

The active component of the catalyst is usually incorporated on the surface of a supporting material and changing that support material can largely affect the properties of the catalyst. There are several compounds like activated carbon, Al<sub>2</sub>O<sub>3</sub>, TiO<sub>2</sub>, SiO<sub>2</sub> and MgO which have been commonly used as supports for cobalt catalysts. Recently attempts were made to use hydrotalcite material as a support material for catalyst. Hydrotalcites are double or sometimes triple layered hydroxides and are generally

---

\* Corresponding author. Tel.: +9251-90855281; fax: +0-000-000-0000 .  
E-mail address: naseem@casen.nust.edu.pk

used as a support material for catalysts used for carbon monoxide methanation[6], auto thermal reforming [7], CO Hydrogenation[8] etc. The active component of hydrotalcite supported catalysts is implanted in the core structure of catalyst instead of surface adsorbing [9].

Attempts were made to use hydrotalcite based catalyst in FTS reactions. Those studies suggest that the high reducibility and high surface areas of hydrotalcite based cobalt catalyst renders them highly active [8]. Apart from that, certain studies also varied the Al/Mg molar ratio in hydrotalcite structure and proposed that lower Mg/Al leads to better distribution of cobalt in the crystal [10]. Recent studies also suggest that hydrothermal method can considerably boost the catalyst activity and selectivity [11]. This study aims towards synthesis of hydrotalcite based cobalt catalyst for FT synthesis by using hydrothermal method and co-precipitation method. Potassium is used as precipitating agent because it increases C5+ selectivity, decreases methanation, increase CO conversion and promotes water gas shift reaction. Apart from that it also helps in increasing the activity of cobalt in the FTS and prevents rapid catalyst deactivation [12]. The prepared catalysts were characterized and difference in their properties was studied.

## **2. Experimental**

### **a. Catalyst Synthesis**

First we prepared hydrotalcite based cobalt catalyst by co-precipitation method (HTCo-Cppt). The metal nitrate solution was prepared by mixing aluminium nitrate (7.03g) magnesium nitrate (8.01g) and cobalt nitrate (7.27 g) in 100 ml deionized water to get a purplish red hue. For preparing precipitating agent solution, potassium carbonate (1.94g) and potassium hydroxide (8.40g) were dissolved in 100ml deionized water to get clear solution. The metal nitrate solution was added to the later solution by drop-wise addition and provided with constant stirring. After complete mixing the pH of the solution was brought down to 8-9 by adding concentrated nitric acid. Then the solution was heated at 80°C for 16 h while constantly stirring to mature precipitates. After that the solution was filtered followed by precipitates washing with distilled water. After washing the precipitates were subjected to oven drying at 80°C overnight to get purple colored solid. The sample was then calcined at 600°C for 7 h in an airtight furnace.

Second we prepare hydrotalcite based cobalt catalyst by hydrothermal method (HTCo-Ht) using the same concentrations of solutions as mentioned in the above method. The only difference between two methods is the process used for maturation of precipitates. The solution was added to a hydrothermal autoclave and heated at 80°C for 16 h. in hydrothermal autoclave we are providing temperature along with pressure whereas coprecipitation process only uses temperature for maturation of precipitates. The precipitates were filtered and washed thoroughly with distilled water and then oven dried at 80°C overnight. After drying, purple colored solid was calcined at 600°C for 7 h in an airtight furnace.

### **b. Catalyst characterization**

The prepared samples were characterized by using various characterization techniques like X-Ray diffraction spectroscopy (XRD), Scanning Electron Microscopy (SEM), Brunauer–Emmett–Teller (BET), Thermal Gravimetric Analysis (TGA) and Fourier Transform Infrared (FTIR). XRD is performed using STOE Powder Diffraction System and SEM and EDS were done with a JEOL, JED 2300 Analysis Station. FT-IR spectra of the prepared samples were recorded at room temperature using PerkinElmer Spectrum 100 Spectrometers. Brunauer–Emmett–Teller (BET) was performed using Tristar II 3020 apparatus whereas nitrogen was used as adsorbate.

## **3. Results and Discussion**

### **a. Scanning Electron Microscope**

SEM images of HTCo-Cppt are shown in Figure 1a. It is quite evident from the figure that the particles are of irregular shape and sizes however when viewed at larger resolution they show relatively plain particle symmetry. It can also be observed that average particle size of samples prepared by coprecipitation method is large as compared to hydrothermal method.

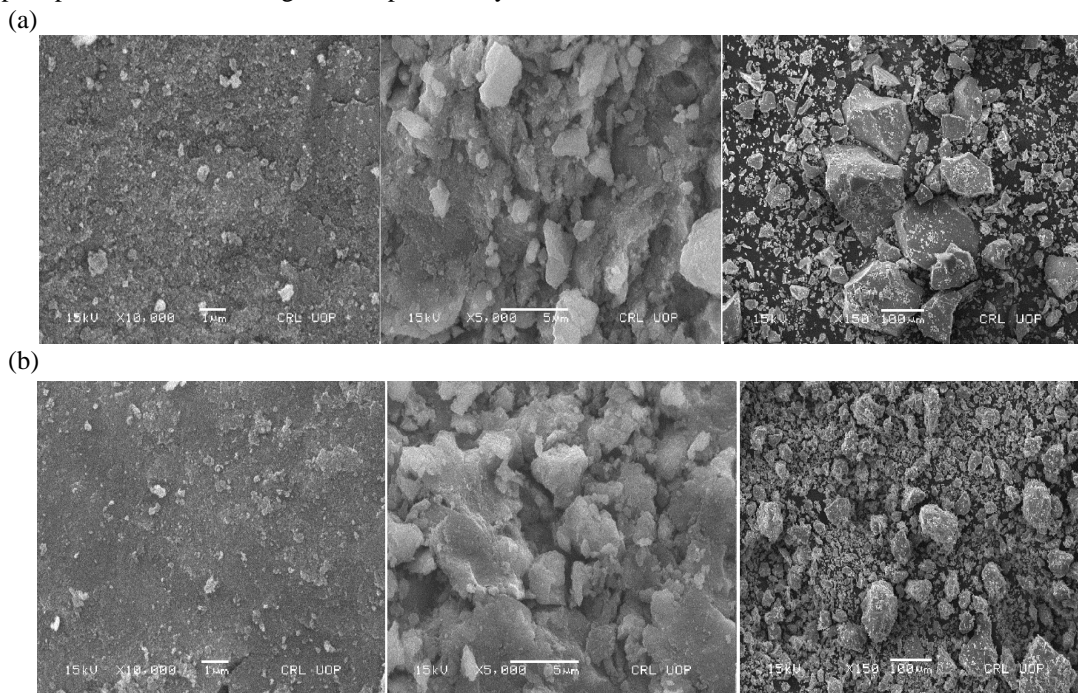


Fig. 1. SEM images of (a) HTCo-Cppt (b) HTCo-Ht.

### b. Energy Dispersive Spectroscopy

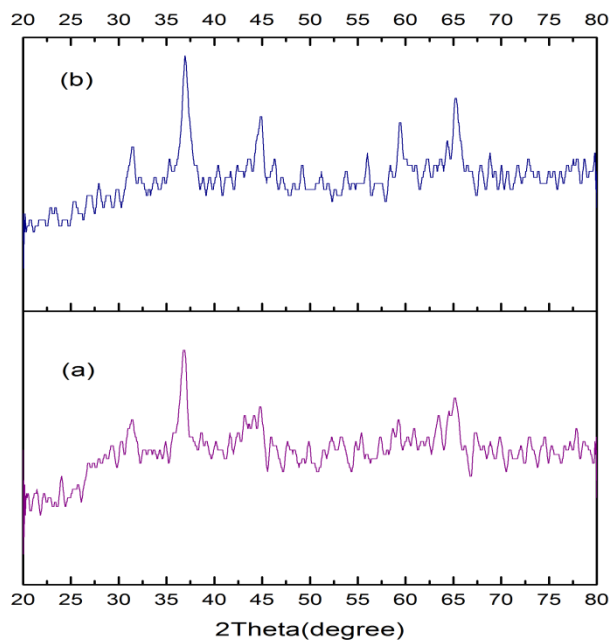
Elemental analysis of the samples is given in Table 1. HTCo-Cppt have approximately 1.02% potassium and HTCo-Ht have around 1.90% potassium. This small percentage may boast a little the activity of catalyst HTCo-Ht. However the cobalt percentage of HTCo-Ht is less than other counterpart. The HTCo-Cppt have less potassium but at the same time its cobalt loading percentage is way more than HTCo-Ht. In other words the EDS suggest that catalyst prepared by coprecipitation method may have more catalytic ability than hydrothermal method.

Table 1. EDS of HTCo prepared by coprecipitation and hydrothermal method

Catalyst	O (%)	K (%)	Mg (%)	Al (%)	Co (%)
HTCo-Cppt	36.07	1.02	11.50	9.75	41.66
HTCo-Ht	38.97	1.90	12.13	10.48	36.52

### c. X-Ray Diffraction Spectroscopy

XRD pattern of HTCo-Cppt and HTCo-Ht are shown in the Figure 2. There peaks around 31°, 37°, 44.8°, 65° which are the characteristics peaks for different planes of cobalt oxide[13]. Cobalt develops into hexagonal close packed structures (hcp) however at high pressure where the magnetism is effectively repressed, we expect a shift from hcp to fcc (face centered cubic structure) [14].



**Fig. 2. XRD Patterns of (a) HTCo-Ht (b) HTCo-Cppt.**

#### **d. Thermal Gravimetric Analysis**

TGA of the HTCo-Cppt sample is given in the Figure 3. The catalyst shows typical hydrotalcite behaviour and give two weight losses. The curve suggests that weight of sample starting to fall till 220 °C. This is due to the hydration water removal from the interlayer space of crystal. Between 220 to 410 °C another weight loss occurs which shows the removal of OH- group from inlayed water molecules [15].

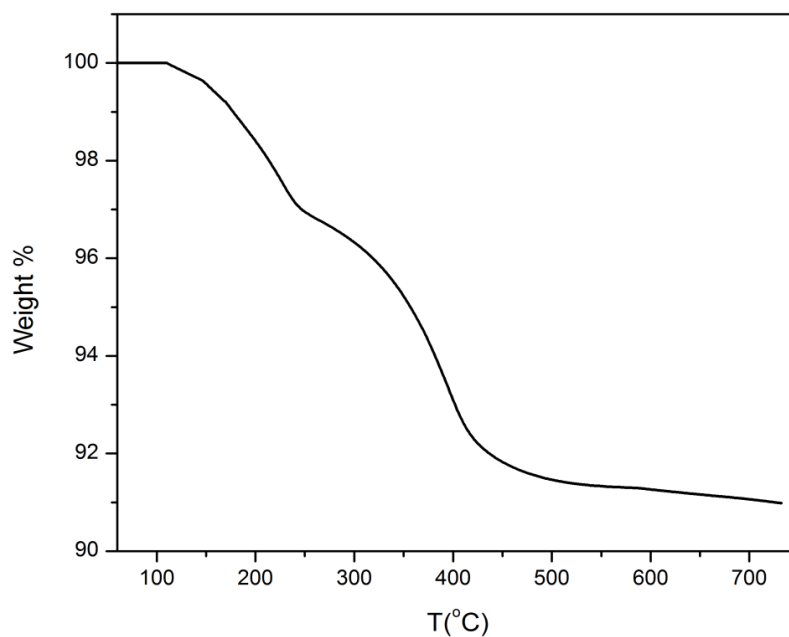


**Fig. 3. TGA Graph of HTCo-Cppt.**

### e. Brunauer–Emmett–Teller

BET of the HTCo-Cppt is shown in the Table 2. The table suggests that the average particle size of the sample is around 52.83 nm. The pore volume is very small so there is a very small chance of diffusion. However the pore size is large and there is a very little chance of blocking of pore mouth. The surface area value shows that the HTCo-Cppt have appropriately large surface area hence there is bigger playground for FTS reaction. The pore size of HTCo-Cppt is 6.33 nm so the majority of the pores fall under the category of mesopores ( $2\text{nm} < \text{size} < 50\text{nm}$ ) [16].

Table 2. BET Analysis of HTCo-Cppt

Catalyst	BET Surface Area ( $\text{m}^2/\text{g}$ )	Pore volume ( $\text{cm}^3/\text{g}$ )	Pore size (nm)	Avg. particle size (nm)
HTCo-Cppt	114.9709	0.1819	6.33	52.836

### f. Fourier Transform Infrared

The FTIR spectra of the HTCo-Cppt shows that there exists a depression around  $3400\text{ cm}^{-1}$  which is due to the hydroxyl stretching [17]. The bending vibrations due to H and OH bond is creating a depression around  $1650\text{ cm}^{-1}$ . There is another depression around  $660\text{ cm}^{-1}$  which is due to cobalt oxide (Co-O stretching) [9]. The calcination of the sample results in the formation of huge bands due to the cobalt oxide phase. The depression around  $550\text{ cm}^{-1}$  is attributed to the  $\text{Al}_2\text{O}_3$  stretching [15].

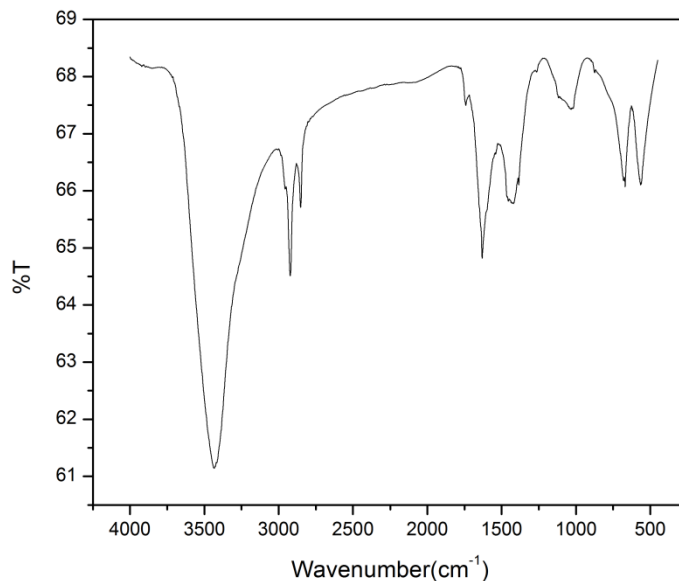


Fig. 4. FTIR Spectra of HTCo-Cppt.

## 4. Conclusion

The Hydrotalcite based cobalt catalysts were prepared using both hydrothermal and coprecipitation methods. The characterization suggests that HTCo-Cppt (Coprecipitation method) have the high cobalt loading and more stable crystal structure as compared to other counterpart. HTCo-Cppt has fairly large surface area which can increase reaction rate. These developed catalyst have potassium in their core structure which itself have the promoting ability for FTS. The overall crystal structure and the properties

of catalyst suggests that using this catalyst (HTCo-Cppt) in FTS can increase the yield and selectivity towards desired hydrocarbons.

### Acknowledgements

- Dr. Naseem Iqbal
- Dr. Nisar Ahmad
- Dr. Tayabba Noor
- Muhammad Arslan
- Saeed Iqbal
- Amin Durrani

### References

- [1] S. Mousavi, A. Zamaniyan, M. Irani, and M. Rashidzadeh, "Generalized kinetic model for iron and cobalt based Fischer–Tropsch synthesis catalysts: Review and model evaluation," *Applied Catalysis A: General*, vol. 506, pp. 57-66, 2015.
- [2] A. Tavasoli, R. M. M. Abbaslou, M. Trepanier, and A. K. Dalai, "Fischer–Tropsch synthesis over cobalt catalyst supported on carbon nanotubes in a slurry reactor," *Applied Catalysis A: General*, vol. 345, pp. 134-142, 2008.
- [3] E. Iglesia, "Design, synthesis, and use of cobalt-based Fischer-Tropsch synthesis catalysts," *Applied Catalysis A: General*, vol. 161, pp. 59-78, 1997.
- [4] A. Y. Khodakov, W. Chu, and P. Fongarland, "Advances in the development of novel cobalt Fischer-Tropsch catalysts for synthesis of long-chain hydrocarbons and clean fuels," *Chemical Reviews*, vol. 107, pp. 1692-1744, 2007.
- [5] G. Jacobs, C. Bertaux, V. R. R. Pendyala, W. D. Shafer, J.-S. Poirier, Q. Xiao, *et al.*, "Fischer-Tropsch synthesis: Cobalt catalysts on alumina having partially pre-filled pores exhibit higher C<sub>5+</sub> and lower light gas selectivities," *Applied Catalysis A: General*, vol. 516, pp. 51-57, 2016.
- [6] L. He, Q. Lin, Y. Liu, and Y. Huang, "Unique catalysis of Ni-Al hydrotalcite derived catalyst in CO<sub>2</sub> methanation: cooperative effect between Ni nanoparticles and a basic support," *Journal of Energy Chemistry*, vol. 23, pp. 587-592, 2014.
- [7] K. Takehira, T. Shishido, P. Wang, T. Kosaka, and K. Takaki, "Autothermal reforming of CH<sub>4</sub> over supported Ni catalysts prepared from Mg–Al hydrotalcite-like anionic clay," *Journal of Catalysis*, vol. 221, pp. 43-54, 2004.
- [8] Y.-T. Tsai, X. Mo, A. Campos, J. G. Goodwin, and J. J. Spivey, "Hydrotalcite supported Co catalysts for CO hydrogenation," *Applied Catalysis A: General*, vol. 396, pp. 91-100, 2011.
- [9] A. Di Fronzo, C. Pirola, A. Comazzi, F. Galli, C. Bianchi, A. Di Michele, *et al.*, "Co-based hydrotalcites as new catalysts for the Fischer–Tropsch synthesis process," *Fuel*, vol. 119, pp. 62-69, 2014.
- [10] A. Forgionny, J. Fierro, F. Mondragón, and A. Moreno, "Effect of Mg/Al Ratio on Catalytic Behavior of Fischer–Tropsch Cobalt-Based Catalysts Obtained from Hydrotalcites Precursors," *Topics in Catalysis*, vol. 59, pp. 230-240, 2016.
- [11] J. Zhang, S. Lu, S. Fan, T. Zhao, and K. Zhang, "Hydrothermal preparation of Fe-Mn catalyst for light olefin synthesis from CO hydrogenation," *Nano Reports*, vol. 1, 2015.
- [12] H. Jahangiri, J. Bennett, P. Mahjoubi, K. Wilson, and S. Gu, "A review of advanced catalyst development for Fischer–Tropsch synthesis of hydrocarbons from biomass derived syn-gas," *Catalysis Science & Technology*, vol. 4, pp. 2210-2229, 2014.
- [13] M. Trépanier, A. K. Dalai, and N. Abatzoglou, "Synthesis of CNT-supported cobalt nanoparticle catalysts using a microemulsion technique: role of nanoparticle size on reducibility, activity and selectivity in Fischer–Tropsch reactions," *Applied Catalysis A: General*, vol. 374, pp. 79-86, 2010.
- [14] C.-S. Yoo, P. Söderlind, and H. Cynn, "The phase diagram of cobalt at high pressure and temperature: the stability of-cobalt and new-cobalt," *Journal of Physics: Condensed Matter*, vol. 10, p. L311, 1998.

- [15] J. Perez-Ramirez, G. Mul, F. Kapteijn, and J. Moulijn, "A spectroscopic study of the effect of the trivalent cation on the thermal decomposition behaviour of Co-based hydrotalcites," *Journal of Materials Chemistry*, vol. 11, pp. 2529-2536, 2001.
- [16] G. Leofanti, M. Padovan, G. Tozzola, and B. Venturelli, "Surface area and pore texture of catalysts," *Catalysis Today*, vol. 41, pp. 207-219, 1998.
- [17] J. T. Klopogge and R. L. Frost, "Fourier transform infrared and Raman spectroscopic study of the local structure of Mg-, Ni-, and Co-hydrotalcites," *Journal of Solid State Chemistry*, vol. 146, pp. 506-515, 1999.